

A

**THE SMAD GENES PLAY ESSENTIAL ROLES IN BODY  
SIZE REGULATION AND MALE TAIL MORPHOGENESIS  
IN CAENORHABDITIS ELEGANS**

by

JIANJUN WANG

A dissertation submitted to the Graduate Faculty in Biochemistry  
in partial fulfillment of the requirements for the degree of Doctor  
of Philosophy, The City University of New York.

2004

UMI Number: 3144149

Copyright 2004 by  
Wang, Jianjun

All rights reserved.

### INFORMATION TO USERS

The quality of this reproduction is dependent upon the quality of the copy submitted. Broken or indistinct print, colored or poor quality illustrations and photographs, print bleed-through, substandard margins, and improper alignment can adversely affect reproduction.

In the unlikely event that the author did not send a complete manuscript and there are missing pages, these will be noted. Also, if unauthorized copyright material had to be removed, a note will indicate the deletion.

**UMI**<sup>®</sup>

---

UMI Microform 3144149

Copyright 2004 by ProQuest Information and Learning Company.

All rights reserved. This microform edition is protected against unauthorized copying under Title 17, United States Code.

ProQuest Information and Learning Company  
300 North Zeeb Road  
P.O. Box 1346  
Ann Arbor, MI 48106-1346

© 2004

JIANJUN WANG

All Rights Reserved

This manuscript has been read and accepted for the Graduate Faculty  
in Biochemistry in satisfaction of the dissertation requirement for  
the degree of Doctor of Philosophy.

9/7/04  
\_\_\_\_\_  
Date

*Cathy Savage-D*  
\_\_\_\_\_  
Chair of Examining Committee

9/10/2004  
\_\_\_\_\_  
Date

*Lesley Davenport*  
\_\_\_\_\_  
Executive Officer

*Wilma Saffa*  
\_\_\_\_\_  
*[Signature]*  
\_\_\_\_\_  
*[Signature]*  
\_\_\_\_\_  
*[Signature]*  
\_\_\_\_\_  
Supervisory Committee

The City University of New York

## Abstract

### **The tissue specific expression and C-terminal mutagenesis of *C. elegans* Smads reveal the mechanisms of body size regulation and male tail morphogenesis**

by Jianjun Wang

Advisor: Professor Savage-Dunn

The Sma/Mab (TGF- $\beta$ ) signaling pathway regulates the body size and male tail morphogenesis. The components include the ligand *dbl-1*, receptors *daf-4* and *sma-6*, intracellular transducers *sma-2*, *sma-3* and *sma-4* (Smads). The mutants of the signaling pathway have small body size and male tail defects, fused sensory rays and crumpled spicules. It is suggested that the Smads cooperate in a heterotrimer manner to regulate the transcription of downstream target genes. The Smad proteins have highly conserved MH1 and MH2 domains connected by a linker region. The last two Serines of receptor responsive Smads are phosphorylated during the activation of the signaling. The crystal structures of mammalian Smads show the MH2 domain is critical for complex formation and receptor activation.

In *C. elegans*, the mechanism of Smad function is still poorly understood. In my studies, using the tissue specific expressed promoters, it is demonstrated that hypodermal expression of *sma-3* is sufficient and necessary for body size rescue. It is supported by the similar experiment with *sma-4* gene. Other groups also reported hypodermal expression of *sma-6*, *daf-4*, and *lon-1* is critical for body size. And *sma-3* expression in the seam cells rescues the body size also. The conclusion is going forward to that SMA-3

presence in *hyp7* is crucial to rescue the body size. The C-terminal mutants of SMA-3 are dominant negative in body size, but they are functional in male tail sensory rays. Pseudophosphorylated SMA-2 is constitutively active in body size rescuing suggests that the phosphorylated SMA-3 plays essential roles in the functional complex. According to all of the combination of different phosphorylated states of SMA-2 and SMA-3, it is suggested that two different kinds of trimers have distinct roles in worm development.

## Acknowledgement

After graduation with Bachelor degree of Science, I am very interested to learn more knowledge in detail of Biochemistry and Molecular Biology. In July 1998, I was excited to get a chance to continue my study toward Ph.D. degree in the Graduate School, the City University of New York, one of my best offers. With encourage of my parents, I come New York City to realize my dream to become a scientist.

The Ph.D. program in Biochemistry provides wonderful courses which teach me more basic knowledge about Biochemistry and Molecular Biology. I am a teaching assistant in Queens College, which provides me experience about teaching and makes me more confident to work in academic in future. I selected Dr Savage-Dunn as my advisor because she has full of experience of Molecular Biology in *C. elegans*, a very popular model organism in research. Interestingly, the loss-of-function mutants of Sma/Mab signaling pathway are small in body size. With the curiosity of the mechanism controlling body size, I began to devote myself into the study of the Smad genes.

Thanks my advisor Dr Savage-Dunn for her patient teaching during the past years. Professor Saffran, Ma, Foster and Patterson are my supervisory committee members. They spent a lot of effort to guide me and gave me suggestion in my research. Thanks to Queens College and Graduate School of CUNY for all of the assistance during my study, especially to Dr Schultz and Dr Davenport, the former and current Executive Officer of the Ph.D. program in Biochemistry.

## Table of Contents

<b>CONTENTS</b>	<b>PAGE</b>
Title	i
Copyrights	ii
Approval Page	iii
Acknowledgement	iv
Abstract	v
Table of Contents	vii
List of Tables	ix
List of Figures	xi
<b>Chapter I General Introduction</b>	<b>1</b>
General description of TGF- $\beta$ signal transduction	1
General Characteristics of <i>Caenorhabditis elegans</i>	13
TGF- $\beta$ signaling in <i>Caenorhabditis elegans</i>	25
Previous experiments characterizing <i>sma-3</i> gene	32
<b>Chapter II The expression of TGF-<math>\beta</math> signal transducers in the hypodermis regulates body size in <i>C. elegans</i></b>	<b>38</b>
Abstract	38
Introduction	39
Material and Methods	42
Results	47
Discussion	59
<b>Chapter III C-terminal mutants of the <i>C. elegans</i> Smads reveal that the targets require different levels of activities</b>	<b>65</b>

Abstract	65
Introduction	66
Material and Methods	69
Results	72
Discussion	91
<b>Chapter IV Other Observations</b>	99
The deletions of two loops abolish SMA-3 activity	99
The long phenotype induced by <i>dbl-1</i> overexpression can be suppressed by the C-terminal mutants of <i>sma-3</i>	101
Seam cell expression of <i>sma-3</i> also rescues the body size	103
<i>sma-4</i> hypodermal expression is sufficient to rescue body size	106
The hairpin intron of <i>sma-2</i> may be a negative regulator	107
<i>eff-1</i> mutants could be suppressed by <i>lon-1</i> in body size	108
<b>Chapter V Conclusion &amp; Discussion</b>	111
The Smad complex in hypodermis regulates body size	111
The role of the Sma/Mab pathway in male tail development	113
Seam-hyp7 fusion may play a role in body size control	116
Smad target genes in <i>C. elegans</i>	117
How does the worm become small?	119
The dauers of small mutants	121
<b>Prospect</b>	124
<b>References</b>	126

## List of Tables

TABLES	PAGE
<b>Table 1.1</b> Mosaic analysis of <i>sma-3</i>	36
<b>Table 2.1</b> The function of tissue-specific <i>sma-3</i> expression constructs in body length regulation <i>sma-3::gfp</i> fusion gene expression pattern and protein localization.	48
<b>Table 2.2</b> The function of <i>sma-3::gfp</i> constructs in male tail patterning	49
<b>Table 3.1</b> The designed C-terminal mutants of <i>sma-2</i> , <i>sma-3</i> and <i>sma-4</i>	73
<b>Table 3.2</b> The C-terminal mutants of <i>sma-3</i> do not rescue the body size of <i>sma-3(wk30)</i> .	74
<b>Table 3.3</b> The C-terminal mutants of <i>sma-3</i> are dominant negative in body size regulation except <i>sma-3-YMY</i> . The domain negative effects can be relieved by elimination of <i>lon-1</i> activity.	75
<b>Table 3.4</b> The C-terminal mutants of SMA-3 can rescue the male tail sensory ray fusion in <i>sma-3(wk30)</i> background.	79
<b>Table 3.5</b> The <i>sma-3</i> C-terminal mutants can not rescue the sensory fusion of <i>sma-6(wk7)</i> .	80
<b>Table 3.6</b> The pseudophosphorylated SMA-2 is constitutively active in body size regulation.	82
<b>Table 3.7</b> The pseudophosphorylation of <i>sma-2</i> can rescue the male tail defects and the double pseudophosphorylation of <i>sma-2</i> and <i>sma-3</i> can not rescue the	82

male tail of *sma-6(wk7)* mutant.

**Table 3.8** The *sma-4* C-terminal mutants functions as same as wild type in 91  
body size regulation.

**Table 3.9** The combinations of SMA-2, SMA-3 of different phosphorylation 95  
states have different effects on body size, male tail sensory rays and spicules.

**Table 4.1** Deletion of the loop WGED or PDIS abolishes SMA-3 activity in 100  
body size regulation.

**Table 4.2** Deletions of WGED and PDIS from SMA-3 show different activity 100  
to rescue the male tail.

**Table 4.3** The long phenotype induced by *dbl-1* overexpression is suppressed 103  
by the dominant negative *sma-3* mutants.

**Table 4.4** Seam expression of *sma-3* can rescue the body size. 105

**Table 4.5** Hypodermal expression of *sma-4* rescues body size. 106

**Table 4.6** *eff-1* null mutants can be suppressed by *lon-1* null mutants in body 109  
size.

## List of Figures

<b>FIGURES</b>	<b>PAGE</b>
<b>Figure 1.1</b> The TGF- $\beta$ related signaling pathways	3
<b>Figure 1.2</b> The X-ray structure of Type II TGF- $\beta$ receptor extracellular domain.	6
<b>Figure 1.3</b> The X-ray crystal structure of phosphorylated Smad2 MH2 domain.	10
<b>Figure 1.4</b> The body structure of a hermaphrodite of <i>C. elegans</i> .	15
<b>Figure 1.5</b> The male tail sensory rays of wild type and <i>sma-3(wk30)</i> mutant.	19
<b>Figure 1.6</b> The cell lineage of male tail sensory rays.	22
<b>Figure 1.7</b> The structure of hypodermis in wild type hermaphrodite.	23
<b>Figure 1.8</b> The TGF- $\beta$ related signaling pathways in <i>C. elegans</i> .	26
<b>Figure 1.9</b> The mutants of Sma/Mab pathway are small in body size.	30
<b>Figure 1.10</b> The SMA-3 protein sequence.	33
<b>Figure 2.1</b> The <i>sma-3::gfp(C)</i> expression stage and pattern in wild type.	51
<b>Figure 2.2</b> The <i>sma-3::gfp(N)</i> expression and localization in different mutant background.	52
<b>Figure 2.3</b> The <i>sma-3</i> expression with tissue-specific promoters.	55
<b>Figure 2.4</b> The distinct intensity of fluorescence in worms with different <i>sma-3::gfp</i> constructs in the <i>sma-3(wk30)</i> background.	56
<b>Figure 2.5</b> Expression of SMA-3::GFP C-terminal fusion protein in different genetic backgrounds.	57

- Figure 3.1** (A) The genomic clone of *sma-2* does not include the two big 83  
introns. (B) The expression pattern of *sma-2::gfp* transcriptional fusion gene.
- Figure 3.2** The yeast two hybrid test of the interaction between *lin-31* and *sma-* 86  
*3* or *sma-2*.
- Figure 3.3** The SMA-3 YMY localizes on the membranes. 87
- Figure 3.4** The SMA-3 C-terminal mutants could activate the negative feedback 88  
loop except for SMA-3 YMY.
- Figure 3.5** Proposed model of the functional complexes of *C. elegans* Smads. 97
- Figure 4.1** Expression pattern of *Pelt-5:sma-3* translational fusion gene in wild 104  
type and *eff-1* mutant background.
- Figure 5.1** The *sma-3:gfpC* expression in male tails. 115
- Figure 5.2** The dauers of *sma-2* and *sma-3* mutants form a special pattern, 122  
parallel to each other.

## Chapter I General Introduction

### General description of TGF- $\beta$ signal transduction

#### *Overview*

Transforming Growth Factor  $\beta$  (TGF- $\beta$ ) signaling pathways have multiple functions in the regulation of cellular events, and have key roles in development and carcinogenesis. The signaling components are conserved in diverse organisms, from worms and fruit fly to human beings (Shi and Massagué, 2003; Derynck and Zhang, 2003; Savage-Dunn, 2001; Hill, 2001). TGF- $\beta$  family members signal through cell surface serine/threonine kinase receptors. The Smad (homologues of *Drosophila* Mad and *C. elegans* Sma) proteins transduce the TGF- $\beta$  signal from the cell surface to the nucleus. There are two types of receptors, type I and type II. Type II receptor kinase is always active. When the ligand (TGF- $\beta$ ) binds the receptors, type II receptor phosphorylates and activates type I receptor. Upon activation, the TGF- $\beta$  type I receptor phosphorylates receptor regulated Smads (R-Smads), which then form complexes with Co-mediator Smads (Co-Smad, not a target of receptor phosphorylation) and accumulate in the nucleus to regulate transcription of a variety of genes that encode crucial determinants of cell fate, i.e. proliferation, differentiation, adhesion and apoptosis (Massagué and Chen, 2000). Smad transcriptional activity is inhibited by the oncogenes, Ski and SnoN. And the activating of the pathway is downregulated by inhibitory Smads (I-Smads), which inhibit receptor

binding with R-Smad and formation of functional Smad complexes and facilitate their degradation (Itoh et al., 2001; Murakami et al., 2003). The Smurf (Smad ubiquitination regulation factor) genes encode E3 ubiquitin ligases (Zhu et al., 1999; Bonni et al., 2001). Their expression is upregulated by the activated Smads in a negative feedback manner. The protein products induce the degradation of the Smads and receptors (Figure 1.1) (Kavsak et al., 2000; reviewed by Shi and Massagué, 2003).

#### *Ligands, the initiators of signaling*

The TGF- $\beta$  superfamily of cytokines, which contain six conserved cysteine residues, are encoded by forty-two open reading frames in human, nine in fruit fly, five in worm (Lander et al., 2001). The superfamily includes two subfamilies, the TGF- $\beta$ /Activin/Nodal subfamily and the BMP (bone morphogenetic protein)/GDF (growth and differentiation factor) /MIS (Muellerian inhibiting substance) subfamily. The signal specificity depends on the sequence variety, i.e. different receptors distinguish their ligands separately. The TGF- $\beta$  ligands inhibit cell proliferation, but BMP ligands enable cell differentiation and control the developmental fate (reviewed by Shi and Massagué, 2003). The BMP related ligand decapentaplegic (*dpp*) has a well-characterized role in pattern formation during *Drosophila* embryogenesis and in larval development. It acts as a long-range morphogen during imaginal disc growth in the wing (Affolter et al., 2001). The active form of a TGF- $\beta$  ligand is a dimer stabilized by hydrophobic interactions and further strengthened by an intersubunit disulfide bridge (Kirsch et al., 2000). The crystal

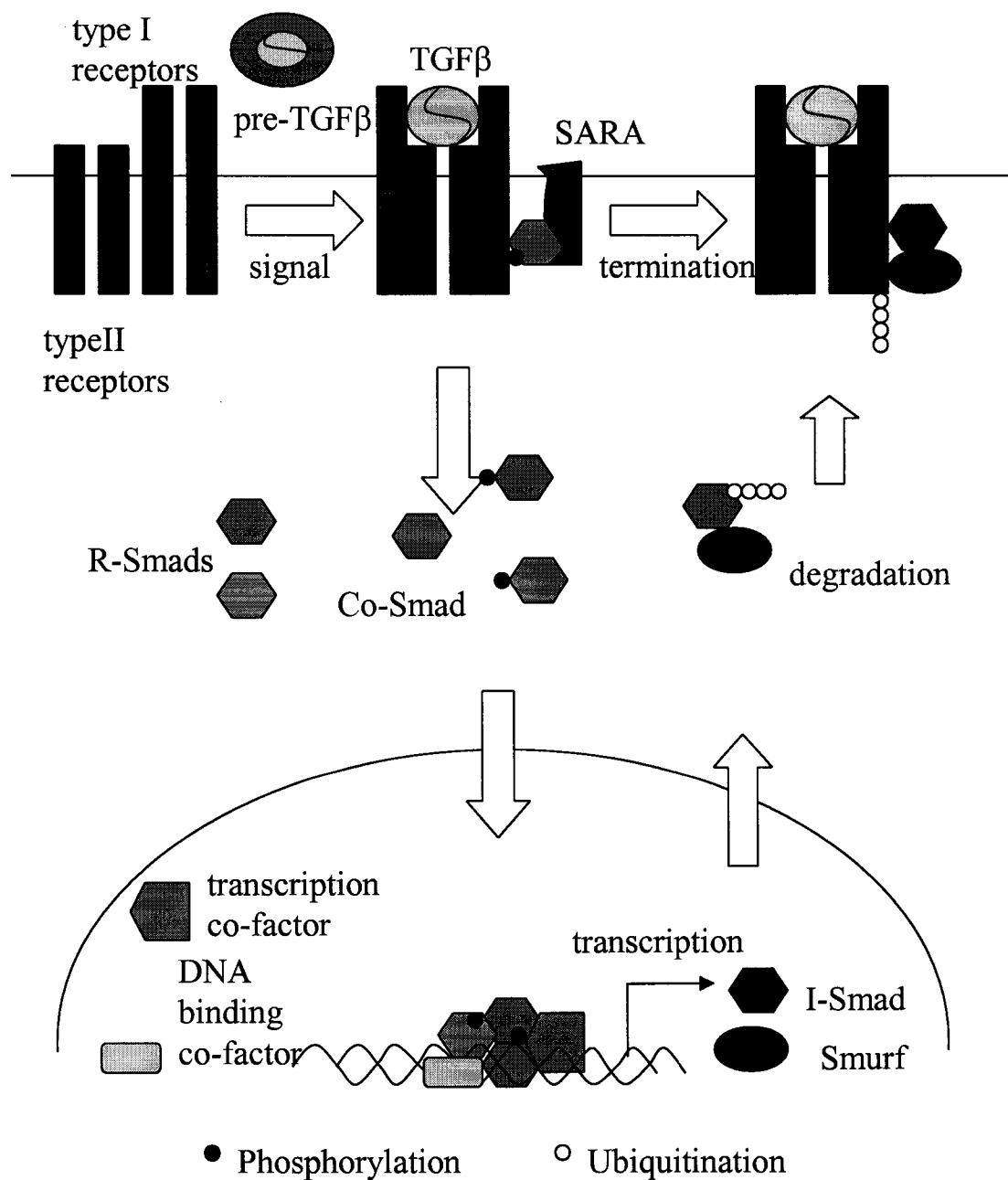


Figure 1.1 TGF  $\beta$  related signaling pathways

structure of the antagonist Noggin bound to BMP-7 shows that Noggin inhibits BMP signaling by blocking the molecular interfaces of the binding epitopes for both type I and type II receptors. The scaffold of Noggin contains a cystine (the oxidized form of cysteine) knot topology similar to that of BMPs. The homologous ligands and their antagonists are likely to have evolved from a common ancestral gene (Groppe et al., 2002).

*There are two types of receptors*

Both types of TGF- $\beta$  receptors are Serine/Threonine kinases. They have an N-terminal extracellular ligand binding domain, a single transmembrane region, and a C-terminal intracellular kinase domain. The type II receptors are thought to be constitutively active. The type I, but not type II receptors, contain a conserved SGSGSG sequence, called the GS box, adjacent to and N-terminal of the kinase domain. The GS domain is phosphorylated by the type II receptor during ligand binding. The ligand interacts with both types of receptors to form an active signaling complex (Massagué, 1998). After phosphorylation, the activated type I receptor is able to bind and phosphorylate R-Smads to conduct the signal downstream. Two distinct models of ligand receptor interaction exist, one exemplified by the BMP subfamily and the other represented by TGF- $\beta$ /Activin subfamily. BMP ligands exhibit a high affinity for the extracellular ligand binding domains of type I BMP receptors and a low affinity for type II receptors. The type I receptor-ligand complex has a higher binding affinity for the type II receptor.

These interactions are predominantly hydrophobic. A knob-and-pocket binding is essential for the interaction between the BMP ligands and the type I receptors (Kirsch et al., 2000). In contrast to the BMPs, TGF- $\beta$  and Activins have a high affinity for the type II receptors and do not interact with the isolated type I receptors (Massagué, 1998). Thus, the ligands bind tightly to the ectodomain of the type II receptors first (Figure 1.2) and this binding allows subsequent recruitment of the type I receptors forming a large complex.

The crystal structure of the ectodomain of the human TGF- $\beta$  type II receptor in complex with the ligand TGF- $\beta$ 3 reveals that the binding occurs at the far ends of the elongated ligand dimer (Hart et al., 2002). This interaction creates two symmetrically positioned concave surface patches, to which the ectodomain of the type I receptor could bind. Binding the ectodomains of two types of receptors, the dimeric ligand induces the conformational change for the intracellular domains of the receptors. The close proximity facilitates the phosphorylation and activation of the type I receptor. The type II receptor kinase phosphorylates multiple Serine/Threonine residues in the TTSGSGSG sequence. The immunophilin FKBP12 inhibits TGF- $\beta$  signaling by binding to unphosphorylated GS domains of the type I receptors (Wang et al., 1996; Huse et al., 1999). The interaction blocks the kinase catalytic center of the type I receptor. By using an in vitro ligation strategy, the type I receptor tetra-phosphorylated in the GS domain was generated. The synthesized protein binds efficiently to Smad2 in vitro and efficiently phosphorylates

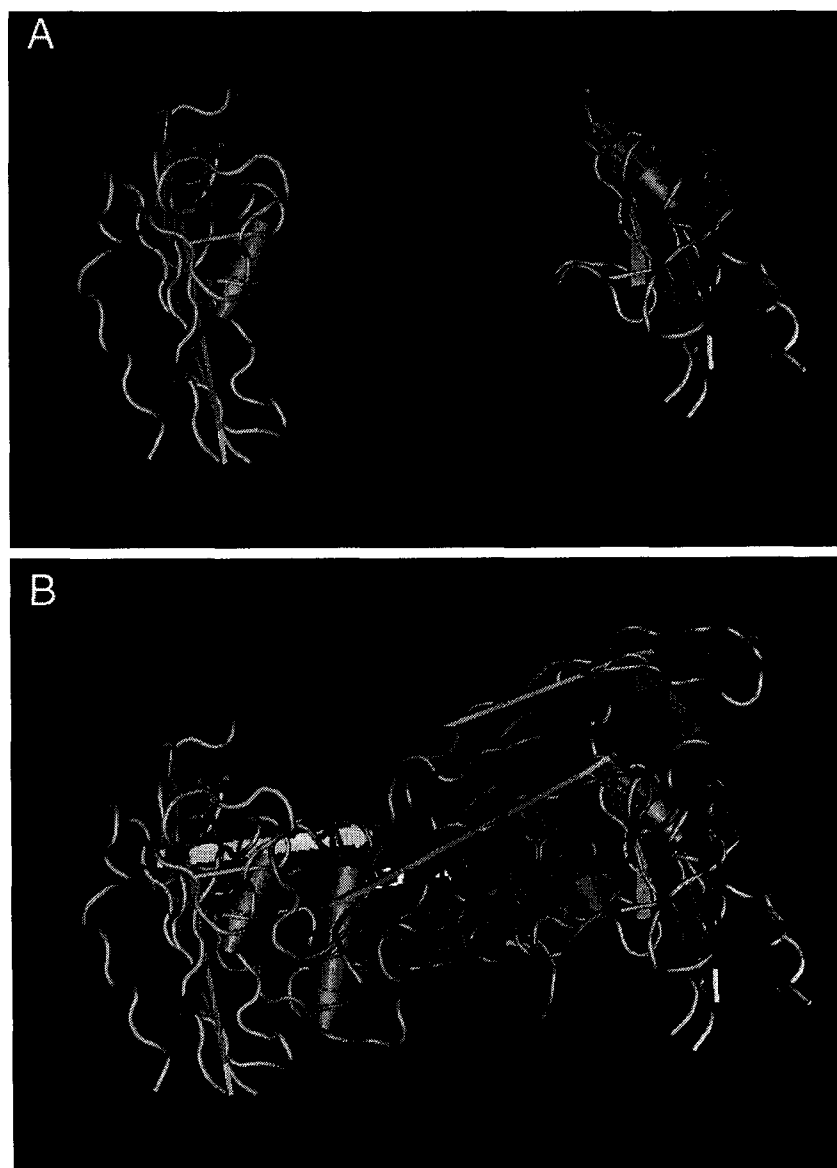


Figure 1.2 The X-ray structure of Type II TGF- $\beta$  receptor extracellular domain. (A) without binding ligand (B) binding with ligand (dimer).

C-terminal Serines of Smad2 (Huse et al., 2001). It cannot be recognized by FKBP12 in vitro. So, the phosphorylation of the GS domain induces the conformational switch from inhibitory protein binding to R-Smad binding.

*Smads are intracellular transducers*

The first intracellular mediator of TGF- $\beta$  signaling, MAD (mothers against dpp), was identified in *Drosophila* (Sekelsky et al., 1995). Soon after, its orthologs were found in *C. elegans* (Savage et al., 1996). The genes *sma-2*, *sma-3* and *sma-4* encode proteins that are required for body size control. Loss-of-function mutants have small (Sma) body size and the male tails are abnormal (Mab). Then, after the discovery of mammalian homologs, the proteins are named Smads (Sma and Mad). There are three classes of Smads. Only R-Smads are the targets of the receptor activation. Smad2 and Smad3 respond to TGF- $\beta$  subfamily signaling and Smad1, Smad5 and Smad8 are specific for signaling of BMP subfamily (Massagué and Wotton, 2000). The R-Smads and Co-Smad (only Smad4) have two conserved functional domains, the N-terminal MH1 (Mad Homolog 1) domain and the C-terminal MH2 (Mad Homolog 2) domain. The two domains are connected with a less conserved linker region (Massagué, 1998). The C-terminus of R-Smad, but not Co-Smad, has a characteristic SSXS motif that was proved to be the sites phosphorylated by the activated type I receptor (Abdollah et al., 1997; Souchelnytskyi et al., 1997). The MH1 domain exhibits sequence-specific DNA binding activity and negatively regulates MH2 domain by auto-inhibition (Hata et al., 1997). Most R-Smads have a nuclear

localization signal, a motif (KKLKK) with multiple positively charged residues (Xiao et al., 2001). The nuclear localization activity is absent in Co-Smad because of a glutamate in the motif. The nuclear accumulation of Co-Smad depends on its association with activated R-Smads. However, Co-Smad also undergoes nuclear shuttling on its own independent of TGF- $\beta$  signaling. There is a leucine-rich nuclear export signal (NES) in Smad4, which regulates the subcellular distribution of Smad4. The NES-dependent cytoplasmic localization of Smad4 is important to achieve optimal TGF- $\beta$  responsiveness in transcriptional activation (Watanabe et al., 2000).

Smads can be specifically immobilized near the plasma membrane by SARA (Smad anchor for receptor activation) through the interaction between the hydrophobic surface of Smad and a peptide sequence of SARA. SARA contains a phospholipid binding FYVE domain. The interaction increases the efficiency of Smad activation by the receptors (Wu et al., 2000). Comparing the MH2 domain of Smads reveals the presence of a much more positively charged surface patch on R-Smad than that of Co-Smad, located next to the L3 loop (the third loop in MH2 domain), which is essential to Smad-Smad complex formation (Hata et al., 1997; Shi et al., 1997) and determines specific interactions between SMAD proteins and TGF- $\beta$  receptors (Lo et al., 1998). This basic patch is postulated to be the binding site for the phosphorylated GS region of the type I receptor (Wu et al., 2000). A cluster of four residues in the L45 loop of the type I receptor kinase domain, and a matching set of two residues in the L3 loop of the Smad MH2 domain

establish the specificity of receptor-Smad interactions (Chen et al., 1998). However, it does not exclude that other sequence elements of R-Smad may also contribute in this interaction (Huse et al., 2001). The crystal structure of phosphorylated Smad2 MH2 domain suggests that the protein forms a homotrimer. The phosphorylated C-terminus pSer-X-pSer motif is nestled in the basic patch (Wu et al., 2001) (Figure 1.3). In the crystal of Co-Smad MH2 domain, the C-terminus is completely flexible and disordered (Shi et al., 1997; Qin et al., 1999). Many experiments demonstrate that the most C-terminal two serines are phosphorylated for Smad activation (Abdollah et al., 1997; Souchelnytskyi et al., 1997). Phosphorylation destabilizes the Smad interaction with the receptor and allows the Smad heteromeric complex to form. The pseudophosphorylated MH2 domain, using glutamate or aspartate to simulate the phosphorylated serines, exhibits a stronger tendency to form a homotrimer as well as heteromeric Smad complex with Smad4 (Chacko et al., 2001). The crystal structure of phosphorylated Smad2 MH2 domain also reveals the significant insight into the mechanism of heteromeric complex formation, especially with Smad4. In the structure, the pSer-X-pSer motif mainly interacts with four positively charged residues in the surface pocket. All of the four residues are conserved in all of the Smads including Smad4, strongly suggesting that R-Smad-Smad4 complexes are stabilized by such an interaction (Wu et al. 2001). So, the pSer-X-pSer motif interacting with the basic surface pocket plays the most important role in Smad function.

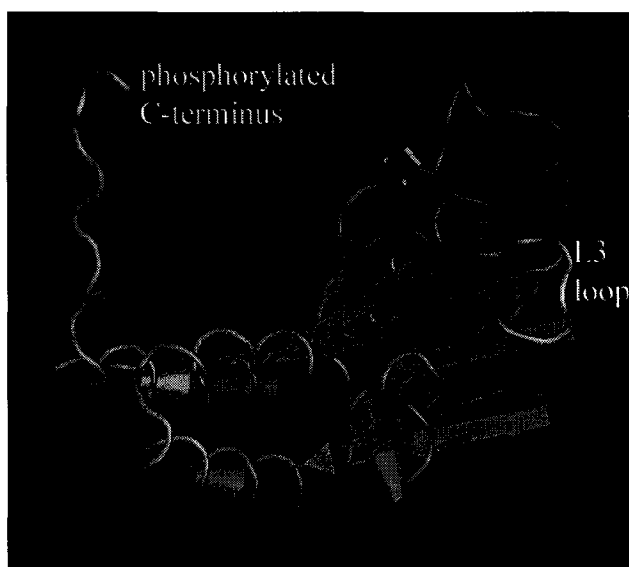


**Figure 1.3** The X-ray crystal structure of phosphorylated Smad2 MH2 domain. The protein forms trimer. The phosphorylated C-terminus interacts with L3 loop of neighbor subunit.

*The Smad linker region has regulation sites*

The Smad linker regions, although not highly conserved, have multiple regulation sites. The serine residues could be phosphorylated by other kinases (Massagué, 2003). It has been shown that Ras-mediated activation of Erk MAP kinase induces the phosphorylation of Smad1, Smad2 and Smad3 at MAP kinase sites in the linker region. This could affect the Smad nuclear import or export process. Such crosstalk results in the attenuation of Smad nuclear accumulation and Smad dependent TGF- $\beta$  signaling (Kretzschmar et al., 1999). Ras is also likely to induce Smad4 degradation. The mechanism is still unclear (Saha et al., 2001). Recently, it is found that phosphorylation of threonine 276 in Smad4 enhances its nuclear accumulation since this might block its nuclear exportation (Roelen et al., 2003). Similarly, calcium-calmodulin-dependent protein kinase II inhibits TGF- $\beta$  signaling through the phosphorylation of the Smad2 linker region using different phosphorylation sites (Wicks et al., 2000).

*The transcription co-factors*

Upon TGF- $\beta$  stimulation, there are hundreds of genes whose expression levels increase or decrease. The activation and repression of gene transcription is regulated by the same proteins, Smads. Target gene selection depends on the cell type specific transcription co-factors (Massagué and Wotton, 2000). The binding affinity and specificity is limited for individual Smads. Smads bind a simple tetranucleotide sequence known as the Smad Binding Element (SBE) (Shi et al., 1998). The transcriptional repression of c-myc is

dependent on direct Smad3 binding to a novel Smad binding site, termed a repressive Smad binding element (RSBE), within the TGF-beta inhibitory element (TIE) of the c-myc promoter (Frederick et al., 2004). Smads must therefore cooperate with each other and transcription co-factors, which include members of different families of DNA binding proteins, such as E-box (TFE3), homeobox (Mixer), forkhead (Fast-1), Jun/Fos, CREBP (reviewed by Massagué and Wotton 2000). The zinc finger transcription co-factor Schnurri was first found in *Drosophila*. It is required for *dpp*-dependent cell fates in the wing development (Torres-Vazquez et al., 2000). Interestingly, the promoter of Smad7 contains two copies of SBE and its expression is activated by both BMP and TGF- $\beta$  signaling without consideration of cell type. Most Smad responsive enhancers have only one copy of SBE.

#### *The regulation of Smad activity*

Ski and SnoN are negative regulators of Smad activity. Ski or SnoN represses Smad signaling by directly binding on Smads and disrupting Smad-Smad or Smad-co factor interaction (Qin et al., 2002; Wu et al., 2002). It has been shown that Ski inhibits Smad activity by binding the L3 loop region through a highly conserved interaction loop (I loop) (Qin et al., 2002; Wu et al., 2002). Smads also bind to the transcription corepressor TGIF (Wotton et al., 1999). Like Ski and SnoN, TGIF is thought to act as an inhibitor of TGF- $\beta$  dependent gene activation, not as a mediator of TGF- $\beta$  dependent gene repression (Shi and Massagué, 2003). There could be two different mechanisms to terminate Smad

signaling. First, dephosphorylation could occur by yet unknown phosphatases (Randall et al., 2002). The other, E3 ubiquitin ligases, Smurfs, could mediate Smad degradation. Smurf1 targets Smad1 and Smad5 for destruction in the cytoplasm (Zhu et al., 1999). However, activated Smad2 is ubiquitinated by Smurf2 in the nucleus (Lo and Massagué, 1999). Smurf1 and Smurf2 also mediate ubiquitination of activated TGF- $\beta$  receptors, leading to their degradation and shutting down the signaling (Ebisawa et al., 2001; Tajima et al., 2003). The inhibitory Smad, Smad7 plays an important role in this process. Smurf1 and Smurf2 form stable complexes with Smad7. The complex could bind activated receptors and both the receptor and Smad7 itself undergo degradation. However, a negative feedback loop activates the transcription of Smad7. Thus, the supply of Smad7 depends on TGF- $\beta$  signaling (Hua et al., 2000). The precise volume and timing of the signal are well controlled by this mechanism. The basally expressed Smad7 localizes to the nucleus until the signaling induces its migration into the cytoplasm. Thus, in signaling from the membrane to the nucleus, every step is precisely regulated and the activity, accumulation, and localization of each component is controlled by a well defined program to ensure the cells respond correctly and the whole body undergoes proposed development (reviewed by Shi and Massagué, 2003).

### **General Characteristics of *Caenorhabditis elegans***

*Caenorhabditis elegans* is a small, free-living soil nematode. It feeds primarily on

bacteria and reproduces with a life cycle of about 3 days under optimal conditions, 20°C, not crowded and plenty of food. There are hermaphrodites (Figure 1.4) and occasionally occurring males (1/500). A young adult is approximately 1.2mm long and 0.3mm wide. Hermaphrodites can reproduce by self-fertilization. They also could mate with males to keep genomic diversity. A single hermaphrodite lays about 400 eggs during adulthood. Juvenile worms hatch and develop through four larval stages, punctuated by molts. The worms become mature after the fourth molt and then live for an additional 15 days (Brenner 1974).

*C. elegans* is a simple organism, both anatomically and genetically. The body is rod-shaped and transparent. An adult hermaphrodite has only 959 somatic nuclei and an adult male has 1031 nuclei. The anatomy, structure and cell lineage have been well studied (Sulston et al., 1984). The haploid genome has six chromosomes (I-V, X). Each chromosome is between 10 and 20M bps and the genome size is about 100M bps. The whole genome has been sequenced and cloned into cosmids and YACs. This has resulted in a map that spans more than 99% of the genes, with only a few gaps at present (Coulson et al., 1995). The representation of the genome in YACs is more complete. This combined with their larger size (average insert size 250kb), allowed these clones to bridge many of the gaps between the cosmids (Coulson et al., 1988). Telomeres of *C. elegans* consist of the repeated hexamer sequence TTAGGC (Wicky et al., 1996). To get a look into the genes of *C. elegans*, projects have been undertaken to obtain end sequences from cDNA

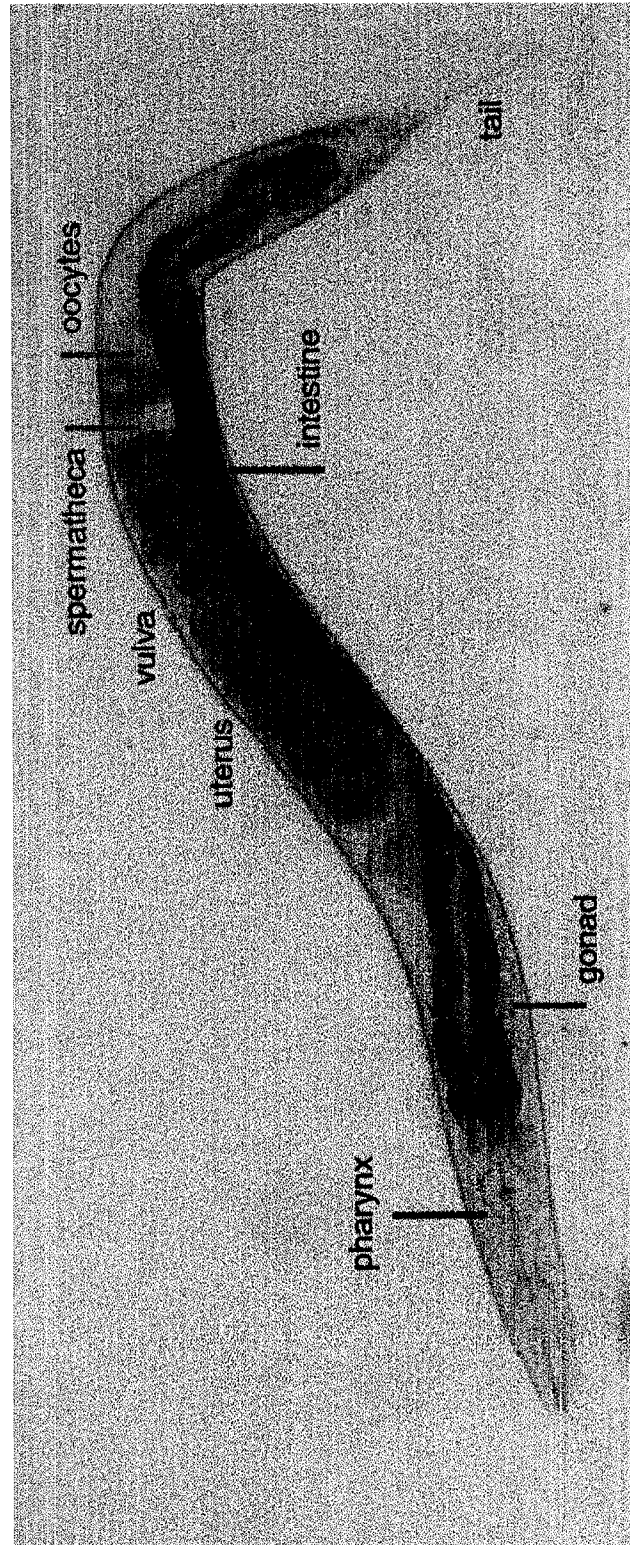


Figure 1.4 The body structure of a hermaphrodite of *C. elegans*.

clones. Such partial sequences or expressed sequence tags (ESTs) can provide insight into a useful fraction of genes. With such sequences, the predicted open reading frames and RNA splicing sites could be confirmed. Currently, most of the 19,000 predicted genes are partially reconfirmed by EST sequences (the *C. elegans* Sequencing Consortium, 1998). Although the genome of the worm is relatively small, many human genes have homologs in the worm genome. It is not surprising that many of the predicted genes fall into families such as G-protein coupled receptors, protein kinases, collagens, zinc finger transcription factors, homeobox proteins, and protein phosphatases (Green et al., 1993).

### *Mutagenesis*

In the *C. elegans* genome, there are transposons, e.g. Tc1 and Tc3. In some strain backgrounds, they could transpose along the genome. When they move into and out of a functional open reading frame, the gene's function could be disrupted by a small deletion or insertion. Some mutants have been generated by such mechanisms (Anderson, 1995). Most mutations are induced by mutagens. EMS is a potent and efficient mutagen for generating point mutations. The common effect is to cause G/C—A/T transitions, although it does produce small deletions, and other chromosomal rearrangements. A potential alternative to EMS is ENU, which has about the same efficiency as EMS but produces both transitions and transversions, as well as some small deletions and other chromosomal rearrangements (Anderson, 1995; De Stasio and Dorman, 2001). Exposure to formaldehyde, X ray-irradiation, UV irradiation, and  $\gamma$ -irradiation causes major

rearrangements such as translocations, large duplications, inversions and deficiencies, which are useful as balancers or for mapping genes to relatively large regions of the genome (Anderson, 1995). When heterologous DNA is injected into the gonad of hermaphrodites, the next generation could carry this DNA as an extrachromosomal array. When the transgenic worms are exposed to X-ray or  $\gamma$ -ray, the array could be integrated into their genomes. After the DNA is integrated, the expression of the genes on the DNA could be stabilized or increased. It is a useful technique to study the gene functions, especially for rescuing mutants or over-expressing genes of interest (Mello et al., 1991).

### *Life Cycle*

The process of fertilization in *C. elegans* occurs when an oocyte passes through the spermatheca, where the leading end of the oocyte appears to engulf a single sperm. The newly fertilized egg exits its prophase arrest state and completes meiosis I and II, extruding two polar bodies at the future anterior end of the embryo. At same time, a hard and impermeable eggshell forms around the embryo (Brenner, 1974). The zygote divides under a pre-determined pattern. During the process, some cells undergo programmed cell death, apoptosis, and the cell bodies are engulfed (Hodgkin, 1999). After several hours in the uterus, the egg is laid and embryogenesis continues. After hatching, worm development proceeds through four larval stages L1-L4. To go to the next stage, the worm molts; a new cuticle is generated and the old one is discarded. Under optimal conditions, *C. elegans* goes through all of the larval stages and becomes an adult. But,

without food, in high temperature, a crowded population, the *C. elegans* can select another developmental plan. The worm is arrested as a dauer larva, an alternative L3 stage. When the conditions get better, the dauer will recover and continue its development into L4 stage. Once a worm goes through L3 stage, it cannot go into the dauer stage (Patterson and Padgett, 2000).

### *The males of C. elegans*

Hermaphrodite self-fertilization makes it easy to maintain strains. To keep the genetic diversity, the male *C. elegans* is also required. But, the male occurs naturally at very low frequency. To generate more males for mating or analyzing, we use mutants with increased chromosomal non-disjunction, e.g. *him-5* (high-incidence of male) (Broverman and Meneely, 1994). The sex of *C. elegans* is determined by the ratio of autosome and X chromosome. A hermaphrodite diploid contains two copies of X chromosomes, but that of male has only one copy of X chromosome and two copies of each autosome. Him genes disrupt X chromosome segregation in meiosis, generating sperms or eggs without X chromosome and producing zygotes with XO genome (Meyer, 2000). The body development of the male is similar to that of hermaphrodite. Specific to males is a fan-shaped tail. An adult male contains nine sensory rays on each side of the tail (Figure 1.5). Each ray contains one sheath cell and two neuron cells. Rays are produced by a sex-specific lineage pattern from some of the lateral hypodermal cells known as seam cells (Sulston and White, 1980). In the center of the male tail, there are spicules. Males



Figure 1.5 The male tail sensory rays of wild type *him-5* and *sma-3(wk30)* mutant. In *him-5*, the arrow points at the healthy spicules. In *sma-3(wk30)*, the arrow points at the crumple spicules and the arrow head indicates the ray 6-7 fusion.

inject sperm into the hermaphrodite vulva and the sperm from males are used preferentially over the hermaphrodite sperm in the spermatheca. The adult arrangement of rays is determined by the placement of ray cells at specific sites in the hypodermis at the L4 stage. Placement of ray cells at specific sites results from the generation of neurons and sheath cells in the hypodermis near to their final positions, and the subsequent refinement of these positions by an active mechanism involving specific cellular associations. A pattern formation mechanism in the hypodermis guides the specification of morphogenetic differences between the rays necessary for correct organelle assembly at specific positions. Two genes of the *C. elegans* HOM-C/Hox gene complex play a role in the pattern formation mechanism. Increasing or decreasing the gene dosage of *mab-5*, an Antennapedia homolog, and *egl-5*, an Abdominal B homolog, results in displacement and fusion of specific rays. These changes are interpreted as anterior or posterior transformations in ray identities. The *C. elegans* HOM-C/Hox gene *mab-5* is required for generation of rays from the descendants of seam cells V5 (ray 1) and V6 (rays 2-6), but not T (ray 7-9) (Kenyon 1986) (Figure 1.6). In *mab-5* mutants, the most anterior ray was generated by V6.pppap, which normally gives rise to ray 4. In the *mab-5(bx54)* mutant, the ray generated by V6.pppap has moved to a position adjacent to the cloaca and extended to the margin of the fan, i.e. it has assumed the morphology of ray 3. Fusion with ray 3 suggests that the fourth ray now not only extends to the fan margin at a more anterior position, but also expresses some cell recognition molecules in common with ray 3. When *mab-5* function decreases, several characteristics of the fourth

ray undergo a posterior-to-anterior transformation (Chow and Emmons, 1994). Thus decreased activity of *mab-5* induces the transformation of the identity of ray 4 to that of ray 3. Interestingly, in a gain of function allele, *mab-5(e1751)* (Hedgecock et al., 1987), ray 1 was located more posteriorly, opened on the ventral surface of the fan or at the fan margin and fused with ray 2. Ray 3 was located more posteriorly, opened on the ventral surface of the fan with ray 4. In homozygous *egl-5(lf)* mutants, ray 6 is lost because the cell V6.ppppa is transformed into a hypodermal cell. The *egl-5* gene plays a role to specify expression of the ray sublineage by a single branch of the V6 lineage (Chisholm, 1991). The identities of ray 4 and ray 6 are sensitive to the ratio between *mab-5(+)* and *egl-5(+)*. As the ratio decreases, the frequency of ray 3 and ray 4 fusion increases. On the contrary, as the ratio increases, the frequency of the ray 4 and ray 6 fusion increases. There are communications between the seam cells to polarize the cell divisions and determine the cell fates (Figure 1.6). The *lin-44* (Wnt) is generated by distal cell and controls the polarity of asymmetric division of T cell (Herman and Horvitz, 1994).

### *The hypodermis and cuticle*

The structure of a worm includes a pharynx in the head. In the body cavity, intestine and gonad are the largest organs taking most of the space. Body movement is controlled by the body wall muscles, which are covered by hypodermis. Muscle and hypodermis form the outer tube of the body. Most of the body surface is covered by one hypodermal cell, hyp7 (Figure 1.7). Hyp7 is a huge syncytium and has 139 nuclei after mid-L3 stage. Even

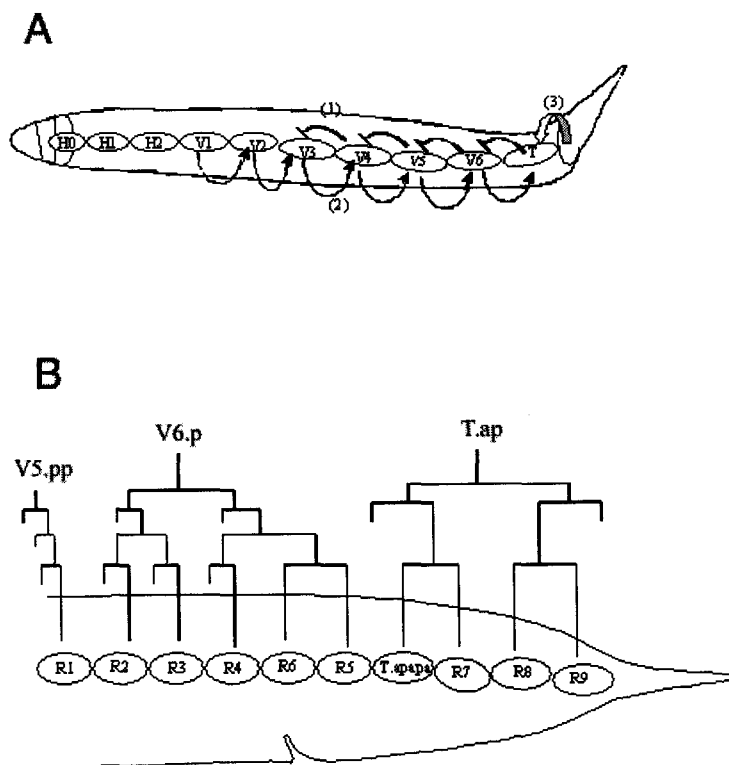


**Figure 1.6** The cell lineage of male tail sensory rays. (A) The effects of signals on lateral epidermal seam cells: (1) Seam cells inhibit their anterior neighbors from generating rays; (2) Seam cells induce stem cell division and polarize the asymmetric divisions of their neighbors; (3) LIN-44(Wnt), expressed by distal cells, orients division polarity in the T lineage. (B) The cell lineage to generate male tail sensory rays. (modified from book *C. elegans II*)

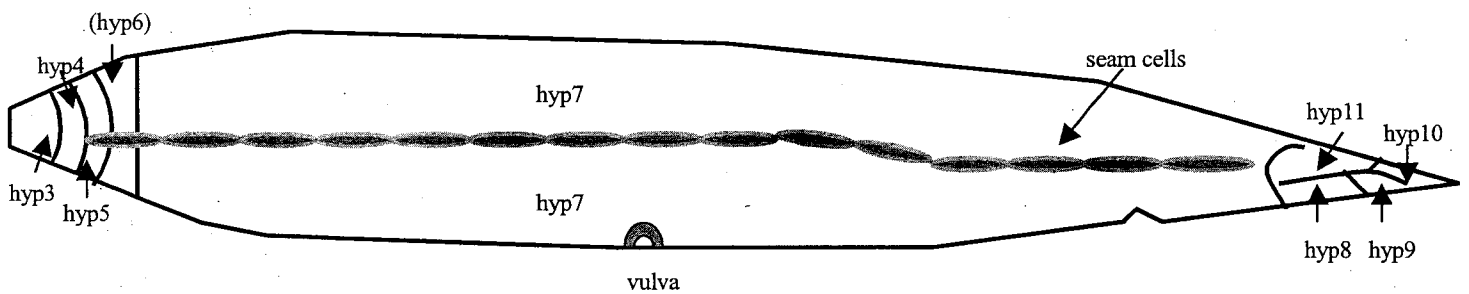


Figure 1.7 The structure of hypodermis in wild type hermaphrodites. The hyp7 takes the most of the surface. The lateral hypodermis, seam cells, connect with each other. (modified from wormatlas.org)

after that, the nuclei of hyp7 still undergo DNA duplication without nuclear division (Hedgecock and White, 1985). Hyp1-hyp5 cells are in the head region and hyp8-hyp12 cover the surface of the tail. The lateral hypodermal cells are called seam cells. During each larval stage, each seam cell divides, the anterior daughter cell fuses into hyp7 and the posterior daughter cell keeps the seam cell identity. Seam cell proliferation is to supply the hypodermis with additional genomes for the purpose of growth (Knight et al., 2002). The exterior of the animal is covered by cuticle. The cuticle is the animal's exoskeleton and is important for maintenance of morphology, protection from external environment. The cuticle has both surface specializations and internal layers that can differ at different developmental stages. Collagen proteins have similar domain structures and several conserved motifs (Kramer, 1994a; Johnstone, 2000). There is a long N-terminal non-Gly-X-Y domain of variable length, a central Gly-X-Y repeat domain, and a variable length C-terminal non-Gly-X-Y domain. Collagen proteins have a high proportion of cysteines and tyrosines, which form intra- and inter-molecular bridges. Thus, the cuticle is a network and has extensive effects on the body growth. The cysteine intervals are likely to be important for directing the formation of disulfide bonds between appropriate molecules in the cuticle. Synthesis of cuticle proteins occurs at high rates during molts and at lower rates between molts (Cox, 1990). Some genes that are involved in determination of overall morphology have been shown to encode cuticle collagens, such as *sqt-1*, *dpy-7*, *rol-6* (Kramer, 1994b). Mutations in these cuticle collagens can generate morphological phenotypes like roller and dumpy. Recently, a new collagen gene,

*lon-3*, has been cloned. The loss of function mutant has a long phenotype (Flemming et al., 2003). This discovery indicates that the small/long phenotypes in the mutants of Sma/Mab pathway (see below) might result from the increased or decreased expression of some collagen genes.

## **TGF- $\beta$ signaling in *Caenorhabditis elegans***

### *Overview*

There are at least five predicted TGF- $\beta$  homologs in the genome of *C. elegans*. Only three of them have been analyzed mutationally, *dbl-1*, *daf-7* and *unc-129*. The *tig-2* gene has high homology to bone morphogenetic protein. But its function is not clear yet. The open reading frame, Y46E12BL.1, has limited similarity to TGF- $\beta$  family ligands. No experiment has been done to characterize this putative TGF- $\beta$  ligand. The intracellular components of the TGF- $\beta$  related pathways are Smad genes including *daf-8*, *daf-14*, *daf-3* (Dauer pathway) and *sma-2*, *sma-3*, *sma-4* (Sma/Mab pathway) (Figure 1.8) (Patterson and Padgett, 2000). The gene *tag-68* and ORF R05D11.1 are also Smad related genes. But their functions are not clear. In sequence alignment, R05D11.1 is mostly related to *sma-2* or human gene Smad5 and its C-terminal residues SSRS belong to R-Smad motif SSXS. But the residue arginine is positive charged and the side chain might have effect on the structure of Smad complex. The protein sequence of *tag-68* is closely related to I-Smad, Smad6 (Newfeld et al, 1999). The strain *tag-68(gk185)* is mild uncoordinated

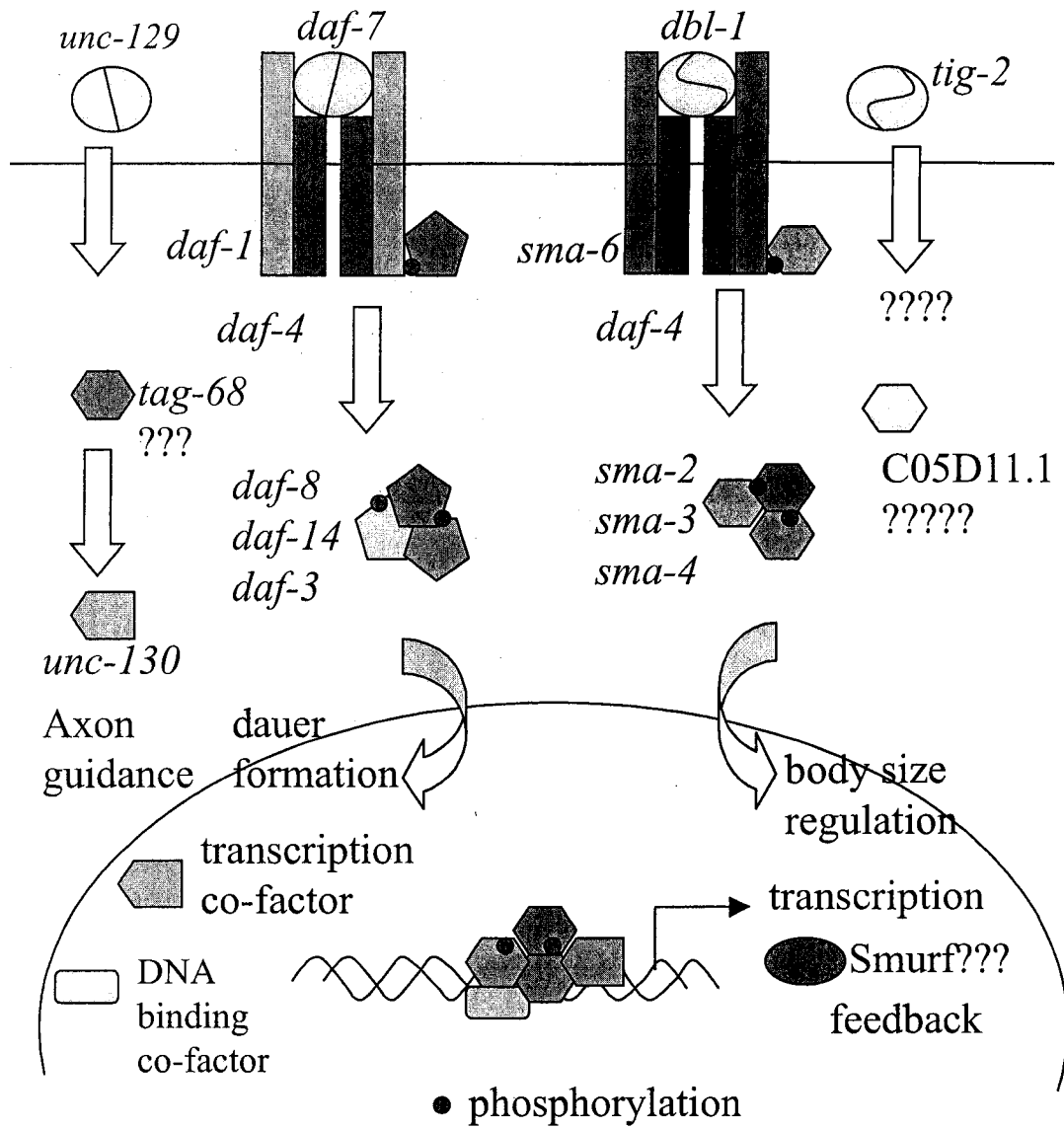


Figure 1.8 TGFβ related signaling pathways in *C. elegans*

(wormbase). Thus, *tag-68* might be a downstream of *unc-129*.

### *unc-129*

The *unc-129* gene is required for guidance of pioneer motoraxons along the dorsoventral axis of *Caenorhabditis elegans* (Colavita et al., 1998). The mutants also have gonad distal tip cell (DTC) migration defects. *unc-129* is expressed in dorsal, but not ventral, rows of body wall muscles. Ectopic expression of UNC-129 from ventral body wall muscle disrupts growth cone and cell migrations that normally occur along the dorsoventral axis. The graded expression of UNC-129 in dorsal body muscles depends on *unc-130* gene, which encodes a forkhead transcription factor (Nash et al., 2000). The cell-specific effects of *unc-130* on ventral, but not dorsal, body muscle expression of *unc-129* accounts for the D/V polarity information required for UNC-129-mediated guidance.

### *Dauer pathway*

Another TGF- $\beta$  ligand, *daf-7*, is required for the regulation of dauer formation. The loss-of-function mutants have a dauer constitutive phenotype and egg-laying defects (Patterson and Padgett, 2000). *daf-7::GFP* fusions are expressed specifically in ASI, a sensory neuron in the cluster near the pharynx, and that expression is regulated by dauer-inducing sensory stimuli. The receptors are encoded by *daf-4* (type II) and *daf-1* (type I) genes. DAF-1 is presumably activated by DAF-4 and then phosphorylates the

R-Smads, DAF-8 and DAF-14. DAF-14 Smad has a highly unusual structure completely lacking the N-terminal MH1 domain found in other Smad proteins. *daf-14* genetically interacts with *daf-8*, and the interaction suggests partial functional redundancy between these two Smad proteins. The *daf-3* gene encodes a Co-Smad. The null mutants of *daf-3* have a dauer-defective phenotype and they can suppress the dauer constitutive phenotype of the loss-of-function of upstream signal components, *daf-7*, *daf-1*, *daf-4*, *daf-8* and *daf-14* (Patterson et al., 1997, Patterson and Padgett, 2000). Thus, the signal from *daf-7* antagonizes *daf-3* activity. DAF-5 is a member of the Sno/Ski superfamily that binds to DAF-3 Co-Smad, suggesting that DAF-5, like Ski/SnoN, is a regulator of transcription in a TGF- $\beta$  superfamily signaling pathway (da Graca et al., 2004). *daf-5* mutants, like *daf-3* null alleles, are dauer-defective. DAF-5 is an unconventional Sno/Ski protein, because DAF-5 acts as a co-factor, rather than an antagonist, of a Smad protein DAF-3. Without upstream signaling, DAF-5 and DAF-3 cooperate in the nucleus to promote target gene expression (da Graca et al., 2004). An upstream regulator of this pathway, KIN-8, is highly homologous to human ROR-1 and ROR-2 receptor tyrosine kinases. A promoter *kin-8::gfp* fusion gene was expressed in ASI neuron and many other neurons as well as in pharyngeal and head muscles. The *kin-8* deletion mutant was isolated and showed constitutive dauer larva formation phenotype. In the mutant, expression of *daf-7::gfp* in ASI was greatly reduced. The Daf-c phenotype was suppressed by *daf-7* cDNA expression or a *daf-3* null mutation (Koga et al., 1999). A human BMP receptor-associated molecule BRAM1 in *Caenorhabditis elegans*, BRA-1, has been

found to bind DAF-1, the type I receptor, through the conserved C-terminal region. A loss-of-function mutation in *bra-1* exhibits robust suppression of the Daf-c phenotype caused by the DAF-7 pathway mutations. Thus, BRA-1 negatively regulates DAF-7 TGF- $\beta$  signaling (Morita et al., 2001).

#### *Sma/Mab pathway*

The Sma/Mab TGF- $\beta$  pathway regulates body size and male tail development. The ligand, *dbl-1*, is expressed primarily in neurons. Loss-of-function mutations in *dbl-1* cause markedly reduced body size and defective male copulatory structures. Conversely, *dbl-1* overexpression causes markedly increased body size and partly complementary male tail phenotypes, indicating that DBL-1 acts as a dose-dependent regulator of these processes (Suzuki et al., 1999). Interestingly, the signaling pathway also uses *daf-4* as the type II receptor, sharing with *daf-7* dauer pathway. The type I receptor *sma-6* is only used in the Sma/Mab pathway. Mutations in *sma-6* generate the reduced body size (Sma) and abnormal male tail (Mab) phenotypes identical to those observed in *daf-4*, but not the dauer constitutive or egg laying defective phenotypes (Krishna et al., 1999). *sma-6* is highly expressed in the hypodermis. Hypodermal expression of *sma-6* is necessary and sufficient for the growth and maintenance of body length (Yoshida et al., 2001).

The intracellular transducers, *sma-2*, *sma-3* and *sma-4* are the Smad homologs. The null mutants of any of the three genes have small body size (Figure 1.9) and male tails have

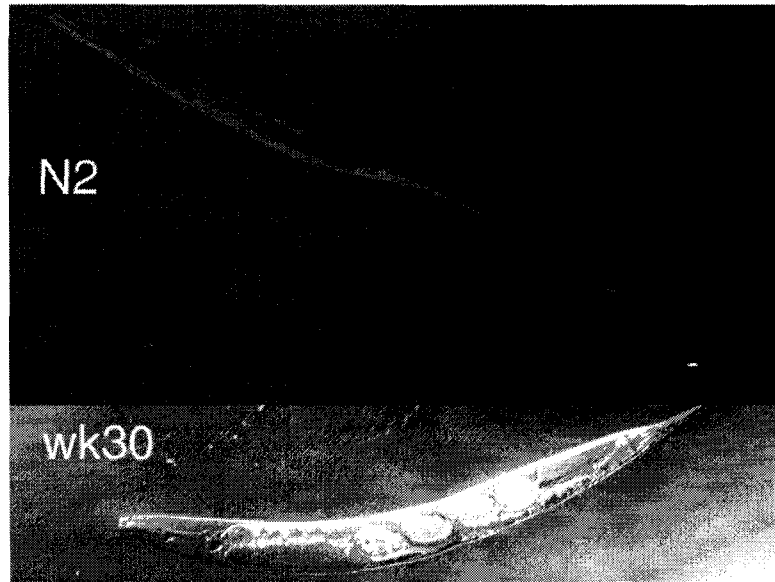


Figure 1.9 The mutants of Sma/Mab pathway are smaller than wild type in body size. N2, wild type; *wk30*, a null mutant of *sma-3*.

sensory ray fusions and the spicules are crumpled at a high percentage (Savage et al., 1996; Savage-Dunn et al., 2000). This phenotype is indistinguishable from that of the *sma-6* null mutants (Figure 1.5). *sma-2* and *sma-3* encode Receptor-regulated Smads and *sma-4* belongs to Common Smad family. A zinc finger transcription co-factor, *sma-9*, homologous to *Drosophila* Schnurri has been cloned by our lab (Liang et al., 2003). The null mutants have small body size, but the defects in the male tail are not as severe as those of *sma-6* mutants. It has been shown that the activity of *sma-9* in body size is only required in the larval stages. After L4 stage, *sma-9* null mutants grow as fast as wild type (Liang et al., 2003). This suggests that the cooperation between Smads and *sma-9* is limited in the larval stage if there is. There should be another transcription co-factor for body size control in adult. Using loss-of-function (small) and gain-of-function (long) *dbl-1* mutants, many small and long mutants have been isolated by genetic screens (Savage-Dunn et al., 2003). The small mutants mainly have defects in body size and the male tail defects are not as severe as *sma-6* mutants. The *lon-1* gene encodes a PR related protein, a putative Smad target gene. The loss-of-function mutants have a long phenotype that is thought to result from an increase in hypodermal ploidy (Morita et al., 2002). It is proved that the hypodermal expression of *lon-1* is sufficient to rescue the long phenotype (Maduzia et al., 2002). Finally, the *lon-3* gene has been shown to encode a putative cuticle collagen that is expressed in hypodermal cells. Morphometric analyses indicate that the *lon-3* loss-of-function phenotype resembles that caused by overexpression of *dbl-1* (Nyström et al., 2003).

## Previous experiments characterizing *sma-3* gene

### *SMA-3 Smad has critical functions in Sma/Mab signaling*

The *sma-3* gene was first characterized molecularly eight years ago. It encodes a Smad protein and cooperates with *sma-2* and *sma-4* to regulate body size and male tail morphogenesis (Savage et al., 1996). The sequence shows that the protein has MH1 and MH2 domain. There is a nucleus localization signal motif, KKLKK in MH1 domain and the C-terminal sequence SMT is the putative phosphorylation site (Figure 1.10). Savage-Dunn (et al., 2000) analyzed the function of the *sma-3* Smad gene. Null mutations in *sma-3* are at least as severe as null mutations of the ligand and type I receptor genes, *dbl-1* and *sma-6*, indicating that the other Smads do not function in the absence of SMA-3. Null mutations in *sma-3* do not cause defects in egg laying or in dauer formation, indicating no overlapping function with the dauer pathway. Using a promoter *sma-3::lacZ* fusion construct, it was shown that the *sma-3* gene is widely expressed at all developmental stages in hermaphrodites and males. The molecular lesions associated with eight *sma-3* alleles of varying severity were determined. The missense mutations cluster in the L3 loop important for Smad function. The differences among the male tail defects suggest that the MH1 domain is not as important as the MH2 domain in male tail morphogenesis.

01 MNGLLHMHGPAVKKLLGWKIGEDEEKWCEKAVEALVKLLKKKNNGCGTLE  
51 DLECVLANPC**T**NSRCITIAKSLDGRLQVSHKKGLPHVIYCRVWRWPDISS  
101 PHELRSIDTCSYPYESSSKTMYICINPYHYQRLSRPQGLNSSMPSPQPIS  
151 SPNTIWQSSGSSTASCASSPSPSVFSEGGGEVQVHQRPPPPFRHPKSWAQI  
201 TYFELNSRVGEVFKLVNLSITVDGYTNPSNSNTRICLGQLTNVNRNGTIE  
251 NTRMHIGKGIQLDNKEDQMIMITNNSDMPVVFVQSKNTNLMMNMPLVKVC  
301 RIPPHSQLCVFEFNLFQMLEQSCNDS DGLNELSKHCFIRISFVKG**WGED**  
351 YPRQDVTST**PC**WLELRLNVPLAYIDQKMKQTPRTNLMEPNSMT

Figure 1.10 The SMA-3 protein sequence. The MH1, MH2 domains and C-terminal phosphorylation sites are underlined. The sites for missense mutation are in bold.

*Cell and organ size measurements in TGF $\beta$  Sma/Mab mutants*

TGF $\beta$  Sma/Mab mutants are the same size as wild-type animals at hatching, but grow more slowly during larval stages and are about 60% of the length of wild type in adulthood (Savage-Dunn et al., 2000), as well as being thinner. This reduction in body size could in principle be due either to reduced cell number or to reduced cell size, or both. No significant change in the number of nuclei in these mutants compared with N2 has been found (Suzuki et al., 1999; Flemming et al., 2000; Nagamatsu and Ohshima, 2004). These results indicate that the small body size phenotype must be due to a reduction in size of some or all of the cells in the animal.

Rafal Tokarz in our lab measured two accessible tissues to determine the extent of cell size reduction in small animals: the seam cells and the pharynx. He took advantage of the *ajm-1::gfp* marker (Mohler et al., 1998), which localizes to the adherens junctions surrounding the seam cells. The seam cell marker was crossed into *sma* mutant backgrounds and fluorescence was observed in the L3 stage. By this stage, *sma* mutant worm length is significantly different from wild type (Savage-Dunn et al., 2000); at later stages the seam cells will fuse with each other and cannot be measured individually. The seam cells in mutant animals are shorter in length than the seam cells of wild-type animals (Wang et al., 2002). In Sma/Mab mutants, the difference in seam cell length is proportional to the difference in overall body length. It was possible that this reduction in seam cell length was offset by an increase in width, so seam cell area was also measured.

Again, he found that seam cell area was reduced in Sma/Mab mutants (Wang et al., 2002). For a negative control, *sma-1* mutants were used. *sma-1* mutants are also small, but they follow a different growth pattern than the TGF $\beta$  Sma/Mab mutants (Savage-Dunn et al., 2000). At the L3 stage, *sma-1* body length is less than the Sma/Mab pathway mutants, but the mean length and area of the seam cells is larger (Wang et al., 2002). The length of the pharynx was also measured in the same worms. Interestingly, in the TGF $\beta$  mutants the pharynx is smaller than in N2, but only slightly so, with the ratios varying between 0.93 and 0.96 of wild type. In *sma-1*, the pharynx is 33% smaller than wild type. Thus, in the small mutants examined, different tissues are reduced in size by different proportions. In the TGF $\beta$  Sma/Mab mutants, but not in *sma-1* animals, the seam cell size is proportional to the body size.

#### *Mosaic analysis of sma-3*

Rafal in our lab also addressed the function of *sma-3* by mosaic analysis. A *sma-3* rescuing genomic fragment was injected with a ubiquitously expressed nuclear localized SUR-5::GFP marker (Yochem et al., 1998) into *sma-3(wk30)* mutants. Animals inheriting the array are wild type in body length, while those without the array are small. Animals were screened for rare loss of the extrachromosomal array in somatic tissues (Wang et al., 2002). A tissue was scored as positive if any cells of the tissue expressed the construct. It was shown that animals with loss of the array in the pharynx or the intestine have wild-type body size (Wang et al., 2002). Rare small worms were also isolated with

expression in the intestine and/or the pharynx. Therefore, expression of SMA-3 in the intestine and the pharynx is neither necessary nor sufficient for regulation of body size. However, expression of *sma-3* in the hypodermis appears to be critical for restoration of wild-type body size. No mosaic worm of wild-type length without *sma-3* expression in the hypodermis were observed. Conversely, no small worm with hypodermal expression was identified.

phenotype	N worms	Intestine	pharynx	Nerve cord	Nerve ring	Body muscle	Hypodermis
Wild type	4	-	+	+	+	+	+
	1	-	-	+	+	-	+
	2	-	-	-	-	+	+
	1	-	-	+	-	+	+
small	1	+	+	-	-	-	-
	1	-	+	-	-	-	-
	1	+	-	-	-	-	-
	1	+	-	-	-	-	-

Table 1.1 Mosaic analysis of *sma-3*. “+” indicates GFP expression in some cells of the tissue. “-” indicates no GFP expression in any cells of the tissue.

**NOTE**

Thanks Rafal Tokarz for his assistance during my beginning period in the lab. Thanks Chow KL, a former member of Emmons lab, for his information about male tail sensory rays.

## Chapter II

### The expression of TGF- $\beta$ signal transducers in the hypodermis regulates body size in *C. elegans*

#### Abstract

In *C. elegans*, a TGF  $\beta$ -related signaling pathway regulates body size. Loss of function of the signaling ligand (*dbl-1*), receptors (*daf-4* and *sma-6*) or Smads (*sma-2*, *sma-3* and *sma-4*) results in viable, but smaller animals because of a reduction in postembryonic growth. We have investigated the tissue specificity of this pathway in body size regulation. We show that SMA-3 Smad is expressed in pharynx, intestine and hypodermis, as has been previously reported for the type I receptor SMA-6. Furthermore, we find that SMA-3::GFP is nuclear localized in all of these tissues, and that nuclear localization is enhanced by SMA-6 activity. Interestingly, SMA-3 protein accumulation is negatively regulated by the level of Sma/Mab pathway activity. Using directed expression of SMA-3, we find that SMA-3 activity in the hypodermis is necessary and sufficient for normal body size. As *dbl-1* is expressed primarily in the nervous system, these results suggest a model in which postembryonic growth of hypodermal cells is regulated by TGF $\beta$ -related signaling from the nervous system to the hypodermis.

## INTRODUCTION

The TGF $\beta$  superfamily, which includes TGF $\beta$ , BMPs and activins, regulates cell growth and differentiation in both vertebrates and invertebrates (reviewed by Massagué, 1998; Raftery and Sutherland, 1999; Hill, 2001; Savage-Dunn, 2001). Signaling initiates when the ligand binds to the type II and type I receptors, both of which are Ser/Thr kinases. During this process, the type II receptor phosphorylates the type I receptor. The activated type I receptor phosphorylates the cytoplasmic Smads. Upon phosphorylation, Smads form a heteromeric complex, translocate into the nucleus and regulate the transcription of downstream genes (Heldin et al., 1997; Wrana and Attisano, 2000; Massagué and Wotton, 2000; Patterson and Padgett, 2000). The Smads are thus the critical intracellular signal transducers for TGF $\beta$ -related signaling.

Smads are separated into three categories, R-Smad, Co-Smad and anti-Smad. R-Smad activity is regulated by the receptors by phosphorylation. Co-Smads are not activated by phosphorylation, but cooperate with R-Smads to form a functional complex. The anti-Smads negatively regulate the TGF $\beta$  pathway, and their expression is dependent upon TGF $\beta$  signaling (Massagué and Chen, 2000). The structure of a Smad comprises conserved MH1 and MH2 domains, separated by a variable linker region. The MH1 domain has the DNA-binding region and nuclear localization sequence (Shi et al., 1998; Xiao et al., 2000). The MH2 domain contains an SSXS motif that is phosphorylated by

type I receptor on the last two serines (Souchelnytskyi et al., 1997). Once phosphorylated, the activated R-Smad forms a heterotrimer with the Co-Smad (Shi et al., 1997; Wu et al., 2001; Qin et al., 1999; Qin et al., 2001).

In the nematode *Caenorhabditis elegans*, we are interested in the TGF $\beta$ -related pathways, the Dauer pathway and the Sma/Mab (small/male tail abnormal) pathway (Patterson and Padgett, 2000; Savage-Dunn, 2001). The Dauer pathway controls entry into and exit from the dauer stage, an L3 larval stage specialized for harsh environmental conditions. Entry into the dauer stage is regulated by environmental cues, such as the availability of food, the population density and temperature. The Dauer pathway is composed of the ligand (*daf-7*), the type II receptor (*daf-4*), the type I receptor (*daf-1*) and the Smads (*daf-8*, *daf-14* and *daf-3*). Loss of function of any factor except *daf-3* results in the dauer constitutive phenotype, in which worms enter dauer even under favorable conditions (Estevez et al., 1993; Ren et al., 1998; Gunther et al., 2000; Inoue and Thomas, 2000). However, the absence of *daf-3* activity gives a dauer defective phenotype, in which worms do not form dauers even under hazard conditions (Patterson et al., 1997).

The ligand for the Sma/Mab pathway, *dbl-1*, is related to *Drosophila dpp* and vertebrate Bone Morphogenesis Proteins (Suzuki et al., 1999; Morita et al., 1999). It functions with the type II receptor *daf-4* and the type I receptor *sma-6* (Estevez et al., 1993; Krishna et al., 1999). The Dauer and Sma/Mab pathways use a common type II receptor, *daf-4*. In the Sma/Mab pathway, *daf-4* and *sma-6* receptors activate the R-Smads, *sma-2* and

*sma-3*. These are thought to form complexes with the Co-Smad, *sma-4*, to propagate the signal into the nucleus (Savage et al., 1996; Savage-Dunn et al., 2000). Loss-of-function mutations in any of the Sma/Mab pathway components result in small body size. In addition, defects of the male tails are seen, including sensory ray fusions and crumpled spicules. Both of the R-Smad proteins, SMA-2 and SMA-3, are crucial for pathway function, suggesting the formation of a heteromeric complex containing two different R-Smad subunits (Savage-Dunn et al., 2000).

The underlying cause of the small body size phenotype is still poorly understood. In theory, the final size of an organ or organism can be determined by the regulation of cell number, cell size, or both. Cell number may be controlled by the regulation of cell division or of cell death. Cell size is usually coordinated with the cell cycle, and often correlates with ploidy (Galitski et al., 1999). Mutants of the Sma/Mab pathway provide an opportunity to study the molecular regulation of body size in a viable animal model. Published reports (Suzuki et al., 1999; Flemming et al., 2000; Nagamatsu and Ohshima, 2004) indicate that these small mutants contain normal numbers of cells. Therefore, some or all cell sizes must be reduced. Measurements of cell and tissue sizes have shown that the reductions in seam cell and *hyp7* sizes are most closely proportional to the change in body size (Wang et al., 2002; Nagamatsu and Ohshima, 2004).

We have addressed the cell and tissue specificity of the Sma/Mab pathway regulation of body size. We characterized the expression and subcellular localization of SMA-3 using

SMA-3::GFP translational fusions. We find that *sma-3* is expressed in the pharynx, intestine and hypodermis. We used directed expression of *sma-3* to determine where it functions to regulate body size. These experiments indicate that the hypodermis is the crucial tissue involved in body size regulation, in agreement with mosaic analysis of *sma-3* (Wang et al., 2002) and directed expression studies of *sma-6* (Yoshida et al., 2001).

## MATERIALS AND METHODS

### Worm strains

Wild type was *C. elegans* strain N2, from which all of the mutants were isolated. Unless otherwise noted, strains were grown at 20°C. All strains used in experiments were cultured as described previously (Brenner, 1974). The following mutations were used: LGII, *sma-6(wk7)*; LGIII, *sma-2(e502)*, *sma-3(wk30)*, *sma-4(e729)*; LGV, *him-5(e1490)*.

Small mutants chosen were either known null mutants or the most severe mutants available. *sma-6(wk7)* has an early stop codon in the extracellular region that results in a null mutation (Krishna et al., 1999). An arginine in the beginning of the linker region in SMA-3 mutates into a stop codon, suggesting *sma-3(wk30)* is a strong allele (Savage-Dunn et al., 2000). In *sma-2(e502)*, the mutation G372D disrupts a critical amino acid in the *sma-2* MH2 domain (Savage et al., 1996). The DNA sequence of the canonical

*sma-4(e729)* allele had not previously been determined. We therefore sequenced the *sma-4* gene from these mutants. Fragments of the *sma-4* gene were amplified by PCR and directly sequenced. *sma-4(e729)* contains a single nucleotide substitution resulting in a Q246 (CAA) to stop codon (UAA) mutation. Therefore, *sma-4(e729)* is an early termination mutation.

### Construction of *sma-3* and GFP fusion genes

An 8 kb *sma-3* genomic fragment was obtained from the cosmid R13F6 by digesting with *Pst*I and subcloning into the vector pBLUESCRIPT SK+ (pCS29). This construct rescues *sma-3(wk30)* mutants. To create GFP fusion constructs, *Mlu*I restriction sites were created in the *sma-3*-coding region, after the start codon (pCS185) or before the stop codon (pCS186) independently, by site-directed mutagenesis (MutaGene kit from BioRad). A GFP *Mlu*I fragment from pPD118.90 (A. Fire) was subcloned into the newly generated *Mlu*I sites, forming two *sma-3::gfp* translational fusion constructs; N-terminal GFP (pCS170) or C-terminal GFP (pCS171). We also created a *sma-3* construct lacking all coding sequences. An *Xho*I-*Mlu*I fragment from pCS185 containing *sma-3* upstream sequences was ligated into *Xho*I-*Mlu*I-digested pCS186 in which upstream and coding regions had been removed leaving only downstream sequences. This *sma-3* construct (pCS210) therefore contains upstream and downstream noncoding sequences but no coding region.

### **Fusion of tissue specific promoters and *sma-3::gfp* coding region**

The promoters used in tissue specific expression of *sma-3::gfp* included *elt-3*, *vha-7*, *dpy-7* (hypodermal); *elt-2*, *vha-6* (intestine); *myo-2* (pharynx); and the third isoform of *tmy-1* (pharynx and intestine) (Gilleard et al., 1999; Oka et al., 2001; Gilleard et al., 1997; Okkema et al., 1993; Fukushige et al., 1998; Anyanful et al., 2001). The *elt-2* and *elt-3* promoters were kindly provided by R. W. Padgett's laboratory (HW373 and HW375). The others were obtained by PCR using N2 genomic DNA as template from worm lysates. The PCR primers used were:

- *tmy-1f*, 5'-AAGTCGACCGAGTAGGTCTCGCCACG-3';
- *tmy-1r*, 5'-ATTCTGCAGAAGTCAGAGGTGT-3';
- *myo-2f*, 5'-AAGTCGACCTCTCCGATTGCTATCATG-3';
- *myo-2r*, 5'-AACTGCAGTGTCTGACGATCGAGGGTT-3';
- *dpy-7f*, 5'-AAGTCGACTGGCGCAAGAGGCAGTGC-3';
- *dpy-7r*, 5'-AACTGCAGTTATCTGGAACAAAATGTAAGA-3';
- *vha-7f*, 5'-AAGTCGACAGGAAATTGTGAGAAG-3';
- *vha-7r*, 5'-AACTGCAGATTACGTCGTTGGTGGA-3';
- *vha-6f*, 5'-AATCTAGAGCATGTACCTTTATAGG-3'; and
- *vha-6r*, 5'-AACCCGGGTAGGTTTTAGTCGCCCTG-3'.

After the PCR products were digested by the appropriate restriction enzymes, the promoters were cloned into pBLUESCRIPT SK+ vector. Next, a *Pst*I fragment

containing the *sma-3::gfp(N)*-coding region was excised from pCS170 (one *Pst*I site derives from the GFP vector pPD118.90) and inserted into vectors containing the heterologous promoters. Thus, after translation, each of the protein products has GFP at the N terminus and SMA-3 at the C terminus.

### **Transformation and integration**

Transformation of constructs into worms was carried out by microinjection (Mello et al., 1991). Unless otherwise stated, the injection solution contains 20 ng/μl of experimental plasmid and 100 ng/μl pRF4 (*rol-6* plasmid). The co-injection of *vha-6::sma-3* and *myo-2::sma-3* includes 20 ng/μl of each. The co-injection of C-terminal *sma-3::gfp* (pCS171) with pCS29, pCS170 or pCS210 contains 10 ng/μl of each experimental plasmid.

We used  $\gamma$ -rays to integrate the *sma-3::gfp(N)* array into *sma-3(wk30)* and the co-injected *sma-3::gfp(C)* with *sma-3* genomic and *sma-3::gfp(C)* with *sma-3* non-coding arrays into N2. More than 100 L4 or young adult worms with each extra-chromosomal array were picked. After exposure to a cesium source, the worms were separated into 20 plates (five worms in each). After starvation, the worms were chunked into new plates. We allowed the worms to recover for 2 days. Each worm carrying the array was picked into a separate plate. After one generation, plates with 100% worms containing the reporter gene (*rol-6*) were selected. The integrated arrays are *qclIs6[sma-3::gfp(N) +*

*rol-6*], *qclIs12[sma-3::gfp(C) + sma-3 + rol-6]* and *qclIs16[sma-3::gfp(C) + sma-3no-code + rol-6]*.

### **Length Measurement**

To assess body length in transgenic animals, cultures were synchronized by bleaching gravid hermaphrodites in order to isolate eggs. These eggs were introduced onto new plates. The body length was measured after 96 hours, in the adult stage. Transgenic (rolling) worms were picked, mounted on slides and measured as described above.

### **Western blot**

Worms were washed off non-starved plates and frozen at -80°C overnight. The boiling buffer (8% SDS+20 mM DTT+100 mM pH 6.8 Tris+10 mM PMSF) was added and the samples were boiled for 5 minutes. The protein concentration was determined and equal amounts of total protein were loaded in each lane. After running the SDS-PAGE gel, the proteins were transferred onto nitrocellulose membrane. The membrane was blocked by 5% BSA in PBS and probed by rabbit anti-GFP antibody (Clontech). The secondary antibody (anti-rabbit) and detection solutions were from the ECL western blotting analysis system (Amersham).

## **RESULTS**

### **Levels of functional activity of *sma-3::gfp* translational fusions**

To determine the expression pattern and subcellular localization of SMA-3 Smad protein, we made two kinds of *sma-3::gfp* translational fusion gene constructs. In pCS170, GFP is inserted at the N terminus, and in pCS171, GFP is inserted at the C terminus. After transformation into *sma-3(wk30)*, the rescuing ability was assessed. Rescue of body size was assessed by measuring worm length 96 hours after embryo collection. Rescue of male tail patterning was assessed by determining the frequency of sensory ray fusions. In the wild-type *C. elegans* male tail are nine bilateral pairs of sensory organs, the sensory rays (Sulston et al., 1980). Each ray is characterized by its unique position, morphology and neurotransmitter usage. The Sma/Mab pathway plays a role in the specification of rays 5, 7 and 9. In mutants, these rays often display characteristics of rays 4, 6 and 8, respectively, resulting in readily observable fusions between rays 4-5, 6-7 and 8-9 (Savage et al., 1996; Suzuki et al., 1999; Morita et al., 1999; Krishna et al., 1999).

The N-terminal *sma-3::gfp* construct is functional, restoring most of the body length (Table 2.1) and rescuing the male tail sensory ray pattern (Table 2.2). However, the C-terminal construct has very little rescuing activity in body length (Table 2.1) and it only partially rescues male tail ray fusions (Table 2.2). When the extra-chromosomal array with the C-terminal construct is crossed into a wild-type background, it even shows a slight inhibition in body length, but does not affect male tail development (Tables 2.1 and

Genotype	Transgene	GFP expression	Length (mm)	Worms
N2	<i>qcEx50[rol-6]</i>	NA	1.15±0.11	44
<i>sma-3(wk30)</i>	<i>qcEx50[rol-6]</i>	NA	0.74±0.05	40
<i>sma-3(wk30)</i>	<i>qcEx24[sma-3::gfpN+rol-6]</i>	H+P+I	1.05±0.08	38
<i>sma-3(wk30)</i>	<i>qcEx42[sma-3::gfpC+rol-6]</i>	H+P+I	0.83±0.07	34
N2	<i>qcEx42[sma-3::gfpC+rol-6]</i>	H+P+I	1.03±0.10	51
<i>sma-3(wk30)</i>	<i>qcEx57[sma-3::gfpC+sma-3::gfpN+rol-6]</i>	H+P+I	1.00±0.11	40
<i>sma-3(wk30)</i>	<i>qcEx44[Pelt-3::sma-3+rol-6]</i>	hyp7	1.04±0.07	40
<i>sma-3(wk30)</i>	<i>qcEx55[Pvha-7::sma-3+rol-6]</i>	hyp7	1.02±0.06	42
<i>sma-3(wk30)</i>	<i>qcEx51[Pdpy-7::sma-3+rol-6]</i>	hyp7	0.94±0.10	32
<i>sma-3(wk30)</i>	<i>qcEx45[Pelt-2::sma-3+rol-6]</i>	Intestine	0.66±0.05	30
<i>sma-3(wk30)</i>	<i>qcEx53[Pvha-6::sma-3+rol-6]</i>	Intestine	0.67±0.04	32
<i>sma-3(wk30)</i>	<i>qcEx52[Pmyo-2::sma-3+rol-6]</i>	Pharynx	0.80±0.06	24
<i>sma-3(wk30)</i>	<i>qcEx54[Ptmy-1(III)::sma-3+rol-6]</i>	Pharynx+ Intestine	0.83±0.06	38
<i>sma-3(wk30)</i>	<i>qcEx56[Pmyo-2::sma-3+Pvha-6::sma-3+rol-6]</i>	Pharynx+ Intestine	0.80±0.05	27

Table 2.1 The function of tissue-specific *sma-3* expression constructs in body length regulation *sma-3::gfp* fusion gene expression pattern and protein localization

Genotype	Transgenes	Sensory ray fusions %			sides
		4&5	6&7	8&9	
<i>him-5(e1490)</i>	None	0	0	6	35
<i>sma-3(wk30); him-5(e1490)</i>	None	22	69	11	55
<i>sma-3(wk30); him-5(e1490)</i>	<i>qcEx24[sma-3::gfp(N)+r ol-6]</i>	0	0	5	148
<i>sma-3(wk30); him-5(e1490)</i>	<i>qcEx42[sma-3::gfp(C)+r ol-6]</i>	2	27	26	84
<i>him-5(e1490)</i>	<i>qcEx42[sma-3::gfp(C)+r ol-6]</i>	0	0	6	106

Table 2.2 The function of *sma-3::gfp* constructs in male tail patterning

2.2), suggesting that it can interfere with wild-type SMA-3 function. The R-Smad C-terminal SSXS motif is the site of phosphorylation and may participate in intermolecular interactions (Wu et al., 2001; Qin et al., 2001). The C-terminal insertion of GFP may disrupt some of these interactions.

Both the N-terminal functional and the C-terminal nonfunctional *sma-3::gfp* constructs

show the same pattern of expression, but the level of fluorescence of the C-terminal construct is much higher. We show the expression of the *sma-3::gfp* C-terminal construct (Figure 2.1). Expression begins late in embryogenesis, and continues through larval stages into adulthood. In larvae, expression is strong in the hypodermis, pharynx and intestine. *sma-3* expression in the hypodermis is seen throughout the large hypodermal syncytium hyp7, but not in the lateral hypodermal blast cells (the seam cells). Nuclear accumulation in all of these tissues is strong. This nuclear localization does not depend on the activity of *sma-6*, however (see Figure 2.5E,F). Expression of the N-terminal construct is similar, although much weaker, even after integration (Figure 2.2A). Again, the nuclear fluorescence is prominent in the pharynx, intestine and hypodermis. We asked whether the nuclear accumulation depends on the activity of other components in the pathway. When the integrated N-terminal construct array (*qcl56*) was crossed into *sma-4(e729)* (Fig2.2C) or *sma-2(e502)* (Figure 2.2E) mutant backgrounds, the nuclear localization did not change significantly. This result is consistent with previous reports that R-Smad nuclear translocation does not require complex formation with a co-Smad partner (Liu et al., 1997). When the array is crossed into *sma-6(wk7)* mutants, the protein became evenly distributed between the cytoplasm and the nucleus in many but not all animals (Figure 2.2G). Thus, the nuclear accumulation of SMA-3::GFP is enhanced by but not dependent on activation by the type I receptor. Determining whether this extensive nuclear localization is characteristic of the endogenous SMA-3 protein must await the development of SMA-3 antibodies.

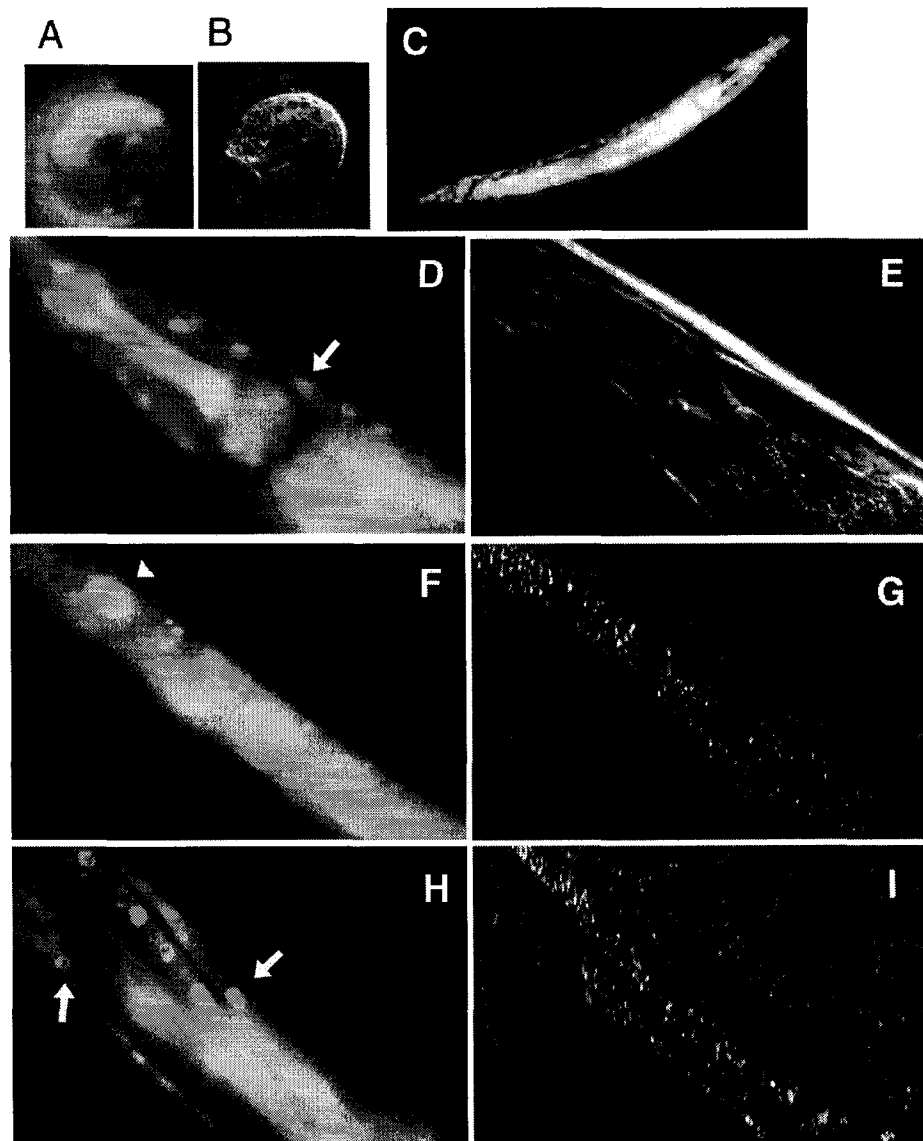


Figure 2.1 The *sma-3::gfp(C)* expression stage and pattern in wild type. (A,C,D,F,H) Direct fluorescence from GFP; (B,E,G,I) Nomarski images of the same samples to their left. (A,B) The expression begins at the late embryo stage, 2.5-fold stage. (C) The gene expression pattern in L3 stage worms. At L4 stage, *sma-3* is expressed in pharynx, head region hypodermis (D,E), intestine (F,G) and body hypodermis (H,I). The arrows indicate the hypodermal nuclei. The arrowhead indicates an intestinal nucleus.

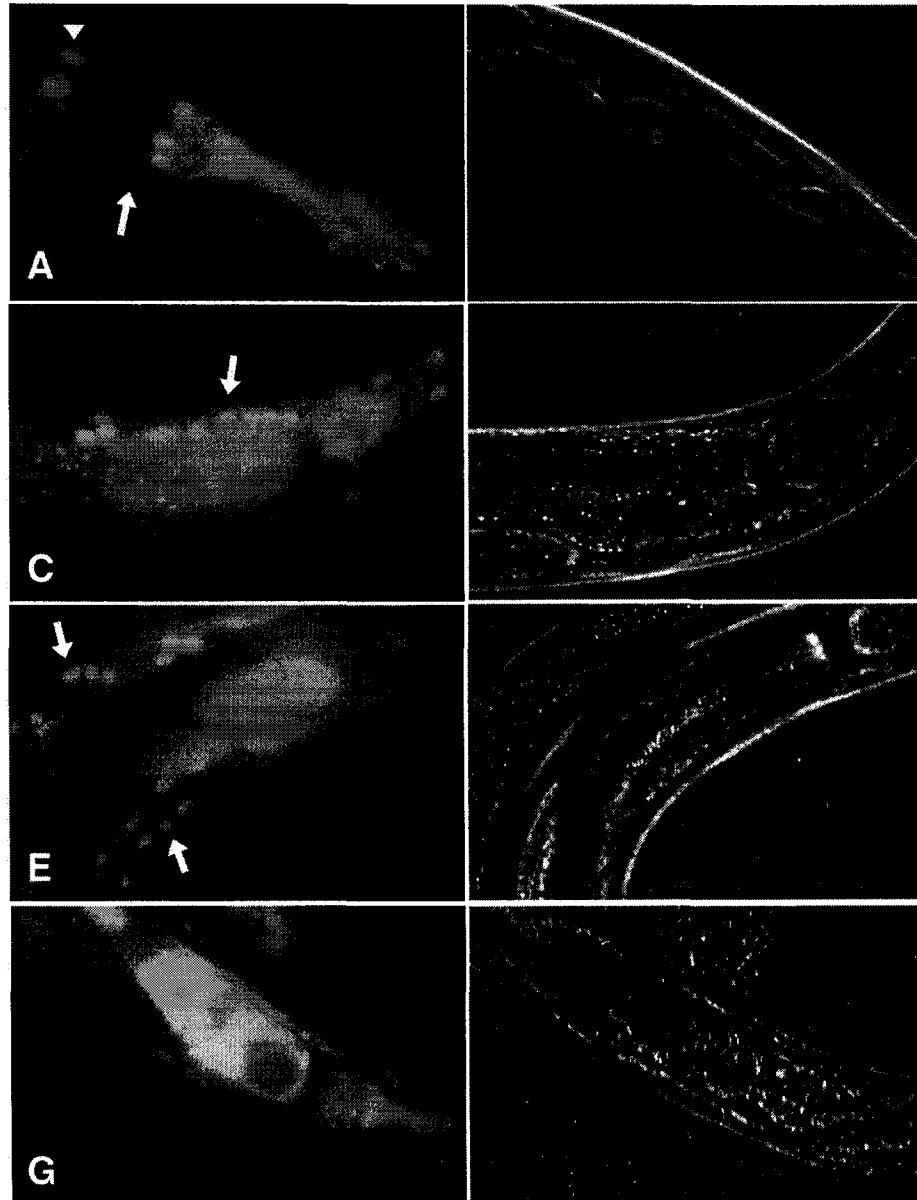


Figure 2.2 The *sma-3:gfp(N)* expression and localization in different mutant backgrounds: (A,B) *sma-3(wk30)*; (C,D) *sma-4(e729)*; (E,F) *sma-2(e502)*; (H,I) *sma-6(wk7)*. (A,C,E,H) show direct fluorescence from GFP; (B,D,F,I) are the Nomarski images of the same samples. The arrows indicate hypodermal nuclei (A,C,E). The arrowhead indicates an intestinal nucleus (A).

### Effects of tissue-specific expression of *sma-3* on body length

To determine the cellular focus of *sma-3* in regulating body length, we created transgenic animals with *sma-3* expression driven by heterologous promoters. Constructs were made with tissue-specific promoters and the *sma-3::gfp* N-terminal fusion. Four types of expression patterns were used. For hypodermal expression, we used *elt-3::sma-3* (Gilleard et al., 1999), *vha-7::sma-3* (Oka et al., 2001) and *dpy-7::sma-3* (Gilleard et al., 1997). These hypodermal promoters function in *hyp7* but not in the seam cells. For pharyngeal expression, we chose *myo-2::sma-3* (Okkema et al., 1993). For intestinal expression, we used *elt-2::sma-3* (Fukushige et al., 1998) and *vha-6::sma-3* (Oka et al., 2001). Finally, for simultaneous expression in the pharynx and intestine, we used *tmy-1* isoform III (Anyanful et al., 2001) as well as a combined injection of *myo-2::sma-3* and *vha-6::sma-3*. We confirmed the expression of SMA-3::GFP in the specified tissues by direct fluorescence (Figure 2.3).

The hypodermal expression of *sma-3* from any of the three hypodermal promoters restores body length to the same extent as the *sma-3* native promoter (Table 2.1). When *sma-3* is only expressed in intestine, there is no effect on the body length. The pharyngeal expression or the co-expression in pharynx and intestine do not increase the body length significantly. Therefore, *sma-3* expression in the hypodermis is sufficient for the regulation of body length.

### SMA-3 protein accumulation

We have found that the nonfunctional *sma-3::gfp* C-terminal construct gives a stronger fluorescent signal than the functional N-terminal construct (Figure 2.4A-D). This difference in intensity was consistent in at least three independent lines for each construct. We also tried lower (10  $\mu\text{g/ml}$ ) or higher (40  $\mu\text{g/ml}$ ) concentrations of the construct in injection mixtures, but the intensity of fluorescence was not different from that with 20  $\mu\text{g/ml}$ . The reduced fluorescence of the *sma-3::gfp(N)* construct could be due to changes in protein folding that affect GFP fluorescence or to reduced protein accumulation.

We hypothesized that the difference in fluorescence is due to differing levels of accumulation of the *sma-3::gfp(N)* and *sma-3::gfp(C)* fusion proteins. There are two possible causes of such differences in accumulation. First, the C-terminal construct could be inherently more stable. Second, SMA-3 degradation could be induced by *sma-3* activity in a negative-feedback loop. To solve this puzzle, we simply mixed the two *sma-3::gfp* constructs together (10  $\mu\text{g/ml}$  each) and microinjected into *sma-3(wk30)* mutants. This mixture can rescue the *sma-3* mutant, in both body length and male tail patterning (Tables 2.1 and 2.2). In other words, the mixture provides *sma-3* activity. However, the level of fluorescence is low, although the C-terminal construct is present (Figure 2.4E,F). This implies that after adding the functional *sma-3* construct, the C-terminal fusion protein could be degraded by an unknown factor. This result also

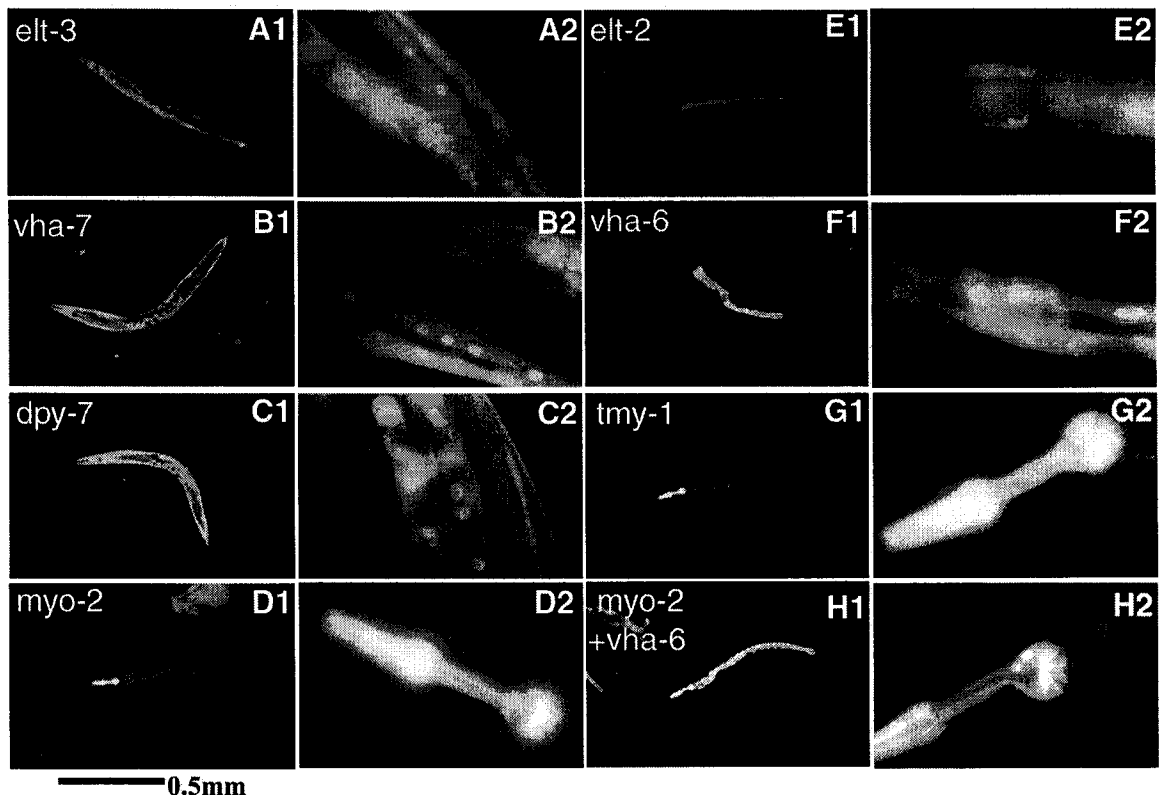


Figure 2.3 The *sma-3* expression with tissue-specific promoters. Worms carrying each array are picked during L4 stage and photographed 24 hours later. The A1-H1 photos (first and third columns) show the overview of the expression pattern and the body size. The A2-H2 photos (second and fourth columns) focus on the region that has strong GFP expression. The tissue specific promoter used in each set is indicated in the A1-H1 photos. Scale bar: 0.5 mm in A1-H1 photos.

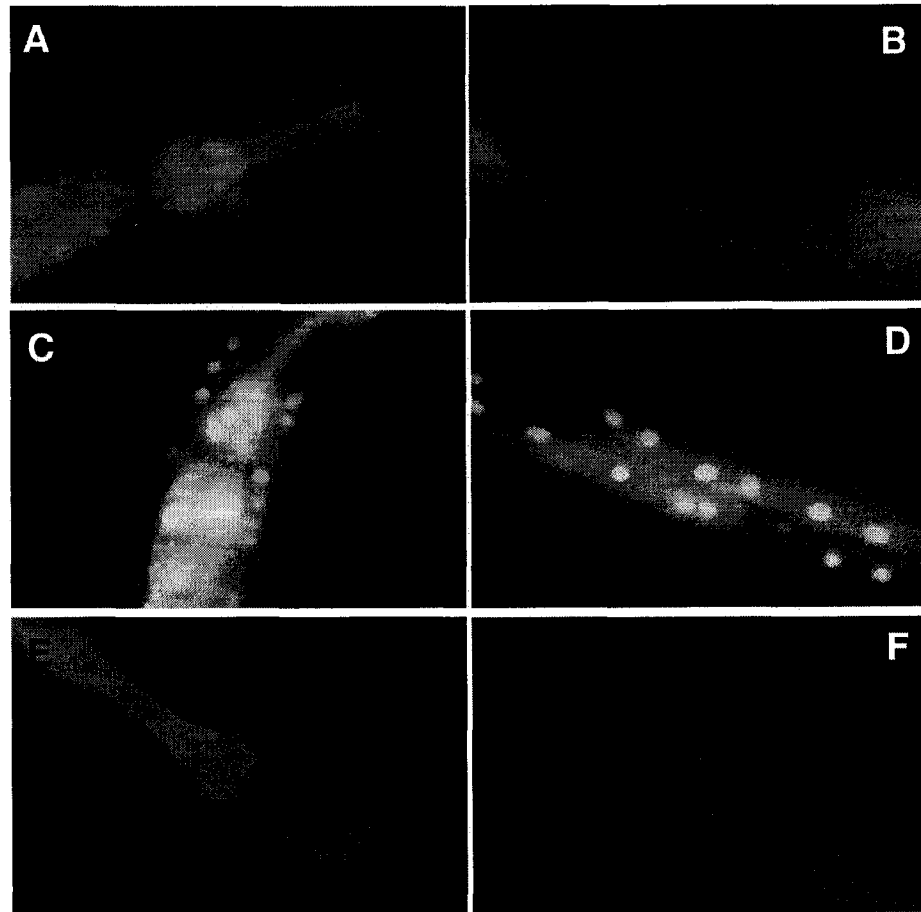


Figure 2.4 The distinct intensity of fluorescence in worms with different *sma-3::gfp* constructs in the *sma-3(wk30)* background. (A,B) *sma-3::gfp(N)*; (C,D) *sma-3::gfp(C)*; (E,F) co-injection of *sma-3::gfp(N)* and *sma-3::gfp(C)*. (A,C,E) The head region; (B,D,F) the body hypodermis. All of the worms (L4 stage) are grown under the same conditions and the photos are taken with the same exposure time.

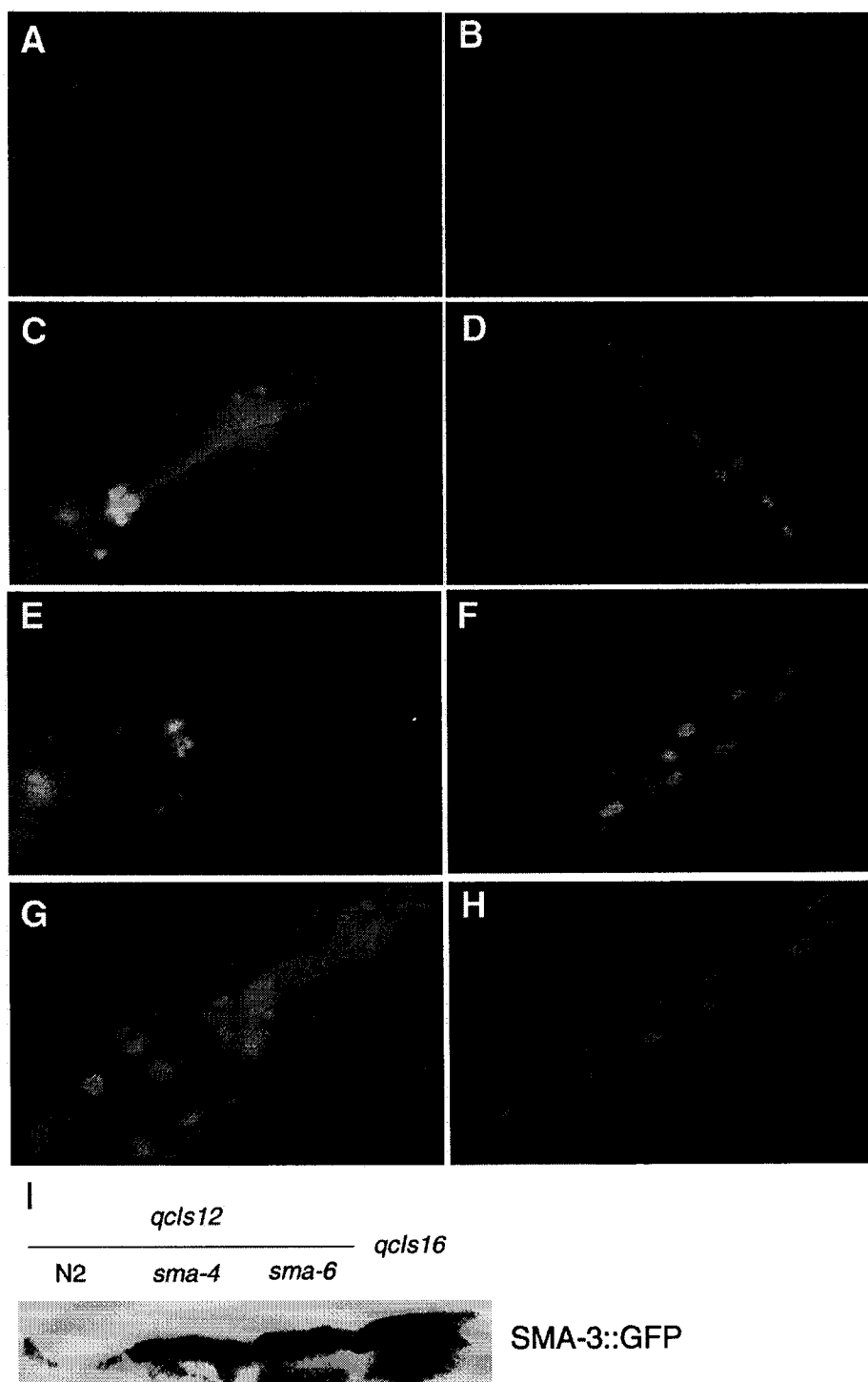


Figure 2.5 Expression of SMA-3::GFP C-terminal fusion protein in different genetic backgrounds. (A-F) *sma-3::gfp* C-terminal fusion was co-injected with *sma-3* genomic fragment, which contains the whole *sma-3* gene sequence. (A,B) *sma-3(wk30)* mutant background. (C,D) *sma-4(e729)* mutant background. (E,F) *sma-6(wk7)* mutant background. (G,H) *sma-3::gfp* C-terminal fusion was co-injected with *sma-3* genomic lacking coding sequences. (I) Western blot of total protein extracts from strains carrying *sma-3::gfp(C)* constructs.

contradicts the model that the difference in fluorescence is due to differences in protein folding that affect GFP fluorescence.

We further tested this model by co-injecting the nonfunctional *sma-3::gfp(C)* (10 µg/ml) construct either with the functional *sma-3* genomic fragment (pCS29) (10 µg/ml) or with a *sma-3* construct in which the coding region had been deleted (pCS210) (10 µg/ml) that would not have SMA-3 activity. In the co-injection with *sma-3* genomic sequences, only a trace amount of GFP fluorescence can be seen (Fig2.5A,B). However, in the co-injection with pCS210, the level of fluorescence remains high (Fig2.5G,H). Thus, under a variety of conditions, *sma-3::gfp* fluorescence levels negatively correlate with SMA-3 activity levels. Finally, we addressed the question of whether a negative-feedback loop requiring other components of the pathway regulates SMA-3 protein accumulation. In fact, an extrachromosomal array carrying *sma-3::gfp(C)* and the *sma-3* genomic fragment shows increased levels of fluorescence in a *sma-4* or *sma-6* mutant background, suggesting that the feedback is dependent on an intact signaling pathway (Figure 2.5C-F).

We verified these results in a western blot using anti-GFP antibody. The extrachromosomal arrays were integrated: *qclIs12* contains *sma-3::gfp(C)* and *sma-3* genomic, *qclIs16* contains *sma-3::gfp(C)* and *sma-3* non-coding genomic. *qclIs12* was crossed into the *sma-4(e729)* and *sma-6(wk7)* mutant backgrounds to determine whether loss of SMA-3::GFP(C) protein accumulation requires active Co-Smad and type I receptor, respectively. Consistent with the results from fluorescence in whole worms,

SMA-3::GFP from *qcls12* in the N2 background is almost undetectable (lane 1). By contrast, a strong band is detectable in the *qcls16* strain (lane 4). In the *sma-4* (lane 2) and *sma-6* (lane 3) backgrounds, SMA-3::GFP levels from *qcls12* increase relative to the levels in a wild-type background. These results are consistent with a negative-feedback loop regulating SMA-3 protein accumulation.

## DISCUSSION

### **The Sma/Mab pathway acts in the hypodermis to regulate body length**

The specification of body size is a poorly understood phenomenon. In recent years, studies have begun to address the molecular mechanisms governing size in animals such as *Drosophila* (Oldham et al., 2000; Johnston and Gallant, 2002; Martin-Castellanos and Edgar, 2002) and *C. elegans* (Flemming et al., 2000; Savage-Dunn et al., 2000). In *C. elegans*, most of the mutants resulting in small body size are defective in components of a TGF $\beta$ -related signaling pathway, the Sma/Mab pathway (Savage-Dunn, 2001). A limited number of additional loci that mutate to a small phenotype have been described (*sma-1*, *sma-5* and *sma-8*), the best studied of which is *sma-1*, a  $\beta_H$ -spectrin homolog (McKeown et al., 1998). An effect of BMP family signaling on cell size may be conserved, as *Drosophila dpp* also regulates cell growth (Martin-Castellanos and Edgar, 2002).

We have previously shown that the Sma/Mab pathway functions postembryonically (Savage-Dunn et al., 2000), in contrast to the embryonic requirement for *sma-1* (McKeown et al., 1998). In this study, we have addressed the tissue specificity of the Sma/Mab pathway in body size regulation and find that the hypodermis is the crucial TGF $\beta$ -responsive tissue involved in body size regulation. The hypodermis of *C. elegans* forms the outer layer of cells surrounding the animal, and it secretes the cuticle (Johnstone, 2000). The largest region of the hypodermis is made up of a single multinucleate syncytium, *hyp7* (Sulston and Horvitz, 1977). Two lateral rows of hypodermal blast cells, the seam cells, divide during each larval stage to form one daughter cell that fuses with *hyp7* and one that remains in the seam. After fusion with *hyp7*, these nuclei undergo endoreduplication (Hedgecock and White, 1985; Flemming et al., 2000). Additional smaller hypodermal cells are present in the head (*hyp1-hyp6*) and the tail (*hyp8-hyp12*).

We conclude that Sma/Mab signal transduction functions in the hypodermis to regulate body size based on (1) the SMA-3 expression pattern; (2) cell and organ size measurements; (3) *sma-3* mosaic analysis; and (4) directed expression of *sma-3*. We have examined SMA-3 Smad expression and subcellular localization using SMA-3::GFP fusion constructs. SMA-3 is expressed in the pharynx, intestine and hypodermis. This expression pattern coincides with the expression pattern of the type I receptor SMA-6 (Krishna et al., 1999; Yoshida et al., 2001). In cell size measurements, the seam cells in

Sma/Mab mutants, but not the pharynx, show a reduction in size similar to the reduction in the body length (Wang et al., 2002). The relative maintenance of pharynx length in Sma/Mab mutants suggests that the expression of Sma/Mab signaling components in the pharynx may serve an unidentified role. Measurement of hyp7 volume (Nagamatsu and Ohshima, 2004) also indicates a decrease in size proportional to the decrease in body volume. Finally, both of the mosaic analysis and tissue-specific expression of *sma-3* indicate that SMA-3 function in the hypodermis is necessary and sufficient for body size regulation (Wang et al., 2002). The hypodermal requirement for SMA-3 is consistent with the results from similar experiments on the receptors *sma-6* (Yoshida et al., 2001) and *daf-4* (Inoue et al., 2000).

Although the seam cells are reduced in size in Sma/Mab mutants, the effect on the seam cells may not be cell autonomous, as neither *sma-3* (Wang et al., 2002) nor *sma-6* (Yoshida et al., 2001) expression is detected in these cells. Furthermore, we have shown that *sma-3* expression from hyp7-specific promoters, which also do not express in the seam cells, is sufficient to rescue the body size in a *sma-3* mutant (Table 2.2). Because the hyp7 and seam cells are joined by gap junctions (David Hall, personal comm) and adherens junctions (Mohler et al., 1998), there could be communication between these tissues without postulating additional extracellular signals. As *dbl-1* is expressed primarily in the nervous system (Suzuki et al., 1999), these results suggest a model in

which postembryonic growth of hypodermal cells is regulated by TGF $\beta$ -related signaling from the nervous system to the hypodermis.

One important question that remains to be addressed is why these cells are smaller. Several possibilities may be considered. One is that reduced DNA content leads to smaller size. Flemming et al., (2000) have proposed that reduced hypodermal ploidy may be the reason for the smaller body size of Sma/Mab mutants, as ploidy can control cell size. The nuclei of the *C. elegans* intestine and hypodermis normally undergo endoreduplication during larval growth (Hedgecock and White, 1985). In late adulthood the hypodermal nuclei in wild type have an average ploidy of 10.7C, and some nuclei have gone through two rounds of endoreduplication (Flemming et al., 2000). It is not clear, however, whether changes in ploidy are sufficient to explain the changes in body size. In fact, a conflicting report finds no evidence of significant changes in hypodermal or intestinal ploidy (Nagamatsu and Ohshima, 2004). Another mechanism that could contribute to smaller cell size is reduced protein synthesis. To test this hypothesis, Rafal tried growing worms on the protein synthesis inhibitor cycloheximide. At concentrations in which the worms could grow, however, they were normal in size. Nagamatsu and Ohshima, (2004) find that the small mutants have significantly lower protein content. But it is more likely to be the effect, not the reason to be small. A third possibility is a change in the cell cycle. By speeding up the cell cycle, small cells could be generated such as is seen in yeast *wee* mutants (Futcher, 1996). Because the small mutants do not develop

more quickly, however, any cell cycle defect could only be in some stage(s) of the cell cycle. In fact, the life cycle, from an egg to the first egg, is much longer for *sma-3(wk30)* than that of wild type (see Chapter V). Finally, metabolic changes could decrease cell size. In *Drosophila* (but not in *C. elegans*) mutations in insulin signaling result in small cells and small animals (Oldham et al., 2000). Similarly, some change in sugar or fat metabolism could underlie the small phenotype.

### **SMA-3 protein accumulation may be regulated by a feedback loop**

Using different SMA-3::GFP fusion constructs, we have obtained evidence that SMA-3 protein accumulation is negatively regulated by the level of SMA-3 and Sma/Mab pathway activity. Furthermore, a negative-feedback loop is consistent with the lack of effect of overexpressing *sma-3*. The overexpression of *dbl-1* ligand induces a long phenotype and male tail sensory ray defects (Suzuki et al., 1999), while the overexpression of *sma-3* does not (data not shown). In other systems, it has been shown that Smads are degraded by the activity of Smurf E3 ubiquitin ligases (Zhu et al., 1999; Zhang et al., 2001; Podos et al., 2001). In human or *Xenopus*, Smurf-1 and Smurf-2 induce R-Smad degradation by the ubiquitin pathway (Zhu et al., 1999; Zhang et al., 2001). Through interaction with the anti-Smad Smad7, Smurf-1 can also induce the degradation of type I receptor (Ebisawa et al., 2001). Smurf-2 enhances the degradation of type I receptor (Kavsak et al., 2000) or SnoN oncogene (Bonni et al., 2001). The target is selected by the Smad with which it interacts. A Smurf gene, *Dsmurf* is found in

*Drosophila*, where it negatively regulates *dpp* signaling in embryonic dorsoventral patterning (Podos et al., 2001). In *C. elegans*, we find several open reading frames with homology to human or *Xenopus* Smurf genes, allowing the possibility that one or more of these genes functions in the Sma/Mab pathway. It will be interesting to determine whether a Smurf gene participates in a negative feedback loop.

**Note:**

The work described in this chapter has been previously published elsewhere (Wang et al., 2002, *Development* **129**: 4989-98).

We thank the Fire Lab for green fluorescence protein vectors and Iva Greenwald Lab for the assistance of DNA integration.

## Chapter III

### **C-terminal mutants of the *C. elegans* Smads reveal that the targets require different levels of activities**

#### **ABSTRACT**

TGF- $\beta$  signaling in the nematode *C. elegans* plays multiple roles in the animal's development. The Sma/Mab pathway controls body size, male tail sensory ray identity and spicule formation and all of the three Smad genes, *sma-2*, *sma-3* and *sma-4* are required for the signaling. Null mutants of any of the three genes have defects as severe as the null mutants of ligand, *dbl-1* or type I receptor, *sma-6*, suggesting that the functional complex is a heterotrimer. Since the C-termini of Smads play important roles in receptor-mediated activation and heteromeric complex formation, we generated C-terminal mutations in the *C. elegans* Smad genes and tested their activities *in vivo* in each of their distinct developmental roles. We show that pseudophosphorylated SMA-3 is dominant negative in body size through a feedback loop, but functional in sensory ray and spicule development. Somewhat differently, pseudophosphorylated SMA-2 is constitutively active in any tissue. The C-terminal mutants of SMA-4 function like wild type suggesting SMA-4 C-terminus is dispensable. Using the combination of different C-terminal mutations in SMA-2 and SMA-3, we find a complex set of requirements for Smad phosphorylation state specific to each outcome.

## INTRODUCTION

TGF- $\beta$ -related ligands, including the BMP subfamily, control the development of organisms by regulating a series of cellular processes including cell growth, cell differentiation, apoptosis and proliferation. In humans, components of the TGF- $\beta$  pathway play important roles in cancer preventing. From cell membrane to nucleus, the signal is conducted by ligands, receptors and intracellular transducer Smads, which are conserved in both invertebrates and vertebrates (Savage-Dunn, 2003; Massagué and Chen, 2000; Patterson and Padgett, 2000; Hill, 2001). The signaling begins when the extracellular ligand binds to the transmembrane type II and type I receptors, which are Ser/Thr kinases. Type II receptor phosphorylates and activates type I receptor (Shi and Massagué, 2003; Mehra and Wrana, 2002). The receptor-regulated Smad proteins (R-Smads) are phosphorylated by the activated type I receptor and form a complex with mediator Smad (Co-Smad, namely Smad4). The complex enters the nucleus to regulate the transcription of target genes (Attisano and Wrana, 2002; Moustakas et al., 2001; Massagué and Wotton, 2000).

Smad proteins contain two highly conserved regions, the MH1 and MH2 domains, located at N- and C-terminus, respectively, connected by a linker region. The linker region is not very conserved and could be the target of activity adjustment (Hata et al., 1997; Massagué, 2003). Two serines/threonines at the C-terminal end of R-Smad proteins

(consensus sequence SS\*XS\*) are the substrates of receptor phosphorylation (Abdollah et al., 1997; Souchelnytskyi et al., 1997). The crystal structures of Smad1 MH2 and phosphorylated Smad2 MH2 provide insight into the structural basis of complex formation (Qin et al., 2001; Wu et al., 2001). The crystal structures show that the phosphorylated C-terminus of Smad2 binds a positively charged pocket of another subunit (Wu et al., 2001). Some studies show that pseudophosphorylated R-Smads with negatively charged C-termini can be constitutively active even without the signal from the ligand or receptors (Chacko et al., 2001; Qin et al., 2001). In addition to phosphorylation by receptors, Smad proteins are regulated by other mechanisms. It has been reported that Smads are ubiquitinated by Smurf proteins, which are E3 ubiquitin ligases that function in a negative feedback loop. Moreover, Smad activity is repressed by the oncoproteins SnoN and Ski, which disrupt Smad complex formation probably by directly binding to Smad proteins (He et al., 2003; Liu et al., 2001).

Most of the TGF- $\beta$  signaling components have been found in *Caenorhabditis elegans*. There are multiple TGF- $\beta$ -related pathways that control different events in *C. elegans* development. Among them, the Sma/Mab and Dauer pathways regulate body size and dauer formation, respectively (Savage et al., 1996; Patterson et al., 1997). They share one type II receptor, *daf-4*. But the type I receptors are different, *sma-6* and *daf-1* (Patterson and Padgett, 2000). When *daf-4* is transformed into human cell lines, the receptor protein binds BMP ligands showing the conservation between these pathway components in

human and *C. elegans* (Estevez et al., 1993). A model for Sma/Mab pathway signaling has been developed based on analogy with biochemical experiments in other systems. The signal begins with ligand DBL-1 binding on the type II receptor DAF-4 and type I receptor SMA-6. The intracellular Smad homologs SMA-2, SMA-3 (R-Smads), and SMA-4 (Co-Smad), propagate the signal by forming a complex and entering the nucleus (Savage-Dunn, 2001). The loss of function of the pathway results in small body size. Furthermore, in the male tail, the sensory rays become fused and the spicules are crumpled (Savage-Dunn et al., 2000). We have previously shown that *sma-3* is expressed in pharynx, intestine and hypodermis. The expression in hypodermis is necessary and sufficient to regulate body size. Also, active *sma-3* turns on a negative feedback loop that reduces SMA-3 protein accumulation (Wang et al., 2002).

We have noted that SMA-3 does not function well with GFP attached to the C-terminus, suggesting that the C-terminus of SMA-3 is indispensable for its activity (Wang et al., 2002). Since the C-terminus is likely the site of phosphorylation, we reasoned that mutating C-terminal residues could provide an opportunity to investigate the roles of Smad phosphorylation *in vivo*. Previous studies using activation of selected target genes in cell lines as an assay have shown that pseudophosphorylated Smads could be constitutively active; however, *in vivo* experiments have not been reported. We have therefore generated C-terminally mutated *sma-3* genes by site-directed mutagenesis. Our results indicate that Smad phosphorylation is not required for nuclear localization, but is

likely required for Smad complex formation and for interaction with transcription co-factors. We also find that different developmental outcomes show differential requirements for Smad C-terminal modification, possibly due to differential affinities for transcription factor binding. Finally, we have created wild-type rescuing and pseudophosphorylated *sma-2* constructs that function differently from the *sma-3* variants. With these data from both *sma-2* and *sma-3*, the signaling mechanisms of the Sma/Mab pathway are better understood.

## **MATERIAL AND METHODS**

### **General methods and worm strains**

*Caenorhabditis elegans* strains were cultured as described by Brenner (1974). The following strains were used: wild-type *C. elegans* variety Bristol strain N2; LGII *sma-6(wk7)*; LGIII, *sma-2(e297)*, *sma-3(wk30)*, *sma-4(e729)*, *lon-1(wk50)*; LG V, *him-5(e1490)*.

### **Cloning of genomic *sma-2***

The *sma-2* ORF is contained within a large genomic region. A big intron (3kb) contains another gene. It is unknown if this gene has any role with *sma-2*. A second large intron (1kb) near the 3' end contains an interesting sequence. The first half is complementary to the second half. During PCR, this intron creates aberrant products. The final rescuing

genomic clone does not include this intron or the big intron (3kb).

### Site-directed mutagenesis

Using MutaGene kit from BioRad, *sma-3* C-terminal mutations were generated by adding primers complementary to the uracil-containing single strand DNA purified from CJ236 *E. coli* strain. After extending by T7 DNA polymerase and ligating by T4 ligase, the DNA is transformed and amplified in DH5 $\alpha$  *E. coli* strain. The mutations are confirmed by DNA sequencing.

Primers for mutagenesis:

DME: GGAACCAATGACATGGAATAATGATT

AMA: GGAACCAAATGCAATGGCATAATGATT

YMY: GAACCAAATTATATGTATTAATGATTTG

Deletion: CGAACTTCATYGAACCAAATTAATGATTTGTAAAA

By chance, we also generated a partial deletion of MT. The C-terminal mutations of *sma-2* and *sma-4* were produced directly by PCR using primers containing the mutations.

The 5' primers are normal and the mutation containing 3' primer sequences are:

Sma-2DID: 3' ATGCGGCCGCTAATCAATATCAGAAATTGGCCGTGGAGT

Sma-4AA: 3' AATCTAGATTATGCTGCTCCAAATTGAGAACTATTTT

Sma-4DD: 3' AATCTAGATTAGTCATCTCCAAATTGAGAACTATTTT

Sma-4SSIS: 3' AATCTAGATTATGATATGGAACTTCCAAATTGAGAAC

### **Transformation and integration**

All of the DNA constructs are amplified in DH5 $\alpha$  E. coli strain and purified by mini-prep kit (QIAGEN). The DNA concentration for injection is 20 $\mu$ g/ml using 100 $\mu$ g/ml *rol-6* marker gene (Mello et al., 1991). For each transformation, at least three lines are observed and data are shown for one representative line. For integration, more than 100 rollers are exposed to 4000rad of gamma ray from CS137 source. They are separated onto 20 new plates. After starvation, they are chunked onto 12cm diameter plates. After recovery, only rollers are picked into individual plates. The plates with pure rollers are integrated worms. The integrated worms are crossed with N2 strain to segregate any unexpected mutation.

### **Body length measurement and male tail analysis**

Eggs are collected from gravid hermaphrodites by bleaching with hypochlorite solution for five minutes. After the eggs are centrifuged and cleaned by M9 buffer, they are spread onto new plates. At 96hours old, the photos are taken and body lengths are measured. The males from non-starved plates are picked at young adult stage. The male tail sensory rays are analyzed. Only the ray fusions are scored.

### **Yeast two hybrid assay**

The cDNAs of interaction partners are cloned into pPC86 and pPDLeu yeast vectors. The yeast strain Mav203 competent cells are cultured at 30 degree until the O.D. value is

about 0.5. After centrifugation, ice cold 0.1M lithium chloride is added. The transformation is conducted by adding 5 $\mu$ g boiled salmon sperm DNA, 0.1M Lithium Acetate, 10% PEG 3350. After adding the DNA and 42°C heat shock for 5 minutes, the yeasts are incubated at 30°C for 30min and spread onto plates without Trp or Leu. The interaction is determined by spreading the transformed yeast onto the plates with 25mM or 50mM 3AT without His.

### **RNA interference**

The whole or partial cDNA of the gene is cloned into pBluescript SK+ vector. After the DNA is purified and dissolved in RNase free water, about 0.5 $\mu$ g DNA is used as template for RNA synthesis for each strand. The both strands of RNA are synthesized by using T3 and T7 RNA polymerase kit (Stratagene). Then, they are mixed, denatured and annealed. The concentration of RNA is determined by loading 1 $\mu$ l solution on agarose gel. The RNA is injected into the gonad and the progenies are scored. RNAi can also be achieved by feeding. The cDNA is cloned into vector pPD129.36 (Fire lab) and transformed into E coli HT 115. The worm is fed on this E. coli transformant to show RNAi phenotype.

## **RESULTS**

### ***sma-3* C-terminal mutants fail to rescue the body size**

Proteins	C-terminus	Description
SMA-3	SMT	Wild type
	DME	pseudophosphorylated
	AMA	Non-phosphorylatable
	YMY	Possibly functional
	$\Delta$ MT	Partially functional
	$\Delta$ SMT	Non-functional
SMA-2	SIS	Wild type
	DID	Pseudophosphorylated
SMA-4	SS	Wild type
	DD	Pseudophosphorylation
	AA	Non-phosphorylatable
	SSIS	Simulate R-Smad

Table 3.1 The designed C-terminal mutants of *sma-2*, *sma-3* and *sma-4*

SMA-2 and SMA-3 have sequence homology with R-Smads. The C-terminal sequence of SMA-3 NSMT is a variant of the canonical SSXS motif. Since the last two serines of R-Smads are phosphorylated during activation (Abdollah et al., 1997; Souchelnytskyi et al., 1997), SMA-3 is likely phosphorylated on the terminal serine and threonine residues. To test the role of the phosphorylation of SMA-3 C-terminus, we generated several *sma-3*

mutant variants (Table 3.1). We hypothesized that the pseudophosphorylated DME mutation might be constitutively active without upstream signaling. Conversely, the unphosphorylatable AMA mutation was expected to be nonfunctional. A YMY mutation was created to test whether the tyrosines could be phosphorylated by the receptor. Finally, we also generated *sma-3* deletion mutants by removing MT or SMT. We tested the ability of *sma-3* C-terminal mutants to rescue the body size of *sma-3(wk30)* mutant worms. The body length was measured in adulthood, 96 hours after egg collection at 20°C. Surprisingly, none of these constructs is functional in rescuing the body size (Table 3.2).

Strain	Transgenes	Body Size (96hrs)	Worms
N2	None	1.17±0.08	30
<i>sma-3(wk30)</i>	None	0.73±0.04	80
	<i>qCIs19(sma-3wt)</i>	1.19±0.10	90
	<i>qCIs7(sma-3-DME)</i>	0.75±0.06	42
	<i>qCIs15(sma-3-AMA)</i>	0.66±0.04	60
	<i>qCIs8(sma-3-YMY)</i>	0.77±0.05	48
	<i>qCIs5(sma-3-ΔMT)</i>	0.74±0.05	54
	<i>qCIs4(sma-3-ΔSMT)</i>	0.73±0.05	42

Table 3.2 The C-terminal mutants of *sma-3* do not rescue the body size of *sma-3(wk30)*.

Strain	Transgenes	Body Size (96hrs)	Worms
<i>sma-3(wk30)</i>	None	0.73±0.04	80
N2	None	1.17±0.08	30
	<i>qcIs7(sma-3-DME)</i>	0.72±0.06	39
	<i>qcIs15(sma-3-AMA)</i>	0.84±0.05	56
	<i>qcIs8(sma-3-YMY)</i>	1.21±0.09	48
	<i>qcIs5(sma-3-ΔMT)</i>	0.74±0.04	45
	<i>qcIs4(sma-3-ΔSMT)</i>	0.79±0.06	44
<i>lon-1(wk50)</i>	None	1.36±0.11	30
	<i>qcIs7(sma-3-DME)</i>	0.93±0.05	31
	<i>qcIs15(sma-3-AMA)</i>	1.10±0.07	36
	<i>qcIs8(sma-3-YMY)</i>	1.26±0.09	32
	<i>qcIs5(sma-3-ΔMT)</i>	1.00±0.05	44
	<i>qcIs4(sma-3-ΔSMT)</i>	1.06±0.06	34

Table 3.3 The C-terminal mutants of *sma-3* are dominant negative in body size regulation except *sma-3-YMY*. The dominant negative effects can be relieved by elimination of *lon-1* activity.

Most strikingly, the pseudophosphorylated SMA-3 DME failed to rescue. This was unexpected since pseudophosphorylated Smad1 and Smad2 have been reported to be

constitutively active (Qin et al., 2001; Petritsch et al., 2000). This result suggests that phosphate groups attached on C-terminus of SMA-3 are required for body size control. The failure of SMA-3 YMY to rescue indicates that the receptor SMA-6 is incapable of tyrosine phosphorylation. The non-functional C-terminal deletions suggest both C-terminal serine and threonine residues are required for SMA-3 activity.

### ***sma-3* C-terminal mutants are dominant negative in body size regulation**

Interestingly, the integrated arrays with each of the mutated *sma-3* genes except for YMY were dominant negative in body size regulation when they are crossed into a wild-type background (Table 3.3). This suggests that these constructs interfere with the function of the wild-type *sma-3* gene. During the cross, we observed that the heterozygotes of the integrated array are a little longer (data not shown), suggesting the inhibition is dose dependent. The SMA-3 DME mutant, which we expected to be constitutively active, is a strong inhibitor. The SMA-3 AMA is the weakest one among the dominant negatives. We can postulate at least two different mechanisms for the inhibition. First, the mutated SMA-3 proteins could compete with wild type SMA-3 by binding to the receptors or other Smad proteins. Alternatively, although these SMA-3 mutants are not functional in body size regulation, they could form partially active complexes with other Smad proteins and activate negative regulators in this pathway. In this case, DME is more likely to be the strongest inhibitor because it is similar to activated Smad and has the greatest tendency to form a heteromeric complex and interact with transcription factors.

We also tested the interaction of *sma-3* mutants with *lon-1*. *lon-1* gene encodes a PR-related protein and it is a target gene of Sma/Mab pathway. It has been reported that *lon-1* expression is downregulated by the Sma/Mab signaling pathway. *lon-1(wk50)* mutants are 20% longer than wild type and their phenotype is epistatic to the small phenotype of Sma/Mab mutants (Maduzia et al. 2002; Morita et al.2002). When the dominant negative constructs of *sma-3* were crossed into *lon-1(wk50)*, an intermediate phenotype, smaller than wild type, is seen for all constructs except the YMY mutant, which retains the long phenotype (Table 3.3). The double null mutant *lon-1sma-3* has a phenotype with body length close to but longer than wild type (Maduzia 2002). Thus, the *sma-3* C-terminal mutations are dominant negative in a *lon-1(wk50)* mutant background, causing a more severe phenotype than *sma-3* null mutations do. This result suggests the C-terminal mutations are different from null mutations in regulating target gene expression. Nevertheless, the worm body lengths are longer in *lon-1* mutant background than in worms containing the same integrated arrays in the wild type background. Thus, inactivation of *lon-1* partially relieves the effect of the dominant negatives. This is consistent with *lon-1* being a target gene downregulated by activated SMA-3, but also indicates that there must be target genes other than *lon-1* regulated by these C-terminal mutant forms.

### ***sma-3* C-terminal mutant forms are functional in male tail sensory ray morphogenesis**

In addition to the small body size, the mutants of the Sma/Mab pathway have male tail defects. Specific sensory rays have fusions and the spicules are crumpled. Since most of the C-terminal mutations we generated were dominant negative in body size control, we asked whether they are also dominant negative in male tail development by crossing them into the *him-5(e1490)* background. There is no defect in any of these transgenic worms (Table 3.4). To test the ability of *sma-3* C-terminal mutants to rescue the male tail defects of *sma-3(wk30)* animals, we cross the integrated arrays into *sma-3;him-5*. The AMA mutation abolishes the phosphorylation site, but still can rescue the male tail sensory rays. Thus, sensory ray development does not require phosphorylated SMA-3. The decreased activity of the deletion suggests a full length SMA-3 is preferred. Maybe only the backbone of the last amino acids is required. The mutation YMY does not rescue at all. Once again it is different from the others. In addition to sensory ray fusions, Sma/Mab pathway mutants have crumpled spicules at 100% penetrance. Among the C-terminal mutations, only SMA-3 DME rescues the male tail spicules in the *sma-3(wk30)* background. Others only repair the spicules a little (Table 3.4). Thus, if we assess their ability to function in the morphogenesis of the spicules, the *sma-3* constructs meet our expectations. The pseudophosphorylated mutants are functional, while the unphosphorylatable forms are nonfunctional. When the integrated arrays were crossed into *sma-6(wk7)*, none of the constructs rescue the male tail defects (Table 3.5). Therefore,

the upstream signal from *sma-6* is still required for male tail development, most likely to induce the phosphorylation of SMA-2.

Strains	Transgenes	Sensory ray fusions			N sides	crumpled spicules%
		%				
		4&5	6&7	8&9		
<i>him-5(e1490)</i>	None	0	0	5	120	0
	<i>qcIs7(sma-3-DME)</i>	0	0	5	188	0
	<i>qcIs15(sma-3-AMA)</i>	0	0	4	166	0
	<i>qcIs8(sma-3-YMY)</i>	0	0	3	94	0
	<i>qcIs5(sma-3-ΔSMT)</i>	0	0	7	120	0
	<i>qcIs4(sma-3-ΔMT)</i>	0	0	6	110	0
<i>him-5(e1490); sma-3(wk30)</i>	None	12	69	28	112	100
	<i>qcIs19(sma-3wt)</i>	0	0	6	100	0
	<i>qcIs7(sma-3-DME)</i>	0	0	7	108	5
	<i>qcIs15(sma-3-AMA)</i>	1	1	9	233	90
	<i>qcIs8(sma-3-YMY)</i>	26	66	52	46	100
	<i>qcIs5(sma-3-ΔSMT)</i>	4	32	30	63	95
	<i>qcIs4(sma-3-ΔMT)</i>	1	1	7	74	88

Table 3.4 The C-terminal mutants of SMA-3 can rescue the male tail sensory ray fusion in *sma-3(wk30)* background.

Strains	Transgenes	Sensory ray fusions			N sides	crumpled spicules%
		%				
		4&5	6&7	8&9		
<i>him-5(e1490)</i>	None	0	0	5	120	0
<i>him-5(e1490);</i>	None	12	52	29	63	100
<i>sma-6(wk7)</i>	<i>qcIs7(sma-3-DME)</i>	6	63	45	200	100
	<i>qcIs15(sma-3-AMA)</i>	8	55	29	124	100
	<i>qcIs8(sma-3-YMY)</i>	14	67	31	132	100
	<i>qcIs5(sma-3-ΔSMT)</i>	14	59	34	112	100
	<i>qcIs4(sma-3-ΔMT)</i>	6	65	30	176	100

Table 3.5 The *sma-3* C-terminal mutants can not rescue the sensory fusion of *sma-6(wk7)*.

### Pseudophosphorylated SMA-2 is constitutively active

We wondered whether there is an absolute requirement for SMA-2 phosphorylation, or whether either SMA-2 or SMA-3 phosphorylation is sufficient for male tail development.

To address this question, we assessed the ability of pseudophosphorylated SMA-2 DID (mutated from SIS) to function in the male tail. We first needed to generate a rescuing *sma-2* clone. We tried to rescue *sma-2(e297)* using *sma-2* upstream sequences plus its cDNA, but it did not work. The genomic DNA of *sma-2* is long including two large introns that proved difficult to clone. We created a construct without the two introns.

After transforming into *sma-2(e297)*, the *sma-2* clone shows rescuing function in both body size and male tail (Table 3.4 & 3.5). This indicates that the two introns are not required for *sma-2* function. A transcriptional fusion of *sma-2* promoter sequences with GFP shows *sma-2* expresses in pharynx, intestine, hypodermis and neurons, similar to the expression pattern of *sma-3* (Figure 3.1). This is consistent with *sma-2* and *sma-3* acting together in the signaling pathway. We generated a SMA-2 DID variant (Table 3.1) by PCR and transformed into *sma-2(e297)*. Interestingly, unlike SMA-3 DME, this pseudophosphorylated Smad could rescue body size although not as efficiently as wild type (Table 3.6). So, the SMA-2 DID is constitutively active in body size control. Just like SMA-3 DME, pseudophosphorylated SMA-2 can also rescue male tail sensory ray fusions and crumpled spicules (Table 3.7). As the pseudophosphorylation of either SMA-2 or SMA-3 could rescue male tail defects, it indicates these constructs could be independent from the receptor *sma-6*. We hypothesized that the pseudophosphorylation of both SMA-2 and SMA-3 could control male tail patterning without upstream signaling. Thus, we integrated both of the constructs into *him-5* and *sma-6(wk7);him-5(e1490)*. In the wild type background, the integrated array is dominant negative in body size but the male tail has no defects (Table 3.6 & 3.7). Although the integrated array has the ability to rescue the male tail sensory ray fusions and crumpled spicules of *sma-2(e297)* or *sma-3(wk30)*, in the *sma-6(wk7)* background, there is no improvement in the male tails at all (Table 3.7). This result suggests that at least one of SMA-2 and SMA-3 should be

Strain	Transgenes	Body Size (96hrs)	Worms
N2	None	1.17±0.08	30
<i>sma-2(e297)</i>	None	0.77±0.06	33
	<i>qcIs39(sma-2wt)</i>	1.19±0.09	45
	<i>qcIs41(sma-2-DID)</i>	1.07±0.09	30

Table 3.6 The pseudophosphorylated SMA-2 is constitutively active in body size regulation.

Strains	Transgenes	sensory ray fusions			N sides	% defected spicules
		%				
		4&5	6&7	8&9		
<i>him-5(e1490)</i>	None	0	0	5	120	0
<i>sma-2(e297);</i>	None	10	63	28	110	100
<i>him-5(e1490)</i>	<i>qcIs39(sma-2wt)</i>	0	0	8	100	0
	<i>qcIs41(sma-2-DID)</i>	0	0	10	95	0
<i>sma-6(wk7);</i>	None	12	52	29	63	100
<i>him-5(e1490)</i>	<i>qcIs42(sma-2-DID+ sma-3-DME)</i>	11	51	22	120	100

Table 3.7 The pseudophosphorylation of *sma-2* can rescue the male tail defects and the double pseudophosphorylation of *sma-2* and *sma-3* can not rescue the male tail of *sma-6(wk7)* mutant.

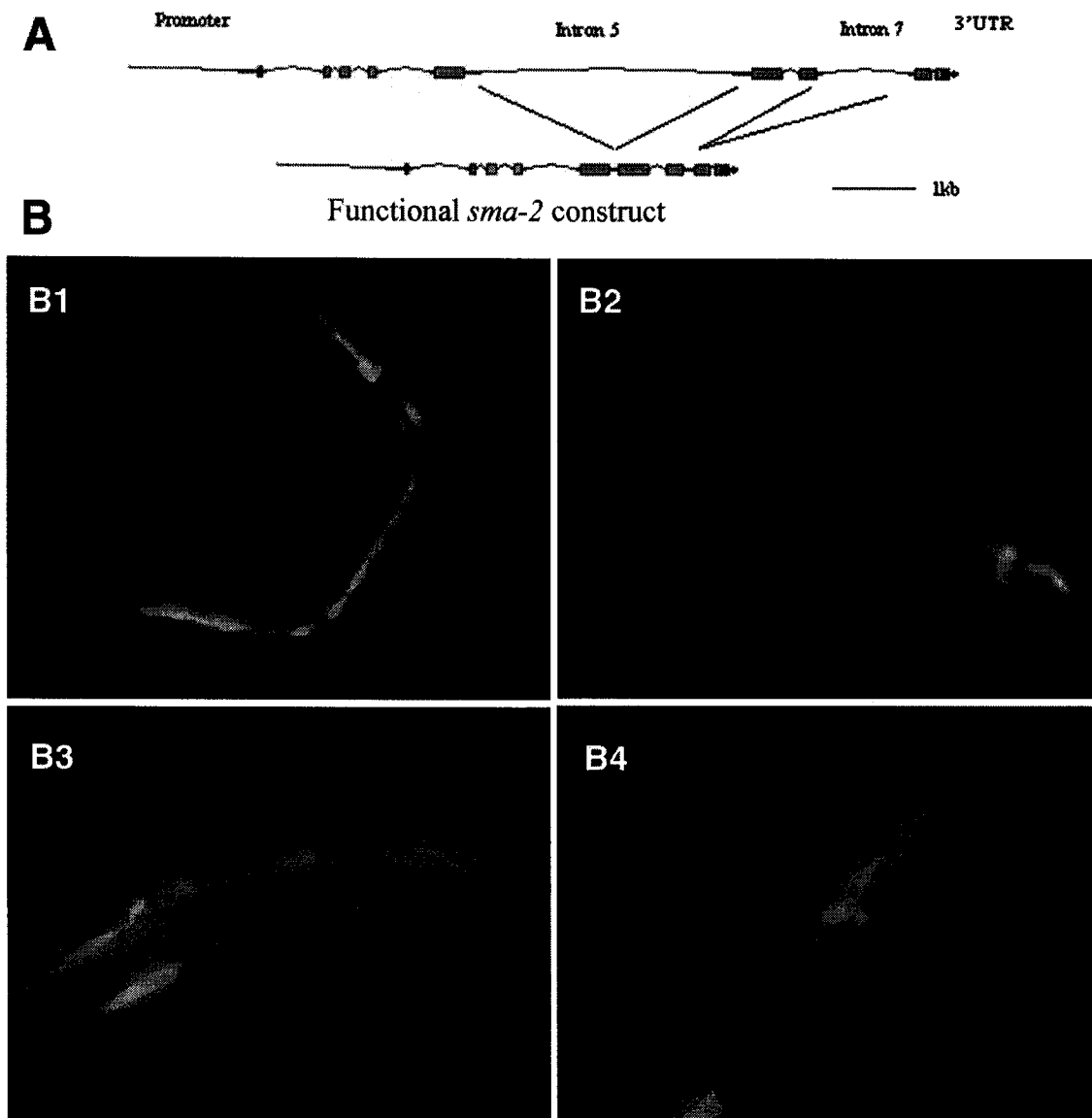


Figure 3.1 (A) The genomic clone of *sma-2* does not include the two big introns. (B) The expression pattern of *sma-2::gfp* transcriptional fusion construct. B1) the whole view; the expression in B2) pharynx, B3) intestine, B4) hypodermis.

truly phosphorylated, rather than pseudophosphorylated, for normal male tail morphogenesis. However, we cannot exclude the possibility that male tail development also requires a Smad independent, but SMA-6 dependent, signaling output.

### **SMA-3 interacts with LIN-31**

It is shown that Smad proteins form complex and MH1 autoinhibits MH2 in the protein-protein interactions (Hata et al., 1997). With the phosphorylation of the C-terminal residues, the intermolecular interaction can be increased. Using the yeast two hybrid, we could not detect any interaction between SMA-2 and SMA-3. Probably, in the yeast strain we used, the Smad proteins are not phosphorylated (data not shown). *lin-31* is implicated in the Sma/Mab pathway because *lin-31* mutant males have crumpled spicules identical to *sma-3* mutants (Baird et. al. 1999). *lin-31* encodes a forkhead transcription factor (Miller et al., 1993). We tested for molecular interactions between LIN-31 and the Smads using the yeast two hybrid system. We detect that wild type SMA-3 interacts with the forkhead transcription factor LIN-31. The SMA-3 DME interacts with LIN-31 more strongly, while the SMA-3 AMA shows much lower affinity (Figure 3.2A). This suggests that the C-terminus of SMA-3 participates in the interaction. It is further possible that the phosphorylation of the SMA-3 C-terminus enhances its interaction with LIN-31. When we tested whether SMA-3 MH1 and MH2 are required for the interaction, we found that both MH1 and MH2 (wild type) interact with LIN-31, but the interaction between MH1 and LIN-31 is much weaker (Figure 3.2B). The interaction between LIN-31 and wild type

SMA-2 or pseudophosphorylated SMA-2 DID is not detectable (Figure 3.2C). The interaction of SMA-4 and LIN-31 could not be tested because of the self-activation of SMA-4. Since *lin-31* mutants have crumpled spicules, but are not small and the male tail sensory rays are normal (Baird et al. 1999), it suggests that the interaction between SMA-3 and LIN-31 is only essential in the development of the spicules. It has been reported that the forkhead transcription factor Fast-1 has a Smad interacting motif (SIM) (Randall et al. 2004). In addition, a novel Smad2 interaction motif, the Fast/FoxH1 motif (FM) is present in all known Fast/FoxH1 family members. The FM is necessary and sufficient to bind active Smad2/Smad4 complexes. The FM only binds phosphorylated Smad2 in the context of activated Smad complexes. Although the FM sequence is not conserved in LIN-31, there could be other motifs in LIN-31 that play similar roles.

### **SMA-3 C-terminal mutant forms have different localization**

We previously reported that *sma-3* expresses in hypodermis, pharynx and intestine from late embryo through the larval and adult stages. When a GFP tag is attached to the N-terminus of SMA-3, the fusion protein is still functional and localizes mainly in the nucleus (Wang et al., 2002). We tagged our SMA-3 mutant forms with N-terminal GFP. All of these mutated proteins were expressed normally and nuclear localized except YMY (Figure 3.3). Although AMA could not be phosphorylated by SMA-6, its presence in the nucleus confirms our previous finding that phosphorylation is not strictly necessary for nuclear localization (Figure 3.3CD). The other dominant negative constructs have similar

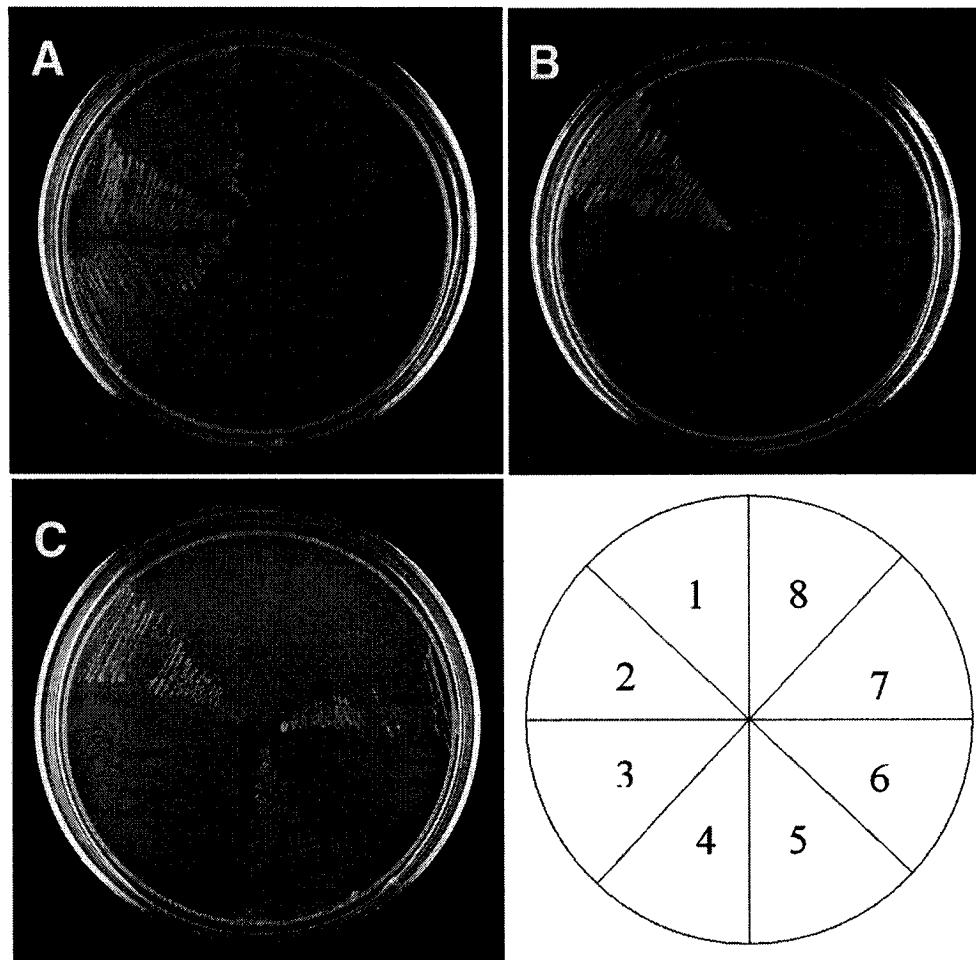


Figure 3.2 The yeast two hybrid test of the interaction between *lin-31* and *sma-3* or *sma-2* (A) The interaction can be detected between *sma-3* and *lin-31* using His selection plate (50mM 3AT). 1) *sma-3*-AMA:*lin-31*, 2) *sma-3*-DME:*lin-31*, 3) *sma-3*:*lin-31*, 4) *lin-31*:vector, 5) *sma-3*-AMA:vector, 6) *sma-3*-DME:vector, 7) *sma-3*:vector, 8) vector:vector. (B) There is no detectable intereaction between *sma-2* and *lin-31* using His selection plate (25mM 3AT). 1) *sma-3*:vector, 2) *sma-3*:*lin-31*, 3) *lin-31*:vector, 4) vector:vector, 5) *sma-2*:*lin-31*, 6) *sma-2*:vector, 7) *sma-2*-DID:*lin-31*, 8) *sma-2*-DID:vector. (C) Both of MH1 and MH2 of *sma-3* can interact with *lin-31* using His selection plate (25mM 3AT). 1) *sma-3*:vector, 2) *sma-3*:*lin-31*, 3) *lin-31*:vector, 4) vector:vector, 5) *sma-3* MH2:*lin-31*, 6) *sma-3* MH2:vector, 7) *sma-3* MH1:*lin-31*, 8) *sma-3* MH1:vector. Note: The *sma-2* or *sma-3* cDNA is inserted into pPDleu vector and *lin-31* cDNA is inserted into pPC86 vector. The yeast strain used for all of the tests is Mav203.

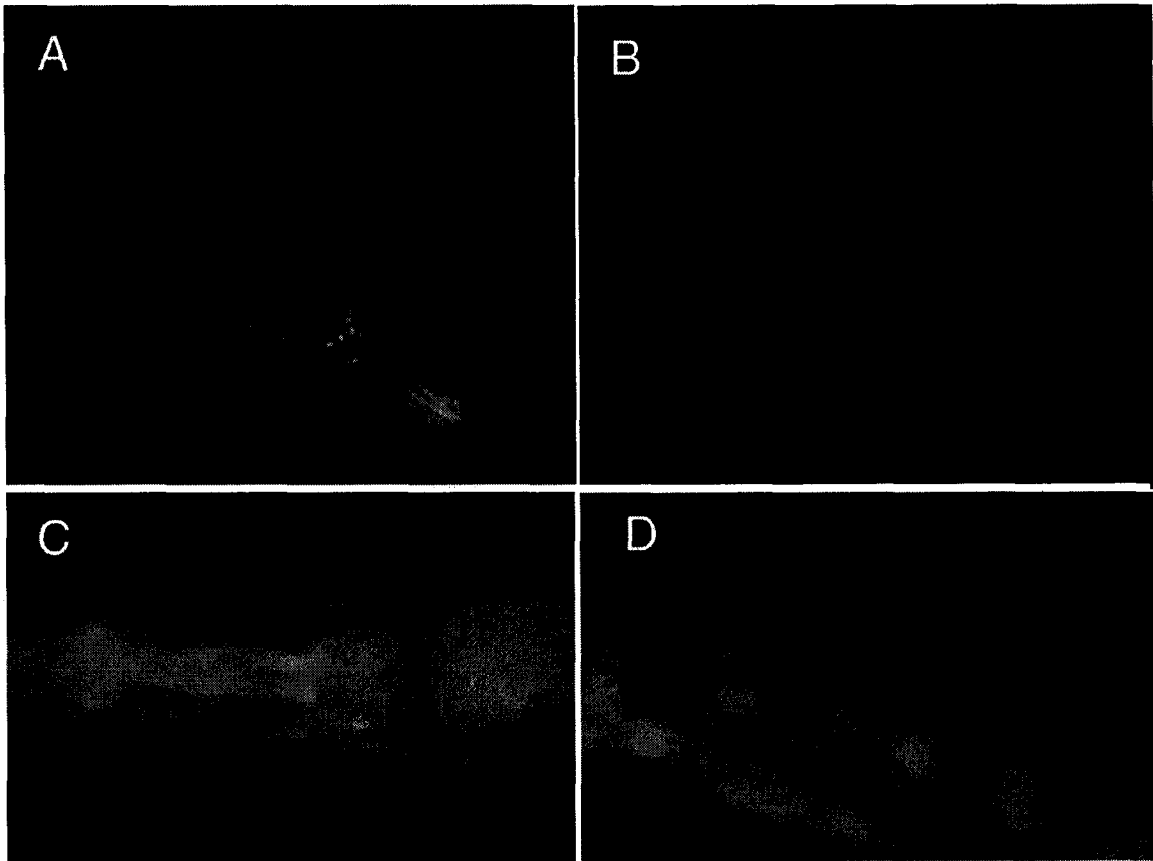


Figure 3.3 The SMA-3 YMY localizes on the membranes. The dominant negative SMA-3 C-terminal mutants accumulate in nucleus similar to wild type SMA-3. (A, B) The SMA-3 YMY protein accumulates on membranes especially nuclear membrane and does not enter the nucleus. (C, D) The SMA-3 AMA protein accumulates in nucleus as same as wild type SMA-3. The other dominant negative SMA-3 mutants have similar localization.

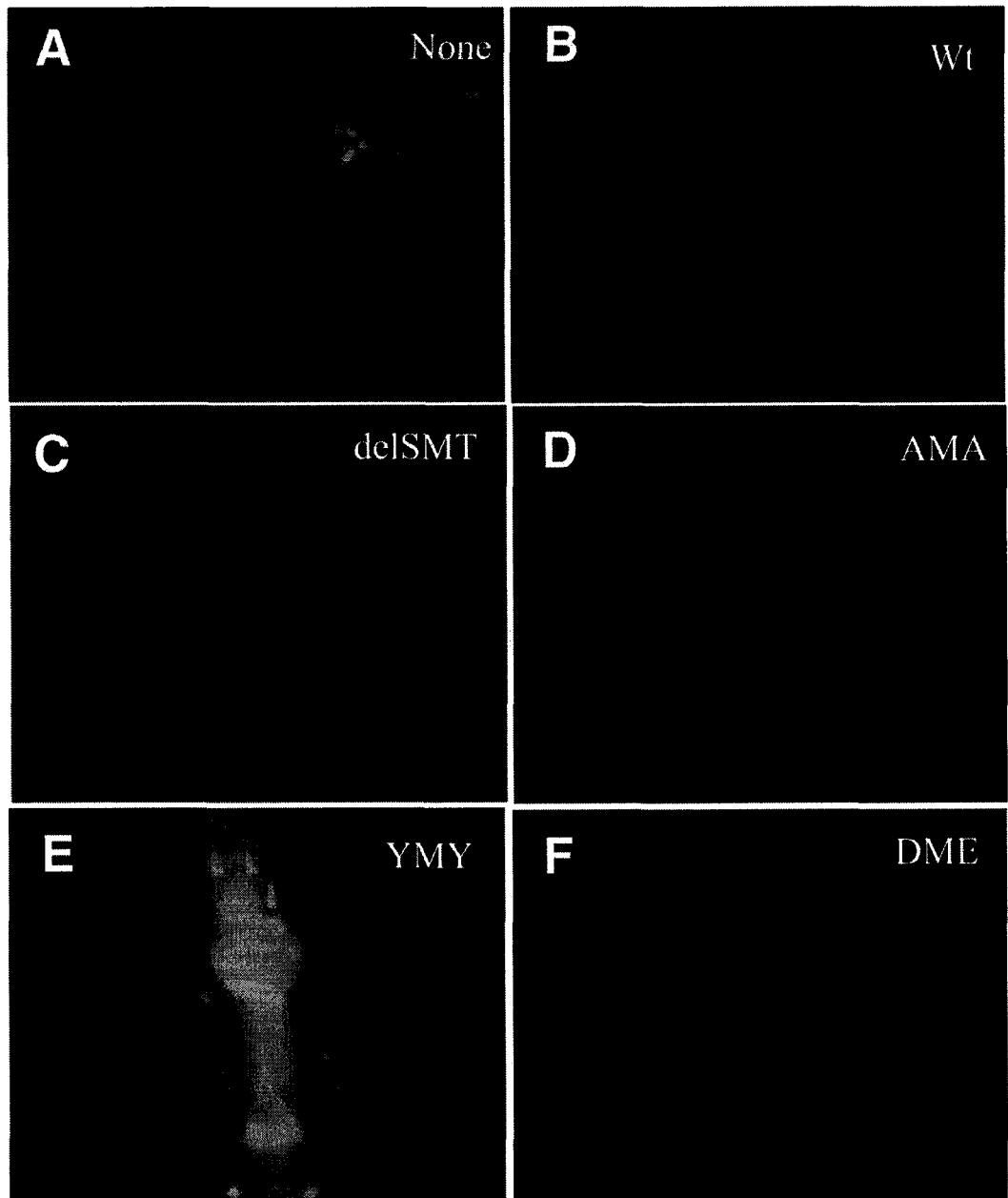


Figure 3.4 The SMA-3 C-terminal mutants could activate the negative feedback loop except SMA-3 YMY. All of the *sma-3* constructs are co-injected with *sma-3:gfpC*. (A) The fluorescence of *sma-3:gfpC* alone, (B) the wild type *sma-3* could activate the feedback loop, which is also shown in (C) *sma-3*DSMT, (D) *sma-3* AMA and (F) *sma-3* DME. (E) *sma-3* YMY shows the protection of the SMA-3:GFPC protein.

localization, but the fluorescence intensity is much lower. The expression of SMA-3 YMY is the most unusual. We find it localizes on membranes, concentrating around the nuclear membrane, but not entering the nucleus (Figure 3.3AB). We see similar localization of SMA-3 YMY in the *sma-6(wk7)* background. Thus, it is unlikely that the membrane localization is induced by SMA-6. It suggests that SMA-3 YMY binds with other molecules located on the membranes. It is unknown if YMY is sufficient for this kind of translocation.

#### **The SMA-3 mutations differ in their abilities to turn on the feedback loop**

When GFP is inserted at the C-terminus of SMA-3, the construct does not have much activity, but accumulates at a high level. Functional SMA-3 can downregulate this SMA-3:GFPC accumulation by a negative feedback loop (Wang et. al., 2002). To assess the mechanism of dominant negativity, we tested whether the SMA-3 C-terminal mutants could turn on the feedback loop. We co-injected the *sma-3::gfp* C-terminal fusion with the mutated *sma-3* genes. The fluorescence intensity shows that the SMA-3 AMA and SMA-3  $\Delta$ SMT downregulate SMA-3::GFPC protein accumulation just like wild type SMA-3. But, with SMA-3 DME, the fluorescence of SMA-3::GFPC is almost undetectable. The SMA-3 YMY behaves more as a protector because the fluorescence of SMA-3::GFPC looks stronger (Figure 3.4).

Thus, the C-terminal mutations retain the ability to turn on the feedback loop that induces

SMA-3 degradation. Since the SMA-3 YMY is not nuclear localized, it is not surprising that it does not turn on the feedback loop. It is clear that SMA-3 YMY is not dominant negative in body size control and it does not rescue *sma-3(wk30)* male tail morphogenesis in part because it never enters the nucleus.

### **The C-terminus of SMA-4 is not important for its activity**

The C-terminal amino acid residues of SMA-4 are two serines, while those of its homolog Smad4 are LD. To test whether these C-terminal serines have any significant function, we produced several mutations of SMA-4. The SS was changed into SSIS (more like an R-Smad), DD (negatively charged) and AA (remove the hydroxyl groups). It is not surprising that all of the three constructs function as well as wild type SMA-4 (Table 3.6). The construct with SSIS can't substitute for any other Smads as it failed to rescue *sma-2* or *sma-3* mutants (data not shown). This suggests, not surprisingly, that the identity of the Smad is not determined by the most C-terminal amino acids, but by the internal sequences which are necessary for receptor activation and subtype-specific functions. The results also tell us that the C-terminus of SMA-4 is different from that of SMA-2 or SMA-3, in that it is dispensable for SMA-4 function. In the crystal structure of the Smad4 MH2 domain, the C-terminus is randomly located (Shi Y et al. 1997), unlike that of phosphorylated Smad2. Probably, the C-termini of Co-Smads are not involved in complex formation or other intermolecular interactions.

Strain	Transgenes	Body Size (96hrs)	Worms
N2	None	1.17±0.08	30
<i>sma-4(e729)</i>	None	0.79±0.05	40
	<i>qcEx58(sma-4wt)</i>	1.19±0.07	42
	<i>qcEx59(sma-4AA)</i>	1.18±0.07	38
	<i>qcEx60(sma-4DD)</i>	1.19±0.08	32
	<i>qcEx61(sma-4SSIS)</i>	1.21±0.09	34

Table 3.8 The *sma-4* C-terminal mutants functions as same as wild type in body size regulation.

## DISCUSSION

### The role of the C-terminus of SMA-3

Several functional roles have been ascribed to the phosphorylation of R-Smad C-termini by type I receptors, most notably the stimulation of heteromeric complex formation and nuclear accumulation. To test the functional roles of Smad C-termini in vivo, we have created SMA-2 and SMA-3 mutant forms and introduced them into wild-type and mutant *C. elegans* strains. Our results are consistent with a role for C-terminal modification in Smad complex formation, but not in R-Smad nuclear accumulation. Furthermore, we

suggest that the phosphorylation of the C-terminus may play a previously unidentified role in transcription co-factor binding. If the C-terminal mutants have different affinities for tissue-specific transcription co-factors, then this would explain their differential abilities to rescue diverse developmental outcomes. Our yeast 2-hybrid experiments testing the interactions of LIN-31 with SMA-3 mutant forms support this conclusion.

The dominant negative effect of SMA-3 DME suggests that with the DME residues, SMA-3 is functional to turn on the feedback loop. However, when the C-terminus is not phosphorylated, the complex does not rescue body size. Thus, the phosphorylated C-terminus of SMA-3 is critical to control transcription of genes necessary for body size regulation. Inside the nucleus, when the MH1 domain of SMA-3 binds DNA, the MH2 domain could bind transcription co-factors. These transcription factors are likely able to distinguish the status of the C-terminus. For body size, only the phosphorylated C-terminus with has a high affinity for the relevant co-factor. Since hypodermal expression of *sma-3* is necessary and sufficient to rescue the body size of *sma-3(wk30)* (Wang et al. 2002), the transcription factors responsible for body size should be expressed in hypodermal cells. In spicule formation, SMA-3 DME is functional because the forkhead transcription factor LIN-31 can interact with pseudophosphorylated C-terminus. This interaction could be strong enough to control the spicule formation. In the sensory rays, the full-length, but non-phosphorylatable SMA-3 is sufficient to rescue the ray fusions. It suggests that phosphorylation of SMA-3 is not strictly required for the sensory

ray development. Thus, we believe that it is likely that the binding requirements of specific transcription factors determine the level of SMA-3 construct activities in different cell types.

### **The complex formation of the SMA proteins**

Smad complex formation has been studied by using gel shift, column elution and crystallization, and different models have been suggested. The main issue is whether the Smads function in a dimer or trimer. A great deal of evidence supports the heterotrimer model. In the crystal structure of the Smad4 MH2 domain (Shi et al., 1997), the protein forms a homotrimer. The most C-terminal amino acids are disordered. In the crystal structure of phosphorylated Smad2 or unphosphorylated Smad1, the C-terminal tail interacts with a positive charged surface of a neighboring subunit in a homotrimer manner (Qin et al., 2001; Wu et al., 2001). Based on this model, the Smad complex in *C. elegans* could be formed through such an interaction. In the sequence alignment, we find all of the positively charged residues are highly conserved among *C. elegans* Smads. The heterotrimer could be formed in different ways. The Smad2-Smad4 trimer contains one Smad4 and two Smad2 molecules (Inman et al., 2002). The complex of Smad4 and pseudophosphorylated Smad3 shows a similar ratio (Chacko et al., 2001). An interaction between R-Smads after phosphorylation is also suggested (Wu et al., 2001). Even the trimer formed by Smad2, Smad3 and Smad4 has been reported (Feng et al. 2000). When *sma-2*, *sma-3* and *sma-4* were first found in *C. elegans*, the heterotrimer model was

suggested because the body size control needs all three of them (Savage et al. 1996). The double and triple mutants of *sma-2*, *sma-3* and *sma-4* do not have more severe phenotypes (Savage-Dunn et al. 2000). *sma-4* is the Co-Smad, which is not a target of activated receptor kinase. The C-terminal mutations of SMA-4 reveal that the last two serines are not important for function, and so are dispensable for complex formation. The R-Smad proteins, SMA-2 and SMA-3, could be phosphorylated during signaling. We cannot exclude the possibility that SMA-2 and SMA-3 form complexes with SMA-4 independently. But such complexes are unlikely to have any easily observed function. In the case of male tail sensory rays, the functional complex must contain both SMA-2 and SMA-3, and at least one of them must be really phosphorylated, instead of pseudophosphorylated. Since SMA-2-DID and SMA-3-DME together fail to rescue any of the defects in *sma-6(wk7)*, it is possible that they do not form a stable complex with SMA-4. In other words, a real phosphorylated C-terminus is required to initiate the complex formation. Because SMA-4 C-terminus is not phosphorylated, we can call it the end of the complex. Which one is the middle subunit? The phosphorylated C-terminus is more negatively charged than other forms and has a stronger tendency to form a homotrimer complex (Wu et al. 2001). Even the pseudophosphorylated Smad1LC has 4278-fold higher trimerization ability than that of wild type (Qin et al. 2001). SMA-4 is not phosphorylated during signaling, thus the autoinhibition between MH1 and MH2 domain could be weak in comparison with unphosphorylated R-Smad. It is likely that phosphorylated R-Smad protein first recruits SMA-4. All of the residues forming the

positively charged pocket are conserved in SMA-4. In the L3 loop region, SMA-4 has even more positively charged residues. Such a dimer could find the third subunit easily

Phosphorylation Status	Body size	Sensory rays	Spicules	Feedback loop
SMA-2-OH, SMA-3-OH	-	-	-	-
SMA-2-Ⓢ, SMA-3-Ⓢ	+	+	+	+
SMA-2-Ⓢ, SMA-3-DME	-	+	+	+
SMA-2-OH, SMA-3-DME	-	-	-	ND
SMA-2-Ⓢ, SMA-3-AMA	-	+	-	+
SMA-2-DID, SMA-3-Ⓢ	+	+	+	ND
SMA-2-DID, SMA-3-DME	-	-	-	ND

Table 3.9 The combinations of SMA-2, SMA-3 of different phosphorylation states have different effects on body size, male tail sensory rays and spicules. “Ⓢ” means phosphorylated C-terminal residues. “+” means functional and “-” means non-functional.

because the structure is more open. Pseudophosphorylated SMA-3 could bind to the SMA-2-SMA-4 dimer and induce the dominant negative effect through a feedback loop. But, it is not functional to regulate the transcription of other target genes, which are responsible for body size control. Other kinds of mutated SMA-3 could bind to the dimer more weakly. Alternately, SMA-2 could bind on the SMA-3-SMA-4 dimer. The results from SMA-2 DID suggest that the complex is stable enough and functional for body size regulation. According to our data on male tails, both kinds of trimers are functional for male tail development. Possibly, both of the complexes could bind the DNA or inhibit the function of unknown proteins, which induces the sensory ray fusions. Thus, different branches of the signaling require different complexes. Based on all of our data (Table 3.9), we propose that body size regulation needs SMA-2-SMA-3-SMA-4 trimer and the feedback loop needs SMA-3-SMA-2-SMA-4 trimer. The male tail does not have any specific requirement (Figure 3.5).

### **Possible mechanisms of the feedback loop**

Feedback loops have been identified in many signaling pathways. It is a common mechanism to regulate signal intensity and efficiency. The activity of transducers is downregulated once the goal has been reached. The cell will be more sensitive to the receipt of new signals. It could be achieved by modification or degradation of the proteins. In vertebrate TGF- $\beta$  pathways, the Ski/Sno and Smurf genes are negative regulators of the pathways (reviewed by Shi and Massagué, 2003). To test the functions

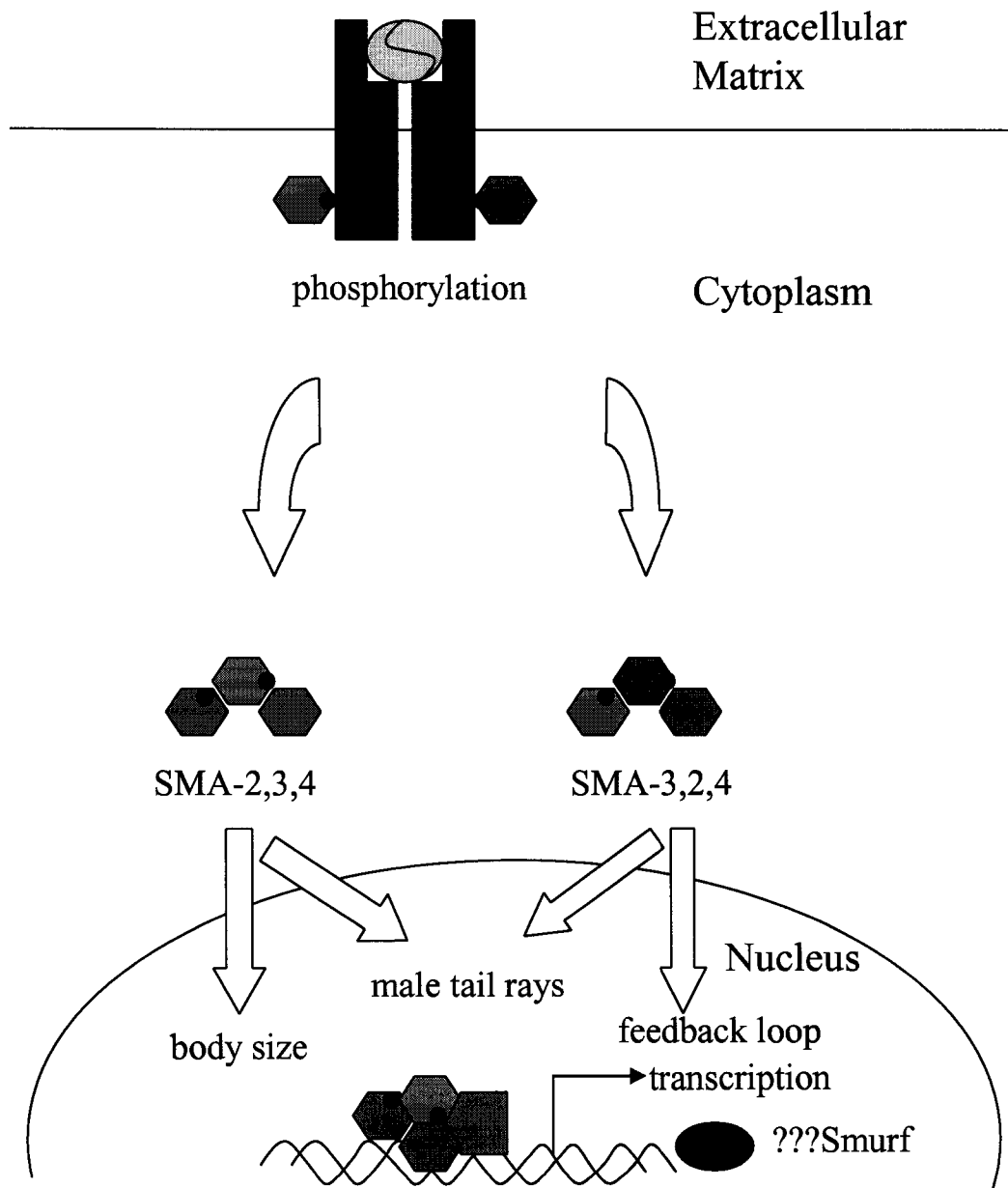


Figure 3.5 The differential activity model of Smad trimers

of *C. elegans* Smurf homologs, we cloned the cDNAs of the three with highest identity, Y64BR4.1a, Y92H12A.2 and F45H7.6. We have previously found that RNAi of *sma-2*, *sma-3* and *sma-4* could phenocopy the mutant phenotypes both by injection or feeding (unpublished data). The RNAi of the Smurf homologs, however, did not give any phenotype. It is possible that only a portion of SMA-2 and SMA-3 is phosphorylated. Under normal conditions, the Smurf and Smad proteins are in a balance. When the Smurf expression is inhibited by RNAi, the Smad concentration increases. But the amount of phosphorylated Smad does not change because the ligand is limiting. Similarly, overexpression of Smad/*sma-3* does not make the worm longer (Wang et al. 2002). The overexpression of ligand *dbl-1* does induce the long phenotype (Suzuki et al., 1999). Additional experiments will be necessary to determine the roles of these Smurf genes or other factors in the feedback loop. It might be possible that the feedback loop in *C. elegans* is completely novel, independent of the Smurf genes.

## NOTE

This part of studies is submitted to EMBO journal. Thanks to Dr Pokay Ma and Joni Seeling for their kindly suggestions on the paper.

Thanks to Kim Lab for *lin-31* construct and the assistance of Kolesnick Lab in the DNA integration.

## Chapter IV

### Other observations

#### The deletions of two loops abolish SMA-3 activity

In the sequence of Smad proteins, there are highly conserved loops that are important for the structure and function. As experiments have shown, the L3 loop in the MH2 domain plays important roles in specificity of receptor recognition and Smad complex formation, and may also interact with other transcription co-factors (Hata et al., 1997; Wu et al., 2000; Shi and Massagué, 2003). Missense mutations identified in *sma-2(e502)* and *sma-3(e491)* result in a glycine changing into arginine or aspartate near the L3 loop (Savage et al., 1996; Savage-Dunn et al., 2000). The mutations show a dominant negative effect on the body size, but an intermediate phenotype in the male tail sensory ray fusions (around 30%-40% in ray 6 and ray 7 fusions). Thus, we designed the partial deletion of the L3 loop in SMA-3 by removing the amino acids, WGED. We also constructed the deletion of the loop PDIS from the MH1 domain. The MH1 domain is responsible for DNA binding and MH2 domain has transcription activation function. Neither of the deletions rescues the null mutant *sma-3(wk30)* and neither are dominant negative in body size (Table 4.1). It suggests that both loops are important for *sma-3* activity in body size regulation. When we look at the male tail, SMA-3 $\Delta$ WGED shows no activity to rescue the male tail ray fusions, but SMA-3 $\Delta$ PDIS partially rescues the ray fusions (Table 4.2). It indicates that the *sma-3* MH1 domain is not as critical as the MH2 domain in male tail

Strain	Transgenic genes	Body Length (96hrs)	Worms
N2	None	1.17±0.08	50
	<i>qcEx23(sma-3ΔWGED)</i>	1.19±0.09	46
	<i>qcEx28(sma-3ΔPDIS)</i>	1.15±0.08	42
<i>sma-3(wk30)</i>	None	0.73±0.04	80
	<i>qcEx23(sma-3ΔWGED)</i>	0.76±0.06	45
	<i>qcEx28(sma-3ΔPDIS)</i>	0.75±0.05	38

Table 4.1 Deletion of the loop WGED or PDIS abolishes SMA-3 activity in body size regulation.

Strain	Transgenic genes	Frequency of ray fusion%			Sides
		4 & 5	6 & 7	8 & 9	
<i>him-5(e1490)</i>	None	0	0	5	120
<i>sma-3(wk30);</i>	None	12	69	28	112
<i>him-5(e1490)</i>	<i>qcEx23(sma-3ΔWGED)</i>	11	62	22	100
	<i>qcEx28(sma-3ΔPDIS)</i>	4	39	25	80

Table 4.2 Deletions of WGED and PDIS from SMA-3 show different activity to rescue the male tail.

sensory rays. This conclusion is supported by the previous data of *sma-3* missense

mutants (Savage et al., 1996; Savage-Dunn et al., 2000). The missense mutations in MH1 domain could give weak alleles and mutants in MH2 domain always have intermediate and strong phenotypes in male tails. The mutant *wk20* has a threonine mutation in the L2 loop of the MH1 domain (Shi et al., 1998). The residue might be involved in autoinhibition because it is located in the L2/L4 double loop region and tumorigenic mutations have been found in this region. The mutations are proven to enhance the autoinhibition between MH1 and MH2 (Hata et al., 1997; Shi et al., 1997; Shi et al. 1998). Both *sma-2(e502)* and *sma-3(e491)*, which have mutations in the L3 loop of the MH2 domain, have intermediate phenotypes in male tails, probably because changing glycine into other amino acids only disrupts the structure in MH2 slightly, not completely abolishing the ability to form a complex, but the activity should be much lower. All of the *sma-2* and *sma-3* mutants are strong alleles in body size. Possibly, the male tail only requires a little Smad activity, but body size needs a high level of activity. To further test this idea, we could create more missense mutations by site-directed mutagenesis or EMS screening.

**The long phenotype induced by *dbl-1* overexpression can be suppressed by the C-terminal mutants of *sma-3***

The dominant negative *sma-3* C-terminal mutants cause small body size in N2 worms. This dominant negative effect can be partially relieved by a *lon-1* null mutation (Chapter III). The overexpression of the ligand, *dbl-1*, also induces a long phenotype (Suzuki et al.,

1999). But, the overexpression of *sma-3* does not induce any new phenotype (Wang et al., 2002). Null mutations of *sma-2* or *sma-3* are not longer than *sma-6*, *daf-4* or *dbl-1* null mutants. Thus, the signal responsible for body size must go through the Smads. The overexpression of *dbl-1*, designated *dbl-1(++)*, probably induces a larger portion of R-Smads to be phosphorylated. Only activated Smad is functional to enable the body to grow longer. Wild type worms with *sma-3* C-terminal mutant constructs are small except those with *sma-3-YMY*. The dominant negative SMA-3 mutants could induce SMA-3 protein degradation. The concentration of wild type SMA-3 protein is surprisingly low to activate downstream gene expression. So, for the body size, the worms carrying the dominant negative *sma-3* genes are just like null mutants, especially worms with *sma-3-DME*. When the C-terminally mutated *sma-3* genes are transferred into *dbl-1* overexpressing worms, all of the worms are small. We failed to generate the homozygous *dbl-1(++);sma-3-DME*, probably because it is lethal. Interestingly, the *dbl-1(++)* worm with *sma-3-YMY* is a little smaller than wild type (Table 4.3). The result indicates that SMA-3-YMY probably gets a chance to enter the nucleus and becomes a weakly dominant negative protein. When the *dbl-1* and *sma-3-YMY::GFP* are injected into wild type worms, the worms with the extrachromosomal array is not long and the fluorescence is almost invisible (data not shown). It indicates that the SMA-3-YMY protein goes into the nucleus and finally is degraded. *dbl-1* overexpression has no effect on body size in the presence of the dominant negative *sma-3* and might release *sma-3:YMY* from the membrane. This result confirms that the DBL-1 signaling for body size act via SMA-3.

The SMA-3 mutants still are dominant negative even in the presence of excessive DBL-1 and can completely block the signal.

Strain	Transgenic genes	Body Length (96hrs)	Worms
N2	None	1.17±0.08	50
<i>sma-3(wk30)</i>	None	0.73±0.04	80
<i>dbl-1(++)</i>	None	1.34±0.11	42
	<i>qcIs15(sma-3-AMA)</i>	0.93±0.06	40
	<i>qcIs8(sma-3-YMY)</i>	1.09±0.06	35
	<i>qcIs5(sma-3-ΔSMT)</i>	0.88±0.05	32
	<i>qcIs4(sma-3-ΔMT)</i>	0.84±0.05	30

Table 4.3 The long phenotype induced by *dbl-1* overexpression is suppressed by the dominant negative *sma-3* mutants.

### Seam cell expression of *sma-3* also rescues the body size

*sma-3* is expressed in intestine, pharynx and hypodermis. In the hypodermal expression of *sma-3*, we never see that it expresses in the seam cells. We want to see if seam expression of *sma-3* also could rescue body size. The *sma-3::gfpN* gene is inserted after *elt-5* promoter, which specifically expresses in seam cells (Koh and Rothman, 2001). We see strong fluorescence in seam cells (Figure 4.1). It is much stronger than that from *Pvha-7:gfp:sma-3*, which expresses in hyp7. This suggests that the Smad feedback loop

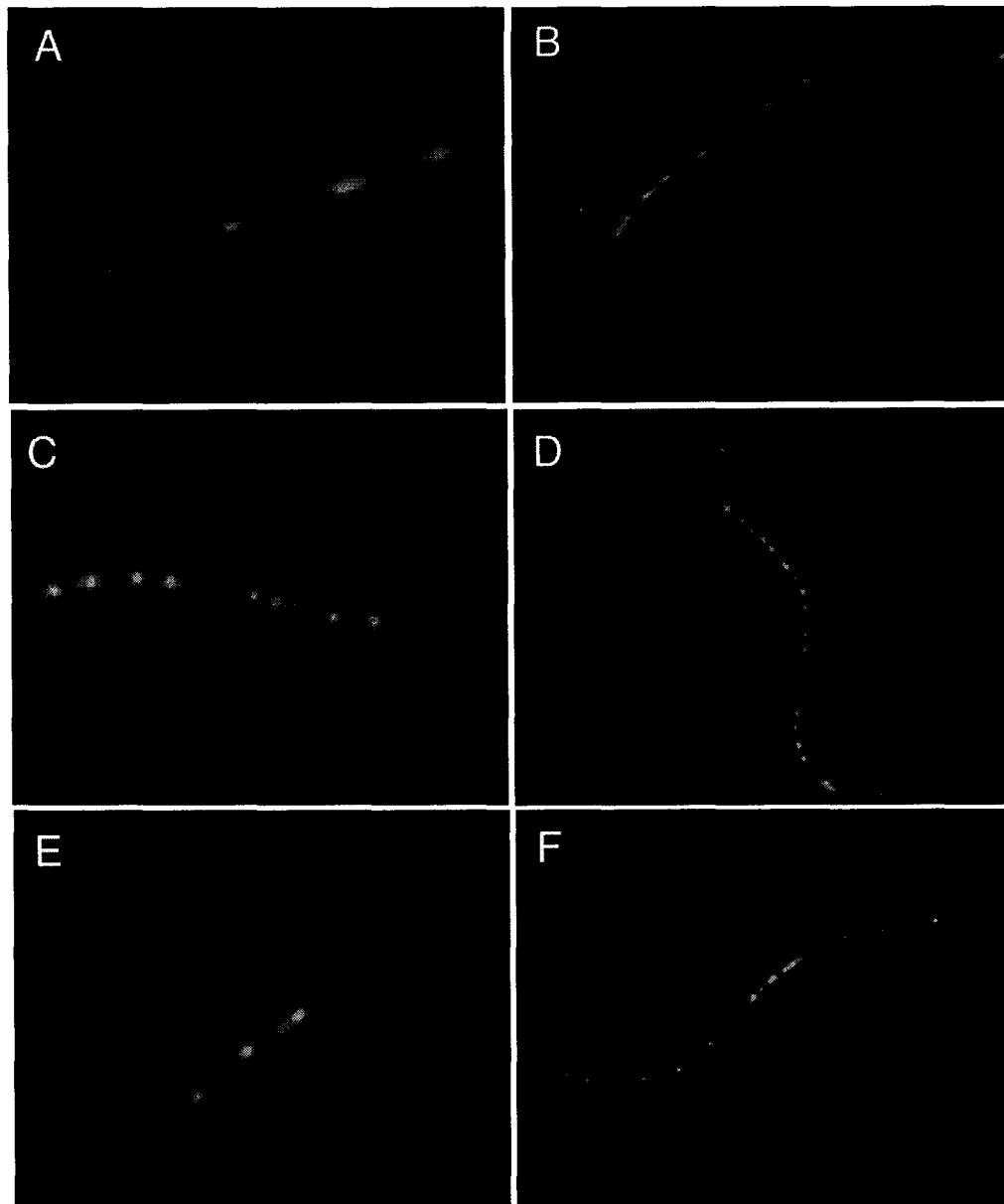


Figure 4.1 Expression pattern of *Pelt-5:sma-3* translational GFP fusion gene in wild type and *eff-1* mutant background. (A,B,C,D) in wild type (E,F) in *eff-1(hy21)* mutant. (A,B) between seam cell mitosis (C,D) during seam cell mitosis. (A,C,E) higher magnification (B,D,F) overview of the seam cells.

does not exist in seam cells. The protein is mainly localized in the nucleus. The integrated array *qcIs18(Pelt-5:gfp:sma-3)* completely rescues the small body size of the mutant *sma-3(wk30)* (Table 4.4). But, we find that there also is weak fluorescence in *hyp7*. This could result from the *elt-5* expression in *hyp7* or from delivery of SMA-3:GFP protein through seam-*hyp7* fusion. The second reason is more reasonable because the fluorescence in *hyp7* is much weaker than that in seam cells.

Strain	Transgenic genes	Body Length (96hrs)	Worms
N2	None	1.17±0.08	50
<i>sma-3(wk30)</i>	None	0.73±0.04	80
	<i>qcIs18(Pelt-5:sma-3)</i>	1.12±0.07	42
<i>eff-1(hy21)</i>	None	0.83±0.05	22
	<i>qcIs18(Pelt-5:sma-3)</i>	0.79±0.05	24

Table 4.4 Seam expression of *sma-3* can rescue the body size.

To confirm this hypothesis, we crossed this integrated array into *eff-1(hy21)*, which is also small in body size (Mohler et al., 2002). The array failed to rescue the *eff-1* mutant. The fluorescence is limited to seam cells and that in *hyp7* is undetectable. We discovered that the protein does not accumulate in some nuclei anymore. This suggests that the nuclear accumulation in these cells requires cell fusion and without it, the cells might lose their identities. In the worm with our construct *Pelt-5:sma-3*, SMA-3 expressed in seam

cells might be phosphorylated and then delivered into *hyp7* and it is functional to rescue body size.

#### ***sma-4* hypodermal expression is sufficient to rescue body size**

The expression patterns of *sma-2* and *sma-3* R-Smad genes have been well studied. It has been shown that hypodermal expression of *sma-3* is necessary and sufficient to rescue body size. But, the expression pattern of *sma-4* is still unclear. It is interesting that a construct without the C-terminus of *sma-4* still can rescue the body size (Baird personal communication). It is reasonable to speculate that *sma-4* also expresses in hypodermal cells. So, we expressed *sma-4* in *hyp7* and seam cells by using *vha-7* and *elt-5* promoters. The result shows that *hyp7* expression of *sma-4* completely rescues the body size, but the seam expression fails to rescue. It has been reported that many of TGF- $\beta$  pathway components express in *hyp7* and *hyp7* expression is sufficient and necessary to rescue body size (Yoshida et al., 2001; Maduzia et al., 2002; Wang et al., 2002).

Strain	Transgenic genes	Body Length (96hrs)	Worms
N2	None	1.17 $\pm$ 0.08	50
<i>sma-4(e729)</i>	None	0.79 $\pm$ 0.05	28
	<i>qcEx67(Pvha-7:sma-4)</i>	1.19 $\pm$ 0.07	32
	<i>qcEx66(Pelt-5:sma-4)</i>	0.83 $\pm$ 0.05	44

Table 4.5 Hypodermal expression of *sma-4* rescues body size.

So, it is not surprising that *hyp7* expression of *sma-4* also rescues body size. In contrast, seam cell expression of *sma-3* also rescues body size, but that of *sma-4* fails to rescue the mutants (Table 4.5). This result might be interesting because the difference might be related to the different roles of *sma-3* and *sma-4*. SMA-4 is not phosphorylated during signaling. SMA-4 protein delivered through seam-*hyp7* fusion might be too dilute. The required concentration of SMA-4 might be much higher than that of SMA-3. Furthermore, phosphorylated SMA-3 is required for body size, and unphosphorylated SMA-3 could negatively compete with activated SMA-3. Co-Smad nuclear localization depends on complex formation. High concentrations of SMA-4 protein could provide a mechanism to increase the likelihood of nuclear accumulation. Thus, the body size regulation has different requirements for SMA-3 and SMA-4 proteins: phosphorylated SMA-3 and a large amount of SMA-4.

#### **The hairpin intron of *sma-2* may be a negative regulator**

Near the 3' end of the *sma-2* gene, there is an intron of about 1kb. Its first half and second half are completely complementary. During the PCR, it gave us a lot of trouble. Using half of the sequence to blast against the worm genome, we find its homologous sequences are all introns. Most of them are in genes related to transcription, such as DNA dependent RNA polymerase I largest subunit. We have shown that the intron is not required for *sma-2* activity because the construct without this intron is still functional (chapter III). But, the *sma-2* gene with only half of the intron cannot rescue the body size at all (data

not shown). Probably, during RNA processing, the intron is removed easily if it is a hairpin. But, if only half of the intron is included in the pre-mRNA, it could be bound with unknown processing proteins that might induce RNA degradation. It might also be possible that alternative splicing of this intron generates another Smad protein, which inhibits SMA-2 function. It has been reported that RNAi could target the pre-mRNA in the nucleus (Bosher et al., 1999). The hairpin intron might be regulated by a similar mechanism. It may be interesting if we could insert the intron into other genes, such as *sma-3* or *sma-4*. The expression of the genes might decrease and the level of activity might be downregulated.

#### ***eff-1* mutants could be suppressed by *lon-1* in body size**

The *eff-1* gene encodes a type I transmembrane protein, which is required for the cell fusions in *C. elegans*. Mutations in the extracellular domain of EFF-1 completely block epithelial cell membrane fusion without affecting other cellular events such as cell generation, patterning, differentiation, and adhesion (Mohler et al. 2002). EFF-1 is a key component in the mechanism of cell fusion, a process essential to normal animal development. Interestingly, the *eff-1* mutants have small body size. The strain *eff-1(hy21)* has an identical body size with *sma-6(wk7)*. This phenotype might result from the absence of the communication between the hypodermal cells, which are supposed to fuse in wild type. In particular, the *hyp7* syncytium is important for collagen synthesis and we have shown *sma-3* expression in *hyp7* is sufficient to rescue body size. Without normal

cell fusion, it is possible that hypodermal cells do not contain enough DNA as template, i.e. the hypodermal ploidy decreases. The cells fused with *hyp7* in wild type worm might lose their identities in *eff-1* mutants. They might be isolated cells and not receive enough information to grow. We speculate that the endoreduplication of their DNA is not activated. The double mutant, *lon-1(wk50); eff-1(hy21)*, has a long phenotype just like *lon-1 (wk50)* alone (Table 4.6). But the shape of the vulva and the tail spike indicate that the *eff-1* mutation is also present. Thus, the small body size of *eff-1* mutants is completely suppressed by *lon-1*. Possibly, cell fusion is required to inhibit *lon-1* expression. Highly expressed *lon-1* may cause the *eff-1* mutants to be small. It will be clear if we look at the *lon-1:gfp* expression in *eff-1* mutant background. It has been reported that the hypodermal

Strain	Body Length (96hrs)	Worms
N2	1.17±0.08	50
<i>eff-1(hy21)</i>	0.83±0.05	32
<i>lon-1(wk50)</i>	1.36±0.11	30
<i>eff-1(hy21);lon-1(wk50)</i>	1.38±0.12	44

Table 4.6 *eff-1* mutants can be suppressed by *lon-1* mutants in body size.

ploidy increases in *lon-1* mutants (Morita et al., 2002). The double mutants, *lon-1(wk50); eff-1(hy21)* may also have increased hypodermal ploidy. Thus, in ploidy, *lon-1* suppresses

*eff-1* and causes the long body size in the double mutant.

## **NOTE**

Thanks to Dr William Mohler for *eff-1(hy21)* and *eff-1(oj55)* strains and Scott Baird for sharing information of *sma-4* gene expression.

## Chapter V

### Conclusion and Discussion

#### The Smad complex in hypodermis regulates body size

The TGF- $\beta$  signaling pathways have multiple roles in *C. elegans* development. The Dauer pathway and Sma/Mab pathway share a common type II receptor, *daf-4*. The *daf-4* null mutants have combination of the defects of the two pathways, i.e., dauer constitutive, egg laying defective, small in body size and male tail ray fusions (Patterson and Padgett, 2000). It has been reported that neuronal expression of *daf-4* could rescue the dauer constitutive phenotype and egg laying defects, and hypodermal expression of *daf-4* could rescue the body size (Inoue et al., 2001). Thus, *daf-4* expression in each tissue has specific role. It is reasonable to assume that *daf-4* expression in other tissues have unknown functions and the defects have not been described yet. The hypodermal expression of SMA-6, the type I receptor of Sma/Mab pathway, rescues the body size (Yoshida et al., 2001). Our study also proves that hypodermal expression of *sma-3* (Wang et al., 2002) and *sma-4*, the Smad genes, rescues the body size. The data from *lon-1* (Maduzia et al., 2002), one possible target gene of the signaling, support the idea that Sma/Mab signaling in the hypodermis is responsible for body size regulation. The model of the pathway could be described as the *dbl-1* ligand is secreted from neurons (Suzuki et al., 1999) and received by hyp7. The signaling induces hyp7 to grow and hyp7 secretes more collagen to make a bigger cuticle. The properties of cuticle could affect the body

size and limit the growth of interior organs.

The activated R-Smads (*sma-2*, *sma-3*) form a heterotrimer with Co-Smad (*sma-4*) and go into the nucleus to regulate downstream gene expression. Each Smad has a DNA binding domain MH1 and transcription activation domain MH2. The MH2 domain is required for the hetero- or homo- oligomerization. But, MH1 represses the hetero-oligomer formation through auto-inhibition (Hata et al., 1997). The hetero-oligomeric interaction is stimulated by the phosphorylation of the C-terminal serines. In the crystals, Smads form homotrimers, which indicates that Smads might function in a heterotrimer (Shi et al., 1997; Qin et al., 1999; Wu et al., 2001; Qin et al., 2001). The three Smad genes in Sma/Mab pathway were predicted to function in a trimer as soon as they were identified (Savage et al., 1996). The triple mutant of the three genes is not smaller than the mutants of any one gene (Savage-Dunn et al., 2000). We designed the C-terminal mutants of *sma-3* and they proved to be dominant negative in body size. But they are functional in male tail sensory rays. This result suggests that the male tail and body size have different requirements of *sma-3*. The body size requires real phosphorylation and male tail does not. The SMA-3 protein accumulation is downregulated by a feedback loop (Wang et al., 2002). The pseudophosphorylated SMA-3-DME is the most powerful one to turn on the feedback loop. It is also the only one that could rescue the crumpled spicules. Thus, SMA-3-DME should have the highest affinity to bind the SMA-2 and SMA-4 dimer. Finally, the double pseudophosphorylation of SMA-2 and SMA-3 has no activity to rescue the male tail. This result suggests that the

trimer formation needs at least one R-Smad to be really phosphorylated.

### **The role of the Sma/Mab pathway in male tail development**

The null mutants of the ligand *dbl-1*, receptors *sma-6*, *daf-4* and Smads *sma-2*, *sma-3* and *sma-4* have male tail defects, fused sensory rays and crumpled spicules. The male tail defects of any Smad null mutants are as severe as those of null mutants in *sma-6*. Therefore, it is unlikely that male tail development is also regulated by additional *sma-6* dependent but Smad independent pathways. The ray 6 and ray 7 fusions have only been found in Sma/Mab pathway mutants. Since there are a lot of small mutants that have no defects in the male tail (Savage-Dunn et al., 2003), body size and male tail morphogenesis might be regulated by different downstream genes. The posterior seam cells V5, V6, and T, are the ancestors of the male tail sensory rays. Ray 6 is generated by cell V6.ppppa and ray 7 is generated by T.apapp. The fusion of these two rays could result from multiple reasons. One possible explanation could be that the ray 7 precursor cell might be more anterior and take the same identity as ray 6 in the Sma/Mab mutants. Thus, the TGF- $\beta$  pathway has a specific role to specify cell identities during male tail development. Maybe one or more of the Smad target genes have the function to control the cell migration or differentiation. The male tail ray identities are regulated by Smad trimers. It does not matter whether phosphorylated SMA-2 or SMA-3 binds SMA-4 protein first. The last subunit to be recruited needs not be phosphorylated at all. As long as it can bind the dimer formed by the other two Smads, even with low affinity, the whole

complex is functional for male tail sensory rays. So, the missense mutations in the amino-terminal MH1 domain of SMA-2 or SMA-3 could still be at least partially functional in male tail rays because only the C-terminal MH2 domain is required for Smad hetero-oligomeric interactions (Hata et al., 1997). The early termination mutants of *sma-3* especially in MH1 domain should be strong alleles in male tail phenotype. But, the missense mutants in MH1 domain of *sma-3* are weak alleles. The missense mutants of *sma-3* MH2 domain are intermediate or strong alleles (Savage-Dunn et al., 2000). There are not many *sma-2* mutants that have been sequenced. Both *sma-2(e1491)*, partial deletion in MH1 domain, and *sma-2(e502)*, missense mutation in the L3 loop of MH2 domain, are intermediate alleles in male tail development.

The gene *mab-21* is required for the choice of alternate cell fates by the cells in the *C. elegans* male tail. It is suggested that *mab-21* acts as part of a short-range pattern-formation mechanism. Each of the changes in cell fate brought about by *mab-21* mutants can be interpreted as a posterior-to-anterior homeotic transformation (Chow et al., 1995). *mab-21* functions cell autonomously for choice of ray identity by ray 6. We observed the *sma-3* expression in ray 5, ray 7 and ray 9. The protein localization is different in *sma-6(wk7)* background (Figure 5.1). As ray 7 frequently takes the identity of ray 6 in *sma-3* mutants, the reason might be the abnormal activation of *mab-21* expression in ray 7. To test this hypothesis, we could look at the transcription level of *mab-21* in the mutants of the TGF- $\beta$  pathway.

The gene *mab-5* has been shown to control the identity of ray 4. When *mab-5* activity

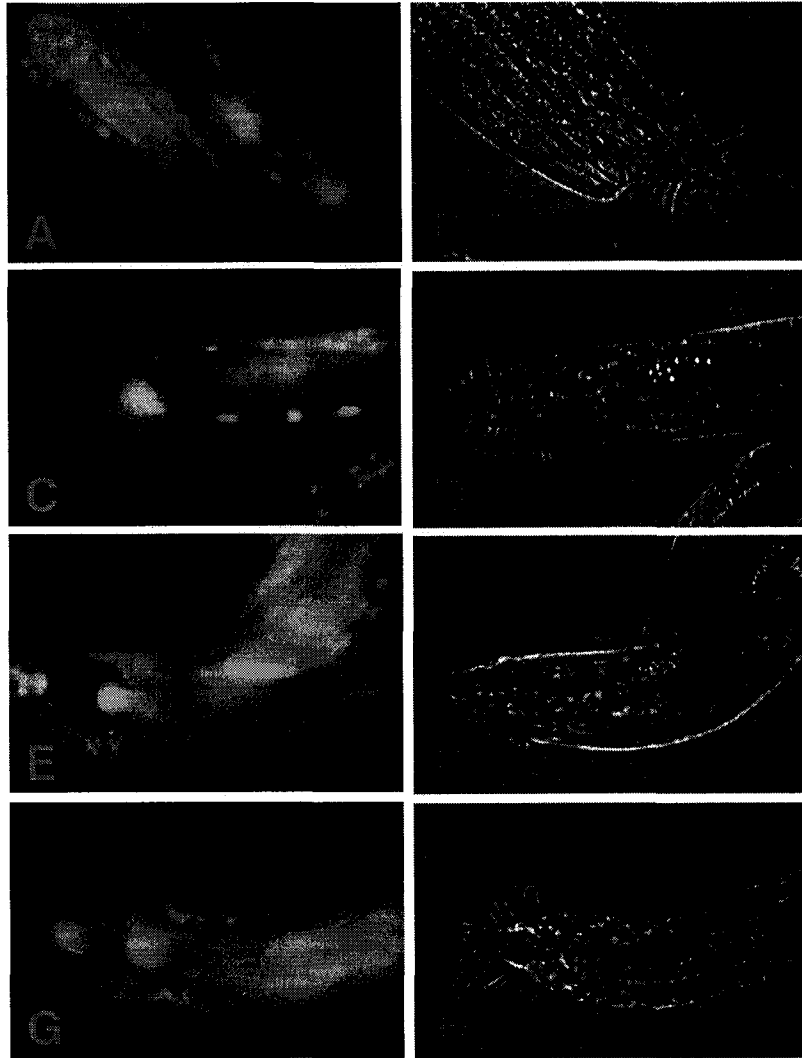


Figure 5.1 The *sma-3:GFP(C)* expression in male tails. (A,B) in wild type; (C,D) in *sma-2(e502)* mutant; (E,F) in *sma-4(e729)*; (G,H) in *sma-6(wk7)*. The arrows show the nucleus localization in some of cells. The arrow heads indicate the ray 6-7 fusions.

decreases, ray 4 undergoes a posterior-to-anterior transformation and takes the identity of ray 3 (Chow and Emmons, 1994). In the *dbl-1* overexpression worms, ray 4 also took the identity of ray 3 and fused with ray 3 (Suzuki et al., 1999). The hypothesis is that *dbl-1* signaling might inhibit *mab-5* expression. It can be tested by looking at *mab-5* expression levels in *dbl-1(++)*, or at the phenotype of *dbl-1* overexpression in *mab-5(e1751)* gain-of-function mutants.

### **Seam-hyp7 fusion may play a role in body size control**

The *hyp7* cell is a syncytium with 139 nuclei in adult worms. It covers almost the whole body except the head and the tail. The cell is like a tube to keep all interior organs organized. The *hyp7* is the major cell to secrete cuticle. So, it has an inner surface, which is in contact with inner organs and separated by body fluid. And its outer side is covered by cuticle, with the seam cells attached at both lateral sides. During each larval stage, each seam cell divides. One daughter cell keeps its identity and the other daughter cell fuses into *hyp7*. There are also similar fusions happening at the ventral and dorsal, and even anterior and posterior sides of *hyp7*. One way to control the body development plan is that the signal is stored in specific cells and the message is delivered by fusion into *hyp7*. For the synthesis of cuticle especially during the molt, the program might be stored in seam cells. The posterior seam cells become sensory rays in male tail development. Seam cell expression of *sma-3* rescues body size, but it does not rescue male tail ray 6 and ray 7 fusions (data not shown). Possibly the T cell, the ancestor of ray 7, has no

expression of *sma-3* from *Pelt-5:sma-3* construct. The *eff-1* mutants are small in body size, but have no fusions of the male tail rays (data not shown). This indicates that the cell fusion defect does not affect ray identities. To test the idea that seam-hyp7 fusion influences body size, we could try hyp7, seam and hyp7-seam expression of *eff-1* by the promoters *vha-7(hyp7)*, *elt-3(hyp7)*, *elt-5(seam)*. Alternatively, we could try to express a dominant negative *eff-1* mutant in the seam cells. The worms will be small.

### **Smad target genes in *C. elegans***

Upon TGF- $\beta$  stimulation, the expression of several hundred genes changes positively or negatively (Kang et al., 2003). Both activation and repression use the same activated Smads. Target gene selection depends on cell type and transcription co-factors. Most of the targets have one or more copies of Smad binding elements (Shi and Massagué, 2003). There are a lot of Smad target genes that have been found in the mammalian TGF- $\beta$  pathway, such as inhibitors of differentiation (Id1, Id2, and Id3), c-myc and p15 (Kang et al., 2003; Feng et al., 2000; Frederick et al., 2004). The I-Smads and Smurf genes are also regulated by the Smad transcription complex. The promoter of Smad7 contains two copies of SBE and its expression is activated by both TGF- $\beta$  signaling and BMP signaling (Denissova et al., 2000). In the absence of TGF- $\beta$  signals, Ski/Sno prevent the activation of transcription by Smad proteins that find their way to the nucleus (Wotton and Massagué, 2001). But in *C. elegans*, not many TGF- $\beta$  target genes and co-factors have been found. *daf-5* is found to be a homologue of Ski (da Graca et al., 2004), which

cooperates with *daf-3* Smad to regulate gene expression. The loss-of-function mutants are dauer defective. The novel component *sma-9*, a *Drosophila* Schnurri homologue, functions to control body size and male tail ray 8 and ray 9 fusions (Liang et al., 2003). But in body size, it is only required during larval stages. Thus, body size regulation in adults needs another transcription co-factor. A few putative Smad target genes have been identified by analyzing the long mutants. One of them, *lon-1*, regulates ploidy and the mutants with increased hypodermal ploidy have a long phenotype (Morita et al., 2002; Maduzia et al., 2002). And the small mutants have decreased hypodermal ploidy. Thus, the small phenotype could be induced by decreased collagen synthesis without enough DNA templates because the body is covered by the cuticle, which is the exoskeleton of the worm. *lon-3* encodes a collagen gene, but the loss-of-function mutant is long and gain-of-function mutant is short (Flemming et al., 2003; Suzuki et al., 2003). Thus, *lon-3* expression should be inhibited by *dbl-1* signaling. To identify other target genes, DNA microarray experiments could be done comparing the expression levels of genes in *dbl-1* loss-of-function mutants to wild type. The results could be confirmed by checking the promoters for SBE sequence and using yeast one hybrid to test the interaction of Smad proteins and the promoters. The target genes should include many collagen genes and cytoskeleton related genes. In the male tail development, although it is unclear, the target genes could be *mab-5*, *egl-5*, *mab-21* and other genes that control the identities of the male tail sensory rays.

### How does the worm become small?

The small worms are not always TGF- $\beta$  pathway defective. Sometimes, it is hard to tell if a worm is dumpy or small. The dumpy worm is shorter but the width is identical to wild type, e.g. *dpy-7* and *sqt-1*. The body shape of small worms look like wild type, but the whole body shrinks, i.e. the volume is smaller. There are many mechanisms that could induce the small body size. Most importantly, the deficiency of collagen synthesis could be the real reason for *dbl-1/sma-6* mutants becomes small. It has been reported that human Smad3 gene stimulates type I collagen transcription in skin fibroblasts (Chen et al., 1999). But, there are also some other mechanisms for worm body size decreasing.

*sma-1* mutants are one type of small worm without defects in the TGF- $\beta$  pathways. *sma-1* gene encodes  $\beta$ -H-spectrin and is required for lumen formation. In *sma-1* mutants, the extent of embryonic elongation is decreased and the *sma-1* larvae, although viable, are shorter than normal. *sma-1* mutants elongate as embryos, but at a lower speed. *sma-1* RNA is expressed in epithelial tissues in the *C. elegans* embryo: in the embryonic hypodermis at the start of morphogenesis and subsequently in the developing pharynx, intestine and excretory cell. SMA-1 is a component of an apical membrane skeleton in the *C. elegans* embryonic hypodermis (McKeown et al., 1998). In *sma-1* mutants, the size of the pharynx decreases dramatically compared with that in TGF- $\beta$  mutants (Wang et al., 2002). There are still many small mutants which have no defects in *dbl-1* signaling.

Another related phenotype is long worms. *lon-1* encodes a PR-related gene and its expression level increases in *sma-6* null mutants (Maduzia et al., 2002; Morita et al.,

2002). The double mutants of *sma-6;lon-1* and *lon-1sma-3* are long, but close to wild type. This result suggests that *lon-1* cannot be the only target gene for body size regulation. The hypodermal ploidy difference becomes obvious only in adults. The ploidy decrease does not explain the small body size of TGF- $\beta$  mutants in larval stages. *lon-3* is another interesting gene, which encodes a collagen protein and shows dosage dependent regulation of body size. The loss-of-function mutants are long and gain-of-function mutants are small. The double mutant *sma-2(502); lon-3(e2175)* is small but a little longer than *sma-2(e502)*. This suggests that *lon-3* could be one of the target genes of *sma-2* and that *sma-2* has more target genes. Double mutants *lon-1;lon-3* are even longer than any single mutant (Nyström et al., 2003). This suggests that *lon-1* and *lon-3* function in parallel to each other. The experiments with tissue specific expression of TGF- $\beta$  components suggest that the hypodermis is the major organ to control the body size. The body surface is mainly covered by hyp7. It is responsible for the collagen synthesis. Interestingly, LON-3 accumulation is upregulated in *dbl-1* loss of function mutants (Suzuki et al., 2003). With LON-3 collagen protein, the cuticle could be thicker or harder to expand which inhibits the body extension. Among Smad target genes, there must be another type of collagen which enables the body to extend and makes the cuticle more permeable. The loss of function of the genes should make the body small or dumpy. The expression of these genes is stimulated by *dbl-1* signaling. Candidate genes are *dpy-2*, *dpy-7*, *dpy-10*, *dpy-13*, *sqt-1*, and *sqt-3*, which are collagen genes and whose loss of function mutants are dumpy or squat (Nyström et al., 2003). The long phenotype of *lon-3*

mutants could be suppressed by *sqt-1* loss-of-function. Possibly the ratio between two kinds of collagens determines the body size.

### **The dauers of small mutants**

The mutants of *dbl-1*, *sma-6*, *sma-2*, *sma-3* and *sma-4* are only small, not defective in dauer formation. But, the behavior of the *sma-2* and *sma-3* null mutants is a little different from the others. As normal, the mutants enter dauer when conditions become more severe, e.g. without food. The shape of the dauers looks similar to the wild type. But the dauer worms aggregate together, parallel to each other (Figure 5.2). This pattern is not found in any other worm. The dauers survive much longer than wild type. Until the plates are completely out of water, the population of worms is always large when they are chunked onto a new plate. This suggests that the *sma-2* and *sma-3* null mutants have a better strategy to survive. It is not clear why it is observed only in *sma-2* and *sma-3* mutants, even not in *sma-4* mutants. In the wild, it is better that the worms spread under the severe conditions. It is good for the species to survive because not everywhere is suitable for living.

What kind of specific activity accounts for such a difference? One possible explanation is that the normal Smad trimer inhibits this behavior. It might be induced by SMA-2 and SMA-4 dimer or SMA-3 and SMA-4 dimer before the worm goes into dauer. The complex could be a trimer with two copies of the same R-Smad (SMA-2 or SMA-3) and one copy of Co-Smad (SMA-4). This hypothesis is supported by the observation that

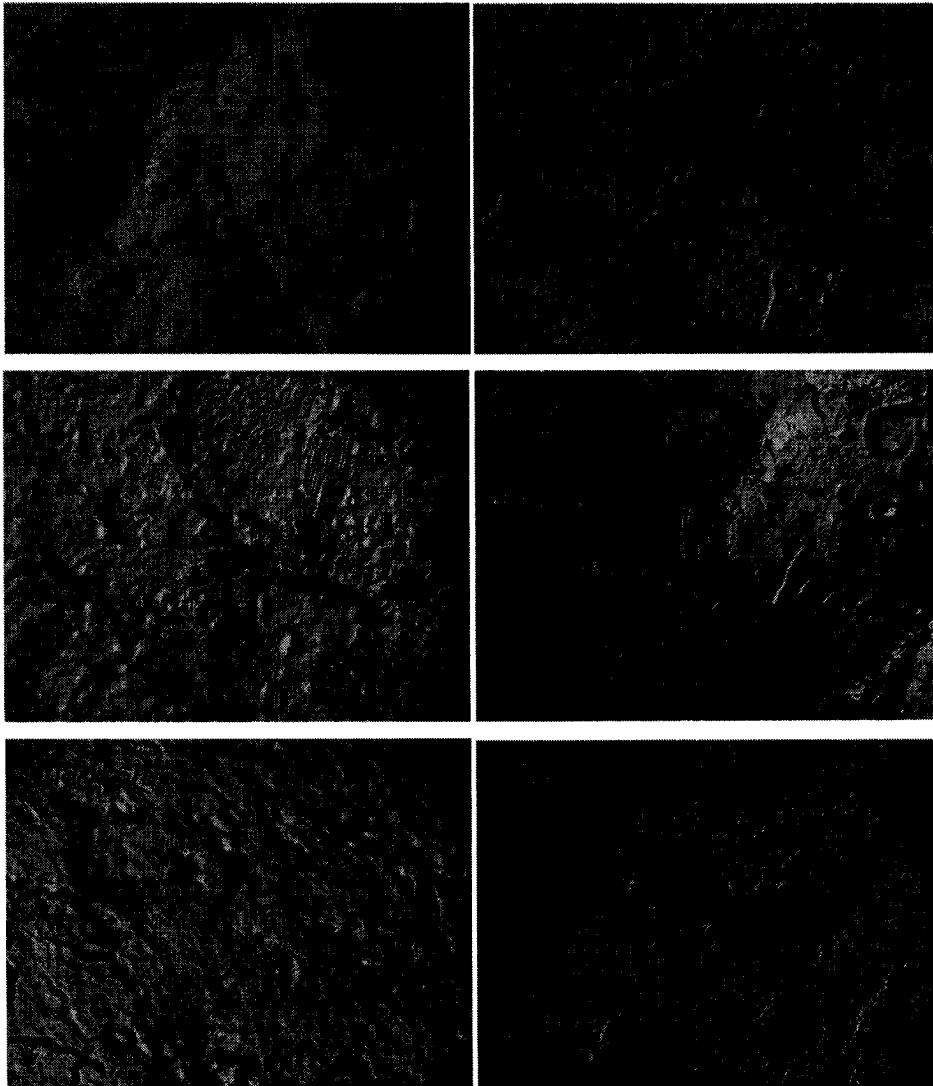


Figure 5-2 The dauers of *sma-2* and *sma-3* mutants form a special pattern, parrallel to each other (the center of each photo). This pattern can not be found in wild type, *sma-6*, *sma-4* or *sma-2sma-3* double mutants.

*sma-3sma-2* double mutants do not form such dauers. It might be interesting if any further investigation suggests new functions of the *C. elegans* Smads.

#### **NOTE**

Some parts of these ideas are supported or come from the book, *C. elegans* II, Cold Spring Harbor Lab Press.

## Prospect

The *C. elegans* is small and easy to deal with. A lot of genes first identified in worm and their homologs are discovered in mammalian genome later. Although the genome size of *C. elegans* is relatively small, it contains most of the homologs of human genes. The sequence of *C. elegans* genome has been completed and the opening reading frames are partially confirmed by expression sequence tags. Thus, the genes are likely to be characterized first in *C. elegans*. At same time, the worm is transparent and the cell lineage is completely studied. It makes all research easy.

Our lab mainly studies the Sma/Mab pathway. We have strong curiosity to learn why the worm becomes small. The Smad proteins have been identified long time ago by Dr Savage-Dunn. But, the knowledge from the genotype to phenotype is not well understood yet. In the future, the study should focus on this question. The transcription co-factors and target genes will be identified and characterized. There are hundreds of Smad target genes. The collagen related genes could be responsible for body size control. The genes critical for cell differentiation could be responsible for the male tail sensory ray fusions. For different cell type and different target genes, the transcription co-factors may be different. The *C. elegans* Smads, *sma-2*, *sma-3* and *sma-4* not only express in hypodermis, which is critical for body size regulation, but also express in intestine and pharynx, even neurons. In these tissues, the proteins could have different roles, which we have not

realized yet. The phenotypes are more difficult to be characterized. In intestine, the Smad genes could involve in the endocytosis. Kim's lab speculates that the Smad genes also are required for immunity (Personal Communication). The wild type becomes mature with the first fertilized egg at 72 hours old under 20°C. But, *sma-3(wk30)* mutant worms need 90 hours to be mature. This suggests that Smad genes including *sma-3* also have roles in the developmental timing. It could be a good project in future.

There are a lot of cross talks between different signaling pathways. In *C. elegans*, the cross talk is not well studied. The cell cycle, cell differentiation, cell death and cell migration pathways may have relation with Sma/Mab pathway. For example, the EGF signaling pathway component Erk might phosphorylated the linker region of Smad proteins. There are many new reports every year especially in mammalian systems. Their relations will be better understood by crossing the mutated worms. To set up a network of the signaling pathways, some novel methods should be invented especially that to analyze a small change. The weak alleles or partially rescues would be tried first.

## References

Abdollah S, Macías-Silva M, Tsukazaki T, Hayashi H, Attisano L and Wrana JL (1997) TBRI phosphorylation of Smad2 on Ser<sup>465</sup> and Ser<sup>467</sup> is required for Smad2-Smad4 complex formation and signaling. *J Biol Chem* **272**: 27678-85

Affolter M, Marty T, Vigano MA, Jazwinska (2001) A Nuclear interpretation of *Dpp* signaling in *Drosophila*. *EMBO J* **20**: 3298-305

Anderson P (1995) Mutagenesis. *Methods Cell Biol* **48**: 31-58

Anyanful A, Sakube Y, Takuwa K and Kagawa H (2001) The third and fourth tropomyosin isoforms of *Caenorhabditis elegans* are expressed in the pharynx and intestines and are essential for development and morphology. *J Mol Biol* **313**: 525-537

Attisano L, Wrana JL (2002) Signal transduction by the TGF- $\beta$  superfamily. *Science* **296**: 1646-1647

Baird SE, Ellazar SA (1999) TGF $\beta$ -like signaling and spicule development in *Caenorhabditis elegans*. *Dev Biol* **212**: 93-100

Bonni S, Wang HR, Causing CG, Kavsak P, Stroschein SL, Luo K and Wrana JL (2001) TGF- $\beta$  induces assembly of a Smad2-Smurf2 ubiquitin ligase complex that targets SnoN for degradation. *Nat Cell Biol* **3**: 587-595

Bosher JM, Dufourcq P, Sookhareea S, Labouesse M (1999) RNA interference can target pre-mRNA: consequences for gene expression in a *Caenorhabditis elegans* operon. *Genetics* **153**: 1245-56

Brenner S (1974) The genetics of *Caenorhabditis elegans*. *Genetics* **77**: 71-94

Broverman SA, Meneely PM (1994) Meiotic mutants that cause a polar decrease in recombination on the X chromosome in *Caenorhabditis elegans*. *Genetics* **136**: 119-127

*C. elegans* II (1997) Edited by Riddle DL, Blumenthal T, Meyer BJ, Priess JR. Cold Spring Harbor Lab Press

Chacko BM, Qin B, Correia JJ, Lam SS, de Caestecker MP, Lin K (2001) The L3 loop and C-terminal phosphorylation jointly define Smad protein trimerization. *Nat Struct Biol* **8**: 248-53

Chen SJ, Yuan W, Mori Y, Levenson A, Trojanowska M, Varga J (1999) Stimulation of

type I collagen transcription in human skin fibroblasts by TGF- $\beta$ : involvement of Smad3.

*J Invest Dermatol* **112**: 49-57

Chen YG, Hata A, Lo RS, Wotton D, Shi Y, Pavletich N, Massagué J (1998) Determinants of specificity in TGF- $\beta$  signal transduction. *Genes Dev* **12**: 2144-52

Chisholm A (1991) Control of cell fate in the tail region of *C. elegans* by the gene *egl-5*. *Development* **111**: 921-32

Chow KL, Hall DH, Emmons SW (1995) The *mab-21* gene of *Caenorhabditis elegans* encodes a novel protein required for choice of alternate cell fates. *Development* **121**: 3615-26

Chow KL, Emmons SW (1994) HOM-C/Hox genes and four interacting loci determine the morphogenetic properties of single cells in the nematode male tail. *Development* **120**: 2579-92

Colavita A, Krishna S, Zheng H, Padgett RW, Culotti JG (1998) Pioneer axon guidance by UNC-129, a *C. elegans* TGF- $\beta$ . *Science* **281**: 706-709

Coulson A, Huynh C, Kozono Y, Shownkeen R (1995) The physical map of the

*Caenorhabditis elegans* genome. *Methods Cell Biol* **48**: 533-50

Coulson A, Waterston R, Kiff J, Sulston J, Kohara Y (1988) Genome linking with yeast artificial chromosomes. *Nature* **335**: 184-186

Cox GN (1990) Molecular biology of the cuticle collagen gene families of *Caenorhabditis elegans* and *Haemonchus contortus*. *Acta Trop* **47**: 269-81

da Graca LS, Zimmerman KK, Mitchell MC, Kozhan-Gorodetska M, Sekiewicz K, Morales Y, Patterson GI (2003) DAF-5 is a Ski oncoprotein homolog that functions in a neuronal TGF- $\beta$  pathway to regulate *C. elegans* dauer development. *Development* **131**: 435-46

De Stasio EA, Dorman S (2001) Optimization of ENU mutagenesis of *Caenorhabditis elegans*. *Mutat Res* **495**: 81-88

Denissova NG, Pouponnot C, Long J, He D, Liu F (2000) Transforming growth factor  $\beta$  inducible independent binding of SMAD to the Smad7 promoter. *Proc Natl Acad Sci USA* **97**: 6397-402

Derynck R, Zhang YE (2003) Smad-dependent and Smad-independent pathways in

TGF- $\beta$  family signalling. *Nature* **425**: 577-84

Ebisawa T, Fukuchi M, Murakami G, Chiba T, Tanaka K, Imamura T and Miyazono K (2001) Smurf1 interacts with transforming growth factor- $\beta$  type I receptor through Smad7 and induces receptor degradation. *J Biol Chem* **276**: 12477-12480

Estevez M, Attisano L, Wrana JL, Albert PS, Massagué J, Riddle DL (1993) The *daf-4* gene encodes a bone morphogenetic protein receptor controlling *C. elegans* dauer larva development. *Nature* **365**: 644-649

Feng XH, Lin X, Derynck R (2000) Smad2, Smad3 and Smad4 cooperate with Sp1 to induce p15(Ink4B) transcription in response to TGF- $\beta$ . *EMBO J* **19**: 5178-93

Flemming AJ, Shen ZZ, Cunha A, Emmons SW and Leroi, AM (2000) Somatic polyploidization and cellular proliferation drive body size evolution in nematodes. *Proc Natl Acad Sci USA* **97**: 5285-90

Frederick JP, Liberati NT, Waddell DS, Shi Y, Wang XF(2004) Transforming growth factor  $\beta$ -mediated transcriptional repression of c-myc is dependent on direct binding of Smad3 to a novel repressive Smad binding element. *Mol Cell Biol* **24**: 2546-59

Fukushige T, Hawkins MG and McGhee JD (1998) The GATA-factor *elt-2* is essential for formation of the *Caenorhabditis elegans* intestine. *Dev Biol* **198**: 286-302

Futcher B (1996) Cyclins and the wiring of the yeast cell cycle. *Yeast* **12**: 1635-46

Galitski T, Saldanha AJ, Styles CA, Lander ES and Fink GR (1999) Ploidy regulation of gene expression. *Science* **285**: 251-254

Gilleard JS, Barry JD and Johnstone IL (1997) *cis*-regulatory requirements for hypodermal cell-specific expression of the *Caenorhabditis elegans* cuticle collagen gene *dpy-7*. *Mol Cell Biol* **17**: 2301-11

Gilleard JS, Shafi Y, Barry JD, McGhee JD (1999) ELT-3: A *Caenorhabditis elegans* GATA factor expressed in the embryonic epidermis during morphogenesis. *Dev Biol* **208**: 265-80

Green P, Lipman D, Hillier L, Waterston R, States D, Claverie JM (1993) Ancient conserved regions in new gene sequences and the protein databases. *Science* **259**: 1711-16

Groppe J, Greenwald J, Wiater E, Rodriguez-Leon J, Economides AN, Kwiatkowski W,

Affolter M, Vale WW, Belmonte JC, Choe S (2002) Structural basis of BMP signalling inhibition by the cystine knot protein Noggin. *Nature* **420**: 636-42

Gunther CV, Georgi LL and Riddle DL (2000) A *Caenorhabditis elegans* type I TGF  $\beta$  receptor can function in the absence of type II kinase to promote larval development. *Development* **127**: 3337-47

Hata A, Lo RS, Wotton D, Lagna G and Massagué J (1997) Mutations increasing autoinhibition inactivate tumour suppressors Smad2 and Smad4. *Nature* **388**: 82-87

He J, Tegen SB, Krawitz AR, Martin GS, Luo K (2003) The transforming activity of Ski and SnoN is dependent on their ability to repress the activity of Smad proteins. *J Biol Chem* **15**: 30540-7

Hedgecock EM, Culotti JG, Hall DH, Stern BD (1987) Genetics of cell and axon migrations in *Caenorhabditis elegans*. *Development* **100**: 365-82

Hedgecock EM and White JG (1985) Polyploid tissues in the nematode *Caenorhabditis elegans*. *Dev Biol* **107**: 128-133

Heldin CH, Miyazono K and ten Dijke P (1997) TGF- $\beta$  signalling from cell membrane to

nucleus through SMAD proteins. *Nature* **390**: 465-471

Herman MA and Horvitz HR (1994) The *Caenorhabditis elegans* gene *lin-44* controls the polarity of asymmetric cell divisions. *Development* **120**:1035-47

Hill CS (2001) TGF- $\beta$  signalling pathways in early *Xenopus* development. *Curr Opin Genet Dev* **11**: 533-40

Hodgkin J (1999) Sex, Cell Death, and the Genome of *C. elegans*. *Cell* **98**: 277-280

Hua X, Miller ZA, Benchabane H, Wrana JL, Lodish HF (2000) Synergism between transcription factors TFE3 and Smad3 in transforming growth factor- $\beta$ -induced transcription of the Smad7 gene. *J Biol Chem* **275**: 33205-08

Huse M, Chen YG, Massagué J, Kuriyan J (1999) Crystal structure of the cytoplasmic domain of the type I TGF  $\beta$  receptor in complex with FKBP12. *Cell* **96**: 425-36

Huse M, Muir TW, Xu L, Chen YG, Kuriyan J, Massagué J (2001) The TGF- $\beta$  receptor activation process: an inhibitor-to substrate-binding switch. *Mol Cell* **8**: 671-82

Inman GJ, Hill CS (2002) Stoichiometry of active smad-transcription factor complexes

on DNA. *J Biol Chem* **277**: 51008-16

Inoue T, Thomas JH (2000) Targets of TGF- $\beta$  signaling in *Caenorhabditis elegans* dauer formation. *Dev Biol* **217**: 192-204

Itoh F, Asao H, Sugamura K, Heldin CH, ten Dijke P, Itoh S (2001) Promoting bone morphogenetic protein signaling through negative regulation of inhibitory Smads. *EMBO J* **20**: 4132-42

Johnston LA and Gallant P (2002) Control of growth and organ size in *Drosophila*. *BioEssays* **24**: 54-64

Johnstone IL (2000) Cuticle collagen genes. Expression in *Caenorhabditis elegans*. *Trends Genet* **16**: 21-27

Kang Y, Chen CR, Massagué J (2003) A self-enabling TGF $\beta$  response coupled to stress signaling: Smad engages stress response factor ATF3 for Id1 repression in epithelial cells. *Mol Cell* **11**: 915-26

Kavsak P, Rasmussen RK, Causing CG, Bonni S, Zhu H, Thomsen GH and Wrana JL (2000) Smad7 binds to Smurf2 to form an E3 ubiquitin ligase that targets the TGF $\beta$

receptor for degradation. *Mol Cell* **6**: 1365-1375

Kenyon C (1986) A gene involved in the development of the posterior body region of *C. elegans*. *Cell* **46**: 477-87

Kirsch T, Sebald W, Dreyer MK (2000) Crystal structure of the BMP-2-BRIA ectodomain complex. *Nat Struct Biol* **7**: 492-496

Knight CG, Patel MN, Azevedo RB, Leroi AM (2002) A novel mode of ecdysozoan growth in *Caenorhabditis elegans*. *Evol Dev* **4**: 16-27

Koga M, Take-uchi M, Tameishi T, Ohshima Y (1999) Control of DAF-7 TGF- $\beta$  expression and neuronal process development by a receptor tyrosine kinase KIN-8 in *Caenorhabditis elegans*. *Development* **126**: 5387-98

Koh K, Rothman JH (2001) ELT-5 and ELT-6 are required continuously to regulate epidermal seam cell differentiation and cell fusion in *C. elegans*. *Development* **128**: 2867-80

Kramer JM (1994a) Structures and functions of collagens in *Caenorhabditis elegans*. *FASEB J* **8**: 329-36

Kramer JM (1994b) Genetic analysis of extracellular matrix in *C. elegans*. *Annu Rev Genet* **28**: 95-116

Kretzschmar M, Doody J, Timokhina I, Massagué J (1999) A mechanism of repression of TGF $\beta$ /Smad signaling by oncogenic Ras. *Genes Dev* **13**: 804-16

Krishna S, Maduzia LL, Padgett RW (1999) Specificity of TGF $\beta$  signaling is conferred by distinct type I receptors and their associated SMAD proteins in *Caenorhabditis elegans*. *Development* **126**: 251-60

Liang J, Lints R, Foehr ML, Tokarz R, Yu L, Emmons SW, Liu J, Savage-Dunn C (2003) The *Caenorhabditis elegans* schnurri homolog *sma-9* mediates stage- and cell type-specific responses to DBL-1 BMP-related signaling. *Development* **130**: 6453-64

Liu F, Pouponnot C and Massagué J (1997) Dual role of the Smad4/DPC4 tumor suppressor in TGF $\beta$ -inducible transcriptional complexes. *Genes Dev* **11**: 3157-3167

Liu X, Sun Y, Weinberg RA and Lodish HF (2001) Ski/Sno and TGF- $\beta$  signaling. *Cyt Growth Factor Rev* **12**: 1-8

Lo RS, Chen YG, Shi Y, Pavletich NP, Massagué J (1998) The L3 loop: a structural motif

determining specific interactions between SMAD proteins and TGF- $\beta$  receptors. *EMBO J* **17**:996-1005

Maduzia LL, Gumienny TL, Zimmerman CM, Wang H, Shetgiri P, Krishna S, Roberts AF, Padgett RW (2002) *lon-1* regulates *Caenorhabditis elegans* body size downstream of the *dbl-1* TGF- $\beta$  signaling pathway. *Dev Biol* **246**: 418-28

Martin-Castellanos C and Edgar BA (2002) A characterization of the effects of *Dpp* signaling on cell growth and proliferation in the *Drosophila* wing. *Development* **129**: 1003-1013

Massagué J (1998) TGF- $\beta$  signal transduction. *Annu Rev Biochem* **67**:753-91

Massagué J (2003) Integration of Smad and MAPK pathways: a link and a linker revisited. *Genes Dev* **17**: 2993-2997

Massagué J and Chen YG (2000) Controlling TGF- $\beta$  signaling. *Genes & Dev* **14**: 627-644

Massagué J and Wotton D (2000) Transcriptional control by the TGF- $\beta$ /Smad signaling system. *EMBO J* **19**: 1745-1754

Mehra A, Wrana JL (2002) TGF- $\beta$  and the Smad signal transduction pathway. *Biochem Cell Biol* **80**: 605-22

Meyer BJ (2000) Sex in the worm counting and compensating X-chromosome dose. *Trends Genet.* **16**: 247-53

McKeown C, Praitis V and Austin J (1998) *sma-1* encodes a  $\beta$ H-spectrin homolog required for *Caenorhabditis elegans* morphogenesis. *Development* **125**: 2087-2098

Mello CC, Kramer JM, Stinchcomb D and Ambros V (1991) Efficient gene transfer in *C. elegans*: extrachromosomal maintenance and integration of transforming sequences. *EMBO J* **10**: 3959-3970

Miller LM, Gallegos ME, Morisseau BA, Kim SK (1993) *lin-31*, a *Caenorhabditis elegans* HNF-3/fork head transcription factor homolog, specifies three alternative cell fates in vulval development. *Genes Dev* **7**: 933-47

Mohler WA, Simske JS, Williams-Masson EM, Hardin JD and White JG (1998) Dynamics and ultrastructure of developmental cell fusions in the *Caenorhabditis elegans* hypodermis. *Curr Biol* **8**: 1087-1090

Mohler WA, Shemer G, del Campo JJ, Valansi C, Opoku-Serebuoh E, Scranton V, Assaf N, White JG, Podbilewicz B (2002) The type I membrane protein EFF-1 is essential for developmental cell fusion. *Dev Cell* **2**: 355-62

Morita K, Chow KL and Ueno N (1999) Regulation of body length and male tail ray pattern formation of *Caenorhabditis elegans* by a member of TGF- $\beta$  family. *Development* **126**: 1337-1347

Morita K, Shimizu M, Shibuya H, Ueno N (2001) A DAF-1-binding protein BRA-1 is a negative regulator of DAF-7 TGF- $\beta$  signaling. *Proc Natl Acad Sci USA* **98**: 6284-88

Morita K, Flemming AJ, Sugihara Y, Mochii M, Suzuki Y, Yoshida S, Wood WB, Kohara Y, Leroi AM, Ueno N (2002) A *Caenorhabditis elegans* TGF- $\beta$ , DBL-1, controls the expression of LON-1, a PR-related protein, that regulates polyploidization and body length. *EMBO J* **21**: 1063-73

Moustakas A, Souchelnytskyi S, Heldin CH (2001) Smad regulation in TGF- $\beta$  signal transduction. *Journal of Cell Science* **114**: 4359-4369

Murakami G, Watabe T, Takaoka K, Miyazono K, Imamura T (2003) Cooperative inhibition of bone morphogenetic protein signaling by Smurf1 and inhibitory Smads. *Mol*

*Biol Cell* **14**: 2809-17

Nagamatsu Y, Ohshima Y (2004) Mechanisms for the control of body size by a G-kinase and a downstream TGF $\beta$  signal pathway in *Caenorhabditis elegans*. *Genes Cells* **9**: 39-47

Nash B, Colavita A, Zheng H, Roy PJ, Culotti JG (2000) The forkhead transcription factor UNC-130 is required for the graded spatial expression of the UNC-129 TGF- $\beta$  guidance factor in *C. elegans*. *Genes Dev* **14**: 2486-500

Newfeld SJ, Wisotzkey RG, Kumar S (1999) Molecular evolution of a developmental pathway: phylogenetic analyses of transforming growth factor- $\beta$  family ligands, receptors and Smad signal transducers. *Genetics* **152**: 783-95

Nyström J, Shen ZZ, Aili M, Flemming AJ, Leroi A, Tuck S (2002) Increased or decreased levels of *Caenorhabditis elegans lon-3*, a gene encoding a collagen, cause reciprocal changes in body length. *Genetics* **161**: 83-97

Oka T, Toyomura T, Honjo K, Wada Y and Futai M (2001) Four subunit isoforms of *Caenorhabditis elegans* vacuolar H<sup>+</sup>-ATPase. Cell-specific expression during development. *J Biol Chem* **276**: 33079–33085

Okkema PG, Harrison SW, Plunger V, Aryana A and Fire A (1993) Sequence requirements for myosin gene expression and regulation in *Caenorhabditis elegans*.

*Genetics* **135**: 385–404

Oldham S, Bohni R, Stocker H, Brogiolo W and Hafen E (2000) Genetic control of size in *Drosophila*. *Philos Trans R Soc Lond B Biol Sci* **355**: 945-952

Patterson GI, Kowcek A, Wong A, Liu Y, Ruvkun G (1997) The DAF-3 Smad protein antagonizes TGF- $\beta$ -related receptor signaling in the *Caenorhabditis elegans* dauer pathway. *Genes Dev* **11**: 2679-90

Patterson GI, Padgett RW (2000) TGF  $\beta$ -related pathways: roles in *Caenorhabditis elegans* development. *Trends Genet* **16**: 27-33

Petritsch C, Beug H, Balmain A, Oft M (2000) TGF- $\beta$  inhibits p70 S6 kinase via protein phosphatase 2A to induce G(1) arrest. *Genes Dev* **14**: 3093-3101

Podos SD, Hanson KK, Wang YC and Ferguson EL (2001) The DSmurf ubiquitin-protein ligase restricts BMP signaling spatially and temporally during *Drosophila* embryogenesis.

*Dev Cell* **1**: 567-578

Qin B, Lam SS, Lin K (1999) Crystal structure of a transcriptionally active Smad4 fragment. *Structure Fold Des* **7**: 1493-503

Qin BY, Chacko BM, Lam SS, de Caestecker MP, Correia JJ, Lin K (2001) Structural basis of Smad1 activation by receptor kinase phosphorylation. *Mol Cell* **8**:1303-1312

Qin BY, Lam SS, Correia JJ, Lin K (2002) Smad3 allostery links TGF- $\beta$  receptor kinase activation to transcriptional control. *Genes Dev* **16**: 1950-63

Randall RA, Howell M, Page CS, Daly A, Bates PA, Hill CS (2004) Recognition of phosphorylated-Smad2-containing complexes by a novel Smad interaction motif. *Mol Cell Biol* **24**:1106-1121

Raftery LA and Sutherland DJ (1999) TGF- $\beta$  family signal transduction in *Drosophila* development: from Mad to Smads. *Dev Biol* **210**: 251-268

Ren P, Lim CS, Johnsen R, Albert PS, Pilgrim D and Riddle DL (1996) Control of *C. elegans* larval development by neuronal expression of a TGF- $\beta$  homolog. *Science* **274**: 1389-1391

Roelen BA, Cohen OS, Raychowdhury MK, Chadee DN, Zhang Y, Kyriakis JM,

Alessandrini AA, Lin HY (2003) Phosphorylation of threonine 276 in Smad4 is involved in transforming growth factor- $\beta$ -induced nuclear accumulation. *Am J Physiol Cell Physiol* **285**: C823-30

Saha D, Datta PK, Beauchamp RD (2001) Oncogenic ras represses transforming growth factor- $\beta$ /Smad signaling by degrading tumor suppressor Smad4. *J Biol Chem* **276**: 29531-7

Savage C, Das P, Finelli AL, Townsend SR, Sun CY, Baird SE, Padgett RW (1996) *Caenorhabditis elegans* genes *sma-2*, *sma-3*, and *sma-4* define a conserved family of transforming growth factor  $\beta$  pathway components. *Proc Natl Acad Sci USA* **93**: 790-794

Savage-Dunn C (2001) Targets of TGF $\beta$ -related signaling in *Caenorhabditis elegans*. *Cytokine Growth Factor Rev* **12**: 305-12

Savage-Dunn C, Tokarz R, Wang H, Cohen S, Giannikas C, Padgett RW (2000) SMA-3 smad has specific and critical functions in DBL-1/SMA-6 TGF $\beta$ -related signaling. *Dev Biol* **223**: 70-76

Savage-Dunn C, Maduzia LL, Zimmerman CM, Roberts AF, Cohen S, Tokarz R, Padgett RW (2003) Genetic screen for small body size mutants in *C. elegans* reveals many TGF $\beta$

pathway components *Genesis*. **35**: 239-47

Sekelsky JJ, Newfeld SJ, Raftery LA, Chartoff EH, Gelbart WM (1995) Genetic characterization and cloning of mothers against *dpp*, a gene required for decapentaplegic function in *Drosophila melanogaster*. *Genetics* **139**: 1347-58

Shi Y, Hata A, Lo RS, Massagué J, Pavletich NP (1997) A structural basis for mutational inactivation of the tumour suppressor Smad4. *Nature* **388**: 87-93

Shi Y, Massagué J (2003) Mechanisms of TGF- $\beta$  signaling from cell membrane to the nucleus. *Cell* **113**: 685-700.

Shi Y, Wang YF, Jayaraman L, Yang H, Massagué J and Pavletich NP (1998) Crystal structure of a Smad MH1 domain bound to DNA: insights on DNA binding in TGF- $\beta$  signaling. *Cell* **94**: 585-594

Souchelnytskyi S, Tamaki K, Engström U, Wernstedt C, ten Dijke P and Heldin CH (1997) Phosphorylation of Ser<sup>465</sup> and Ser<sup>467</sup> in the C terminus of Smad2 mediates interaction with Smad4 and is required for transforming growth factor- $\beta$  signaling. *J Biol Chem* **272**: 28107-28115.

Sulston JE, Albertson DG and Thomson JN (1980) The *Caenorhabditis elegans* male: postembryonic development of nongonadal structures. *Dev Biol* **78**: 542-576

Sulston JE, Schierenberg E, White JG, Thomson JN (1983) The embryonic cell lineage of the nematode *Caenorhabditis elegans*. *Dev Biol* **100**: 64-119

Sulston JE, White JG (1980) Regulation and cell autonomy during postembryonic development of *Caenorhabditis elegans*. *Dev Biol* **78**: 577-97

Sulston JE and Horvitz HR (1977) Post-embryonic cell lineages of the nematode, *Caenorhabditis elegans*. *Dev Biol* **56**: 110-156

Stroschein SL, Wang W, Zhou S, Zhou Q, Luo K. Negative feedback regulation of TGF- $\beta$  signaling by the SnoN oncoprotein. *Science* **286**: 771-774

Suzuki Y, Morris GA, Han M, Wood WB (2002) A cuticle collagen encoded by the *lon-3* gene may be a target of TGF- $\beta$  signaling in determining *Caenorhabditis elegans* body shape. *Genetics* **162**: 1631-39

Suzuki Y, Yandell MD, Roy PJ, Krishna S, Savage-Dunn C, Ross RM, Padgett RW, Wood WB (1999) A BMP homolog acts as a dose-dependent regulator of body size and male

tail patterning in *Caenorhabditis elegans*. *Development* **126**: 241-250

Tajima Y, Goto K, Yoshida M, Shinomiya K, Sekimoto T, Yoneda Y, Miyazono K, Imamura T (2003) Chromosomal region maintenance 1 (CRM1)-dependent nuclear export of Smad ubiquitin regulatory factor 1 (Smurf1) is essential for negative regulation of transforming growth factor- $\beta$  signaling by Smad7. *J Biol Chem* **278**: 10716-21

Tan PB, Lackner MR, Kim SK (1998) MAP kinase signaling specificity mediated by the LIN-1 Ets/LIN-31 WH transcription factor complex during *C. elegans* vulval induction. *Cell* **93**: 569-580

The *C. elegans* Sequencing Consortium (1998) Genome sequence of the nematode *C. elegans*: a platform for investigating biology. *Science* **282**: 2012-2018

Torres-Vazquez J, Warrior R, Arora K (2000) *schnurri* is required for dpp-dependent patterning of the *Drosophila* wing. *Dev Biol* **227**: 388-402

Wang J, Tokarz R, Savage-Dunn C (2002) The expression of TGF $\beta$  signal transducers in the hypodermis regulates body size in *C. elegans*. *Development* **129**: 4989-4998

Wang T, Li BY, Danielson PD, Shah PC, Rockwell S, Lechleider RJ, Martin J,

Manganaro T, Donahoe PK The immunophilin (1996) FKBP12 functions as a common inhibitor of the TGF $\beta$  family type I receptors. *Cell* **86**: 435-44

Watanabe M, Masuyama N, Fukuda M, Nishida E (2000) Regulation of intracellular dynamics of Smad4 by its leucine-rich nuclear export signal. *EMBO Rep* **1**: 176-182

Wicks SJ, Lui S, Abdel-Wahab N, Mason RM, Chantry A (2000) Inactivation of smad-transforming growth factor  $\beta$  signaling by Ca(2+) calmodulin dependent protein kinase II. *Mol Cell Biol* **20**: 8103-11

Wicky C, Villeneuve AM, Lauper N, Codourey L, Tobler H, Muller F (1996) Telomeric repeats (TTAGGC) $_n$  are sufficient for chromosome capping function in *Caenorhabditis elegans*. *Proc Natl Acad Sci U S A* **93**: 8983-8

Wotton D, Massagué J (2001) Smad transcriptional corepressors in TGF $\beta$  family signaling. *Curr Top Microbiol Immunol*. **254**: 145-164.

Wrana JL (2002) Phosphoserine-Dependent regulation of protein-protein interactions in smad pathway. *Structure* **10**: 5-7

Wrana JL and Attisano L (2000) The Smad pathway. *Cytokine Growth Factor Rev* **11**:

5-13

Wu G, Chen YG, Ozdamar B, Gyuricza CA, Chong PA, Wrana JL, Massagué J, Shi Y (2000) Structural basis of Smad2 recognition by the Smad anchor for receptor activation. *Science* **287**: 92-97

Wu JW, Krawitz AR, Chai J, Li W, Zhang F, Luo K, Shi Y (2002) Structural mechanism of Smad4 recognition by the nuclear oncoprotein Ski: insights on Ski-mediated repression of TGF- $\beta$  signaling. *Cell* **111**: 357-67

Wu JW, Hu M, Chai J, Seoane J, Huse M, Li C, Rigotti DJ, Kyin S, Muir TW, Fairman R, Massagué J, Shi Y (2001) Crystal structure of a phosphorylated Smad2. Recognition of phosphoserine by the MH2 domain and insights on Smad function in TGF- $\beta$  signaling. *Mol Cell* **8**: 1277-89

Xiao Z, Liu X, Henis YI, Lodish HF (2000) A distinct nuclear localization signal in the N terminus of Smad3 determines its ligand-induced nuclear translocation. *Proc Natl Acad Sci USA* **97**: 7853-58

Yochem J, Gu T and Han M (1998) A new marker for mosaic analysis in *Caenorhabditis elegans* indicates a fusion between hyp6 and hyp7, two major components of the

hypodermis. *Genetics* **149**: 1323-1334

Yoshida S, Morita K, Mochii M, Ueno N (2001) Hypodermal expression of *Caenorhabditis elegans* TGF- $\beta$  type I receptor SMA-6 is essential for the growth and maintenance of body length. *Dev Biol* **240**: 32-45

Zhang Y, Chang C, Gehling DJ, Hemmati-Brivanlou A and Derynck R (2001) Regulation of Smad degradation and activity by Smurf2, an E3 ubiquitin ligase. *Proc Natl Acad Sci USA* **98**: 974-979

Zhu H, Kavsak P, Abdollah S, Wrana JL and Thomsen GH (1999) A SMAD ubiquitin ligase targets the BMP pathway and affects embryonic pattern formation. *Nature* **400**: 687-693